Roles of the mitochondrial fatty acid synthesis II (mtFASII) pathway in mitochondrial function and signaling

By

Hayley Boyd Clay

Dissertation
Submitted to the Faculty of the
Graduate School of Vanderbilt University
in partial fulfillment of the requirements
for the degree of

DOCTOR OF PHILOSOPHY
in

Neuroscience
August, 2016
Nashville, Tennessee

Approved:
Aaron Bowman, Ph.D.
Bruce Carter, Ph.D.
Laura Dugan, M.D.
Sandra Zinkel, M.D., Ph.D.
Deborah Murdock, Ph.D.

To Hank, for your unfailing belief in me.
And to Caroline—you can do anything.

ACKNOWLEDGEMENTS

I would like to thank the Vanderbilt Neuroscience program for providing an excellent education through the program coursework, financial support through the program's training grant, and professional encouragement from the program administration. I am particularly grateful for the support of Mark Wallace and Doug McMahon and the administrative help I received through Mary Michael-Woolman, Roz Johnson, and Beth Sims.

Thank you to Dave Hachey and Wade Callahan at the Vanderbilt Mass Spectrometry Core Laboratory for their help with my ability to understand and analyze mass spectrometry data and for their technical support in teaching me how to prepare my samples. I am also grateful for the services provided by Metabolon, Inc. and the MUSC Lipidomics Core.

I am very grateful to my thesis committee—Aaron Bowman, Bruce Carter, Laura Dugan, and Sandy Zinkel—for their excellent advice and thought-provoking discussions. The time and effort spent attending committee meetings, reading committee updates, and reviewing manuscripts are greatly appreciated.

None of my work would have been possible without my advisor Debbie Murdock. I am so grateful that she took me into her lab at all, and also so thankful for her generosity of kindness, advice, support, and patience. The amount of scientific knowledge I gained from you cannot be measured—her mentorship has truly taught me to think like a scientist. She has been a wonderful mentor and friend, and made graduate school the best experience it could be. I remember my time in the Murdock laboratory with great fondness.

I am also indebted to my labmates, Sabrina Mitchell and Angie Parl. I learned so much from you and would not have been able to complete my work without you. I appreciate all the bench work pointers and troubleshooting, and I am grateful for the time you spent discussing my

data and writing, editing, and rewriting manuscripts. I enjoyed working with you more than I can say, and I consider both of you my friends.

To my wonderful friends—specifically Sudipta Chakraborty, Chris Muller, Jamie and James Saxon, and Christi and Will French—I am so grateful for your emotional support, listening ears, and ability to distract me from the stress of graduate school. I will always be thankful for coffee and lunch breaks, venting sessions, weekend trips, and TV nights. Each of you improves my quality of life, and I hope that I am able to return the favor.

I am so very grateful for my family of origin. To my mom Jamie and stepfather Matt, you provided me with the upbringing and encouragement that enabled me to succeed academically. To my sister Megan, I am so thankful for your love and support and for making me laugh. I am thankful also for my in-laws, Patty, David, Sam, Sara, and Mike. You have always shown a great interest in my work, and I am so glad to call you family.

Lastly, I want to thank my new family—my husband Hank and our sweet baby Caroline. Hank, I really would not be here without you. You have supported me at every turn, keeping me sane, comforting me, and being the daily encouragement I needed to keep going. Caroline, you are so new and bring so much hope for the future. I hope that earning my Ph.D. will show you that you can do anything you set your mind to do. There are no words to describe how much I love you two.

LIST OF TABLES

LIST OF FIGURES

LIST OF ABBREVIATIONS

4'PP ..... 4'phosphopantetheine

AAA ..... ATPase associated with diverse cellular activities

ABAD ..... amyloid-beta-binding alcohol dehydrogenase

ABC ..... ATP-binding cassette

ACP ..... acyl carrier protein

ACSF3 ..... acyl-CoA synthetase F3

AD ..... Alzheimer's disease

ADP ..... adenosine diphosphate

AHL ..... N-acyl homoserine lactone

AMP ..... adenosine monophosphate

ANOVA ..... analysis of variance

ATF5 ..... activating transcription factor 5

ATFS-1 ..... activating transcription factor associated with stress 1

ATP ..... adenosine triphosphate

ATPase ..... ATP monophosphatase

B. subtilis ..... *Bacillus subtilis*

B. taurus ..... *Bos taurus*

Bax ..... B-cell CLL/lymphoma 2-associated X protein

BF_3 ..... boron trifluoride

BSA ..... bovine serum albumin

C ..... carbon

c-Jun ..... Jun proto-oncogene

C. elegans ..... *Caenorhabditis elegans*

C/EBPβ ..... CCAAT-enhancer-binding protein β

Ca^{2+} ..... calcium

cAMP ..... cyclic adenosine monophosphate

CDP ..... cytidine diphosphate

Cem1 ..... condensing enzyme with mitochondrial function 1

CerS ..... (dihydro)ceramide synthase

CGT ..... ceramide galactosyltransferase

CHOP ..... CCAAT-enhancer-binding protein homologous protein

CI ..... complex I

ClpP ..... caseinolytic mitochondrial matrix peptidase proteolytic subunit

CMAMMA ..... combined malonic and methylmalonic aciduria

CO_2 ..... carbon dioxide

CoA ..... coenzyme A

Com ..... competence protein

Cs_2SO_4 ..... cesium sulfate

CSF ..... competence and sporulation factor

CSSG ..... cysteine-glutathione disulfide

DMEM ..... Dulbecco's modified eagle medium

DNA ..... deoxyribonucleic acid

DNAJC19 ..... DnaJ homolog subfamily C, member 19

DTNB ..... 5,5'-dithiobis-(2-nitrobenzoic acid)

DTT ..... dithiothreitol

DVE-1 ..... defective proventriculus 1

E. coli ..... *Escherichia coli*

EDF ..... extracellular death factor

EGFP ..... enhanced green fluorescent protein

ELISA ..... enzyme-linked immunosorbent assay

ER ..... endoplasmic reticulum

ER-UPR .....ER unfolded protein response

ESI ..... electrospray ionization

ETC.....electron transport chain

Etr1p .....2-enoyl-thioester reductase protein

Fab.....fatty acid biosynthesis

FACLS4 .....acyl-CoA synthetase long-chain family member 4

FAS .....fatty acid synthesis

FASN ..... fatty acid synthase

FBS .....fetal bovine serum

FDR..... false discovery rate

G6PD .....glucose-6-phosphate dehydrogenase

GC/MS .....gas chromatography/mass spectrometry

GG ..... double glycine

GMP.....guanosine monophosphate

GPAM .....mitochondrial glycerol-3-phosphate acyltransferase

GPAT ..... glycerol-3-phosphate acyltransferase

GSH .....glutathione

GSSG..... glutathione disulfide

GTPase..... guanosine triphosphate monophosphatase

H ..... hydrogen

H_2O ..... water

H_2O_2 ..... hydrogen peroxide

HADH2..... 3-hydroxyacyl-CoA dehydrogenase type 2

HPLC .....high performance liquid chromatography

HSCBR4 .....*Homo sapiens* carbonyl reductase 4

HSHSD17B8 ..... *Homo sapiens* hydroxysteroid (17β) dehydrogenase 8

HSHTD2 ..... *Homo sapiens* 3-hydroxyacyl-ACP dehydratase 2

Hsp60 ..... heat shock protein 60

Htd2 ..... 3-hydroxyacyl-ACP dehydratase 2

I ..... iodine

i-AAA ..... inner mitochondrial membrane AAA

IMM ..... inner mitochondrial membrane

JNK ..... c-Jun N-terminal kinase

KAR ..... 3-ketoacyl reductase

KAS ..... β-ketoacyl-ACP synthase

KD ..... knockdown

KHDR ..... 3-ketodihydrosphinganine reductase

LAE ..... lipoate activating enzyme

LC ..... liquid chromatography

LC-MS ..... liquid chromatography-mass spectrometry

LC-MS/MS ..... liquid chromatography-tandem mass spectrometry

LIAS ..... lipoic acid synthase

LIPT1 ..... lipoyl transferase

LIPT2 ..... octanoyl transferase

LIT ..... linear ion trap

LTQ ..... linear trap quadrupole

m-AAA ..... matrix AAA

m/z ..... mass-to-charge ratio

MACS ..... magnetic assisted cell sorting

MCAT ..... malonyl-CoA:ACP transacylase

MECR ..... mitochondrial *trans*-2-enoyl-CoA reductase

MEK ..... mitogen-activated protein kinase kinase

Mg ..... magnesium

$MgCl_2$ ..... magnesium chloride

MOPS ..... 3-(*N*-morpholino)propanesulfonic acid

MRPP ..... mitochondrial RNase P protein

MS ..... mass spectrometry

MS^2 ..... tandem mass spectrometry

mtDNA ..... mitochondrial DNA

mtHsp70 ..... mitochondrial heat shock protein 70

mtRNAse ..... mitochondrial RNase

mtUPR ..... mitochondrial unfolded protein response

MURE ..... mitochondrial unfolded protein response element

N. crassa ..... *Neurospora crassa*

NAD ..... nicotinamide adenine dinucleotide

NADP ..... nicotinamide adenine dinucleotide phosphate

nDNA ..... nuclear DNA

NDUFAB1 ..... NADH dehydrogenase (ubiquinone) 1, α/β subcomplex 1

NDUFB2 ..... NADH dehydrogenase (ubiquinone) 1, β subcomplex 2

NDUFS3 ..... NADH dehydrogenase (ubiquinone) Fe-S protein 3

Oar1p ..... 3-oxoacyl-ACP reductase

ODC ..... ornithine decarboxylase

ORF ..... open reading frame

OX ..... overexpression

OXPHOS ..... oxidative phosphorylation

PCR ..... polymerase chain reaction

PDH ..... pyruvate dehydrogenase

PHB2.....prohibitin 2

PhrC.....phosphatase RapC inhibitor

PKCζ.....protein kinase C ζ

PLA2.....phospholipase A2

PP1.....protein phosphatase 1

PP2A..... protein phosphatase 2A

PPAR.....peroxisome proliferator-activated receptor

PPP..... pentose phosphate pathway

PPTase.....phosphopantetheine:protein transferase

pSG5.....pregnancy specific β-1-glycoprotein 5

Rap.....response regulator aspartate phosphatase

RNA..... ribonucleic acid

RNase P..... ribonuclease P

RNAseq..... RNA sequencing

ROS.....reactive oxygen species

RPM.....RNA component of mitochondrial RNase P

RPP14..... ribonuclease P/MRP 14 kDa subunit

RT-PCR.....reverse transcription PCR

S..... sulfur

S. cerevisiae..... *Saccharomyces cerevisiae*

S1P.....sphingosine-1-phosphate

S1PR..... S1P receptor

shRNA.....short hairpin RNA

siRNA.....short interfering RNA

SMPD5.....sphingomyelin phosphodiesterase 5

SPG-7..... spastic paraplegia 7/paraplegin

SPHK ..... sphingosine kinase

Spo ..... sporulation protein

SPT ..... serine palmitoyltransferase

SSAT ..... spermidine/spermine-N'-acetyltransferase

SV40 ..... simian vacuolating virus 40

TCA ..... tricarboxylic acid

TLC ..... thin layer chromatography

TNB ..... 5-thio-2-nitrobenzoic acid

TNFα ..... tumor necrosis factor α

TOM22 ..... translocase of the mitochondrial outer membrane 22

tRNA ..... transfer RNA

UBL-5 ..... ubiquitin-like 5

UHLC/MS/MS ..... ultrahigh performance liquid chromatography/tandem mass spectrometry

UPLC ..... ultrahigh performance liquid chromatography

UV ..... ultraviolet

V. fischeri ..... *Vibrio fischeri*

YME1L1 ..... *YME1-like 1 ATPase*

α-KGDH ..... α-ketoglutarate dehydrogenase

Table of Contents

CHAPTER I

INTRODUCTION

Three types of fatty acid synthesis

Synthesis of straight chain, saturated fatty acids largely occurs in three main pathways: FASI, FASII, and mitochondrial FASII (mtFASII). FASI occurs in the cytoplasm of eukaryotic cells via the dimeric, multifunctional enzyme FASN.[1] FASII occurs in prokaryotes and uses individual, monofunctional enzymes for each step of the pathway. Because mitochondria are evolutionarily linked to bacteria, mtFASII behaves similarly to prokaryotic FASII—mtFASII employs a separate enzyme for each step of the fatty acid synthesis pathway.

Despite these separate systems for fatty acid synthesis, the reactions involved in all three pathways are largely the same. Fatty acid synthesis is cyclical in nature, with the addition of two-carbon units to the acyl chain per reaction cycle. Generally, fatty acid synthesis begins with the carboxylation of acetyl-CoA to malonyl-CoA via acetyl-CoA carboxylase. Additionally, acyl carrier protein (ACP), the nascent fatty acid's mode of transport through the reaction cycle, must be activated by pantetheinylation, which is the ACP synthase-mediated addition of a labile prosthetic group derived from CoA. In the initial reaction cycle, both a molecule of acetyl-CoA and malonyl-CoA are activated by the replacement of CoA with ACP by ACP-S-acetyltransferase and ACP-S-malonyltransferase, respectively. Acetyl-ACP and malonyl-ACP are then combined to form 3-ketoacyl-ACP via β-ketoacyl-ACP synthase. The tail-end carbon is reduced by 3-ketoacyl-ACP reductase, producing 3-hydroxyacyl-ACP. 3-hydroxyacyl-ACP dehydratase removes a water molecule from 3-hydroxyacyl-ACP, forming enoyl-ACP. Finally, enoyl-ACP is reduced by enoyl-ACP reductase, producing acyl-ACP. This acyl-ACP can re-enter the pathway at its initial step, combining with malonyl-ACP via β-ketoacyl-ACP synthase.

Depending on the fatty acid synthesis system in question, typical product chain lengths range between four and 16 carbons.[1, 2] FASI products are used toward the synthesis of palmitate.[1] In bacteria, FASII is the only *de novo* source of fatty acids, so all newly synthesized bacterial lipids are derived from FASII products. In eukaryotes, the roles of mitochondria-derived fatty acids are not known, and there is no evidence to support their inclusion in phospholipids. MtFASII products are, however, known to contribute to lipoic acid synthesis, a pathway that will be discussed later.

The components of mtFASII

MtFASII, like bacterial FASII, relies on a series of monofunctional enzymes to catalyze the reactions required for fatty acid synthesis (Figure 1). MtFASII occurs in the mitochondrial matrix, and it is the only fatty acid synthesis pathway within the mitochondria, although mitochondria are able to obtain lipid molecules from elsewhere in the cell. Below is an overview of the enzymes involved in the mtFASII pathway.

Phosphopantetheine:protein transferase (PPTase)

Phosphopantetheine:protein transferase (PPTase) catalyzes the transfer of the acyl-carrying phosphopantetheine group from CoA to ACP.[3-6] Human and yeast PPTases were identified by their sequence similarity with bacterial homologs, and human PPTase expression is highest in mitochondria-rich tissues such as heart, kidney, and liver.[3, 4, 7]

Yeast contain two PPTases, one for FASI and one for mtFASII.[6] A BLAST search of the human genome, however, only found one PPTase homolog.[7, 8] This single human PPTase is capable of converting both cytosolic and mitochondrial apo-ACP to holo-ACP, but localization studies found it to be a cytosolic protein.[3, 7] If the known human PPTase is the only PPTase in the cell, mitochondrial ACP would need to be imported into the mitochondria after conversion to

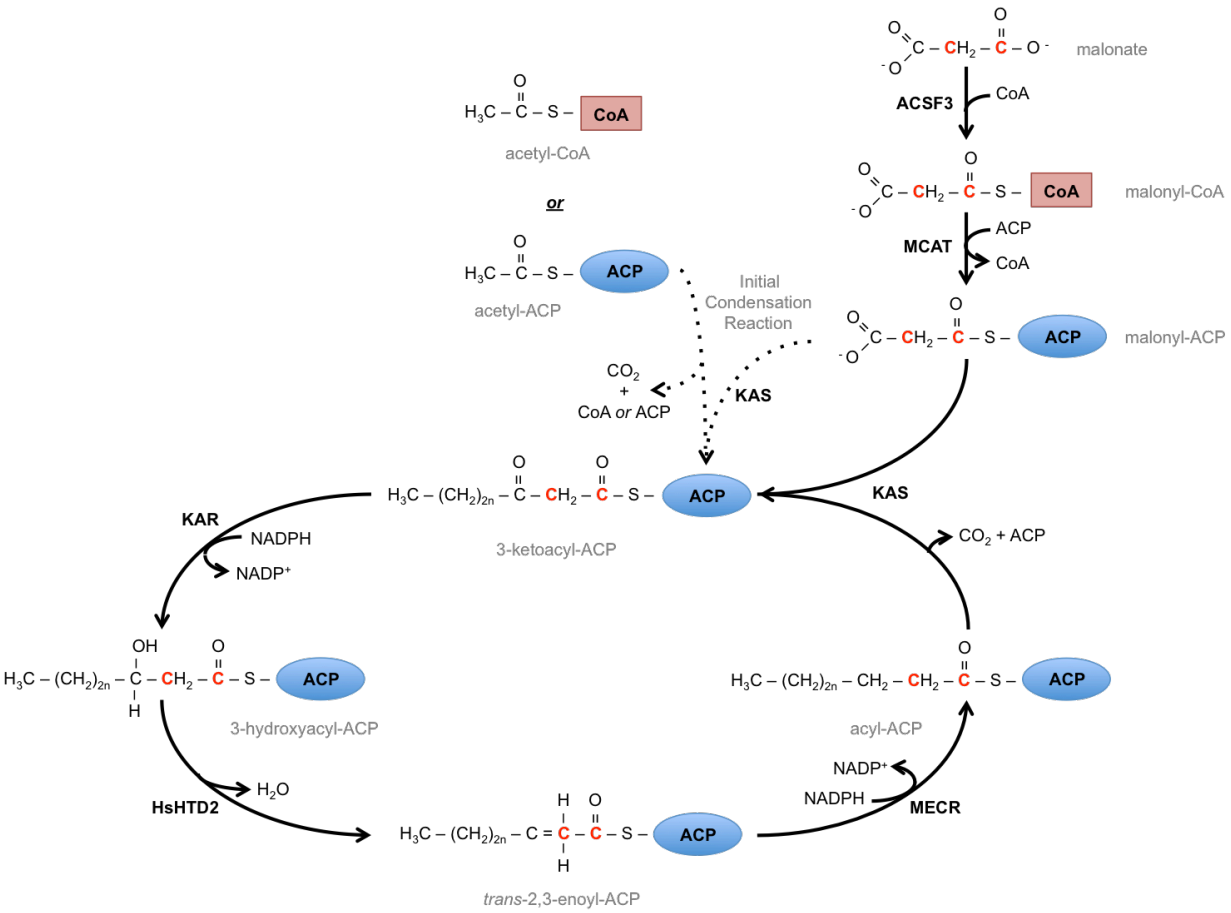

Figure 1. The mtFASII pathway.
In the mitochondria, ACSF3 links malonate to CoA, producing malonyl-CoA. MCAT then transfers the malonyl moiety from malonyl-CoA onto ACP, resulting in malonyl-ACP. KAS performs the initial condensation reaction of the mtFASII pathway, consending malonyl ACP with acetyl-CoA, acetyl-ACP, or acyl-ACP derived from previous mtFASII cycles. The initial condensation reaction produces 3-ketoacyl-ACP. KAR then reduces 3-ketoacyl-ACP, producing 3-hydroxyacyl-ACP. HsHTD2 then dehydrates 3-hydroxyacyl-ACP to *trans*-2,3-enoyl-ACP. Finally, MECR reduces *trans*-2,3-enoyl-ACP to acyl-ACP. Adapted from Schonauer et al, 2008.[9]

its mature form in the cytosol. There is no known mechanism for such a process. Given the presence of cytosolic and mitochondrial PPTases in yeast, it is likely, then, that human mitochondrial PPTase has simply not yet been identified.

PPTase functions as a monomer composed of two highly similar subdomains.[7, 8] In the interdomain cleft, PPTase binds Mg^{2+} and CoA, followed by binding of ACP.[3, 8] Substrate

binding to PPTase induces a hinge-like movement in which the two subdomains move closer to one another.[8]

Acyl-CoA synthetase F3 (ACSF3)

Acyl-CoA synthetase F3 (ACSF3) carries out the first step of mtFASII, which is the linkage of malonate, and to a lesser extent methylmalonate, onto CoA.[10, 11] Human ACSF3 was identified based on its homology to similar enzymes in other species.[12] Consistent with its mitochondrial localization, ACSF3 has highest expression in brown adipose, liver, and kidney.[12] Though malonyl-CoA is found in the cytosol, ACSF3 is the only source of malonyl-CoA in the mitochondria.[11] In its mature form, ACSF3 is a roughly 60-kDa protein.[12] Information regarding the structure and mechanism of action of ACSF3 has not been published.

Malonyl-CoA:ACP transacylase (MCAT)

Malonyl-CoA:ACP transacylase (MCAT) catalyzes the movement of the malonyl moiety of malonyl-CoA onto ACP, creating malonyl-ACP.[6] Yeast MCAT (MCT1) was identified based on its homology to bacterial FabD.[3, 6, 13] Data regarding MCAT's expression across tissues is not available. MCAT is a monomeric protein with an active site buried between two subdomains. Binding of the substrate results in a hinge-like movement, bringing the two subdomains into closer proximity. MCAT is specific for malonyl-CoA and for mitochondrial ACP.[3]

Beta-ketoacyl-ACP synthase (KAS)

Beta-ketoacyl-ACP synthase (KAS) catalyzes the condensation of acetyl- or acyl-ACP and malonyl-ACP, producing 3-ketoacyl-ACP.[3, 6] This step of mtFASII elongates the malonyl- or acyl-ACP chain by two carbons.

KAS was first identified in yeast by a random mutagenesis screen for respiratory-deficient phenotypes.[14] Sequencing of the gene revealed similarities to β-ketoacyl synthases of other species.[14] The human KAS was identified based on its 85% identity with the mouse gene,

and human KAS shows similarity to *Escherichia coli* KASII.[3, 15, 16] Data regarding KAS's expression across tissues is not available.

KAS functions as a dimer, and substrates bind in a pocket within the dimer interface, the end of which contains the active site.[3, 6, 16] Interestingly, little conformation change occurs when KAS binds an acyl chain of up to six carbons, but KAS does undergo conformation change to elongate the binding pocket for acyl chains longer than six carbons.[16]

KAS shows preference for certain acyl chain lengths: KAS has the fastest kinetics for acyl chains 6 and 10 carbons long, indicating that C8 and C12 acyl chains are potentially important products of the mtFASII pathway.[3, 15]

3-ketoacyl reductase (KAR)

3-ketoacyl reductase (KAR) catalyzes the reduction of 3-ketoacyl-ACP to 3-hydroxyacyl-ACP in an NADPH-dependent manner.[3, 6, 10] KAR is the only enzyme in the mammalian mtFASII pathway that contains two separate proteins, HSHSD17B8 and HSCBR4.[17]

The components of KAR were identified by sequence similarity to the yeast homolog Oar1p and bacterial FabG.[3, 18] Transfection of yeast *oar1* deletion mutants with genes for either component of the KAR protein resulted in only partial complementation of the mutant's respiratory deficient phenotype.[18, 19] When cotransfected, however, HSHSD17B8 and HSCBR4 fully rescued the *oar1* deletion phenotype, possibly indicating an interaction between the two proteins.[18, 19]

HSHSD17B8 and HSCBR4 copurified in a 1:1 stoichiometry, and size exclusion chromatography revealed a complex weighing roughly 110 kDa.[18] Given that HSHSD17B8 and HSCBR4 individually weigh 28.3 kDa and 26.6 kDa, respectively, the KAR complex functions as a heterotetramer.[18]

Both HSHSD17B8 and HSCBR4 are composed of a seven-stranded β-sheet covered in α-helices.[3, 17] The dimers of each protein interface through two α-helices, while the interaction

between the two dimers occurs at the β-sheet.[17] The HSCBR4 subunit of KAR first binds NADPH, which produces a conformation change that uncovers the active site, allowing the binding of 3-ketoacyl-ACP.[3, 17, 20]

Cytosolic KAR contains a catalytic domain and a structural domain, so it is possible that one of the mitochondrial KAR proteins serves a purely structural function.[17] Because mutation of HSCBR4 results in functional abnormality while mutation of HSHSD17B8 does not, it is likely that HSCBR4 serves as KAR's catalytic domain and HSHSD17B8 serves as a structural domain.[17] Data regarding KAR's mechanism of action or substrate specificity are not available.

3-hydroxyacyl-ACP dehydratase (HSHTD2)

Human 3-hydroxyacyl-ACP dehydratase (HSHTD2) catalyzes the dehydration of 3-hydroxyacyl-ACP to *trans*-2,3-enoyl-ACP. Identifying Htd2p, the yeast homolog of bacterial FabA, was difficult due to a lack of sequence similarity.[6] The yeast FabA homolog, however, was identified through a functional screen: monitoring a library of yeast mutant strains for the inability to lose a mitochondrial-targeted FabA plasmid revealed Htd2p to be the yeast FabA homolog.[6] To identify the human homolog, HSHTD2, a cDNA library of human transcripts was screened against *htd2*-Δ mutant yeast for complementation.[21]

HSHTD2 localizes to the mitochondria and is most highly expressed in heart and liver, both of which are mitochondria-rich tissues.[3, 6, 21, 22] HSHTD2 is an 18.8-kDa protein and has a "hotdog" fold structure in which an α-helix is wrapped in an anti-parallel β-sheet.[3] Data regarding HSHTD2's mechanism of action or substrate specificity are not available.

Mitochondrial trans-2-enoyl CoA reductase (MECR)

Mitochondrial *trans*-2-enoyl CoA reductase (MECR) catalyzes the last step of the mtFASII pathway.[3] MECR reduces *trans*-2,3-enoyl-ACP to acyl-ACP in an NADPH-dependent manner.[3, 6, 23] Mammalian MECR was identified based on its homology with the fungal 2-enoyl-thioester reductase protein (Etr1p), and MECR is highly conserved across species.[23]

Consistent with its role in the mtFASII pathway, MECR is localized to the mitochondria.[23] One study reported MECR translocating to the nucleus with PPARα, but that finding has not been replicated.[24] Published confocal imaging data from our laboratory confirms that fluorescent signal from a MECR-EGFP fusion protein overlaps with MitoTracker Red staining.[25]

MECR functions as a homodimer, with each subunit weighing 37 kDa.[3, 23, 26] Each MECR monomer is composed of an N-terminal catalytic domain and a C-terminal cofactor-binding domain, between which is a cleft that binds NADPH.[26] The interface between the two MECR monomers occurs at the cofactor-binding domain.[26] In addition to the NADPH-binding site, MECR contains a groove that fits ACP's recognition helix.[26] Importantly, the MECR catalytic domain contains a pocket leading to the active site that is long enough to accommodate a 16-carbon acyl chain.[3, 26]

MECR's activity is maximal for C8 and C12 acyl chains in humans. In *Bos taurus*, mtFASII was shown to synthesize up to 14-carbon acyl chains, but it is possible, given the depth of MECR's acyl chain pocket that mammalian mtFASII is actually capable of synthesizing 16-carbon acyl chains.

Acyl carrier protein (ACP)

Acyl carrier protein (ACP) shuttles the nascent fatty acid to the various enzymes of mtFASII. ACP is a 10-kDa protein that is highly conserved across species, and mammalian ACP can complement ACP deletion in *E. coli*.[3, 27] ACP is initially translated in an apo form but is converted to a holo form upon transfer of a 4'phosphopantetheine (4'PP) group from CoA onto a conserved serine residue.[3, 28-30] This 4'PP group serves as the site of nascent fatty acid binding.[6]

The major feature of ACP is its four-helix bundle surrounding a hydrophobic central cavity. Acylated ACP houses the nascent fatty acid in this pocket, which can expand by slight conformation change to accommodate longer chain lengths.[3, 31]

Helix 2 of ACP serves as a recognition helix, where ACP binds mtFASII components. Since ACP must shuttle the acyl chain to several different enzymes, its association with each mtFASII component must be reversible. Thus, binding of ACP to mtFASII enzymes is weak.[3]

Mammalian ACP was originally identified as a subunit of complex I (CI) of the electron transport chain (ETC), and it has been found to copurify with CI.[3, 27, 28] Multiple other studies, however, have found that less than half of ACP is membrane-bound, and that ACP is mainly a soluble matrix protein.[29, 32, 33] It is noteworthy that in *Saccharomyces cerevisiae*, which have no CI, deletion of ACP1 also leads to a respiratory-deficient phenotype.[34, 35]

Roles of mtFASII

Lipoylation

Though mtFASII is conserved from mitochondria's bacterial origins, the reason for its conservation is not completely understood. Loss of mtFASII functionality does not alter the cell's overall lipid composition, indicating that mtFASII does not make a significant portion of the cell's fatty acids.[3, 14, 36] In yeast mitochondria, however, both Cem1p (KAS in humans) and ACP mutants showed changes in levels of cardiolipin and phosphatidylethanolamine, indicating that mtFASII may play a role in mitochondrial lipid content.[3, 14, 36] The inclusion of mtFASII products into phospholipids has not been shown.[3]

MECR, the last enzyme in the mtFASII pathway, can accommodate up to 16-carbon fatty acids, and rat liver mitochondria were shown to produce long-chain fatty acids.[3, 26, 37] Bovine mtFASII is known to synthesize at least 14-carbon fatty acids, while plant mitochondria have been shows to produce 16-carbon fatty acids.[2, 3, 32, 38] In several species, however, one of the main products of mtFASII was shown to be octanoic acid, which is a precursor for lipoic acid synthesis.[2, 3, 38] Most studies of mitochondrial fatty acid synthesis, however, have been limited to analysis of what fatty acids are still bound to ACP and are not able to identify what fatty acids have been released from ACP.

Lipoic acid is a prosthetic group that acts as a swinging arm on select mitochondrial proteins: the E2 subunits of pyruvate dehydrogenase, α-ketoglutarate dehydrogenase, and branched-chain α-ketoacid dehydrogenase, as well as the H protein of the glycine cleavage system.[9, 19, 39-41] In each case, the lipoic acid group interacts directly with the reaction intermediates, shuttling them between the components of the multienzyme complex to which the lipoic acid is bound.[39, 41]

Lipoic acid can be synthesized in either a *de novo* process or through a salvage pathway. In the *de novo* pathway, octanoic acid is added to H protein via octanoyl transferase (LIPT2) through an amide linkage on a lysine residue.[19, 39, 40] Next, two of octanoic acid's carbon atoms are replaced with sulfur atoms by lipoic acid synthase (LIAS).[39, 40, 42] These sulfur atoms then bind each other, forming a ring structure to which reaction intermediates attach.[40] After synthesis on H protein, lipoic acid can be transferred to E2 subunits of other enzymes by lipoyl transferase (LIPT1).[19, 40, 43] In the salvage pathway of lipoic acid synthesis, free lipoic acid from the diet is activated to lipoyl-GMP by lipoate activating enzyme (LAE) followed by transfer to the target protein via LIPT1.[41, 43]

Evidence for mtFASII's involvement in lipoic acid synthesis is extensive. When radiolabeled malonate, which exclusively feeds into mtFASII, was incubated with mitochondrial matrix extract, the tracer was seen attached to H protein, which is lipoylated.[2, 38, 44] In *E. coli*, radiolabel from octanoyl-ACP was later found in the lipoylation domain of the pyruvate dehydrogenase complex, again indicating that FASII-derived octanoate can serve as the precursor for lipoic acid synthesis.[45]

MtFASII enzymes are required for lipoic acid synthesis. Knockdown (KD) of ACP, PPT2, ACC, MCAT, and HSHTD2 have all been found to reduce protein lipoylation levels and overall cellular lipoic acid content.[3, 4, 6, 9, 10, 19, 34, 46, 47] The lipoylation defects of mtFASII mutants are not secondary to respiratory deficiency since other respiratory-deficient controls were analyzed as well, but no lipoylation defects were seen.[43, 46] Loss of lipoylation, either through mtFASII KD or

loss of lipoic acid attachment, reduces activity of TCA cycle enzymes that are normally lipoylated.[46]

Respiration

The mtFASII pathway is involved in mitochondrial respiration, as any knockdown of mtFASII components results in respiratory deficiency.[3, 6, 10, 19, 22, 48] This phenomenon is most comprehensively characterized in yeast, but deficiencies have also been noted in *Caenorhabditis elegans*, *Mus musculus*, *Neurospora crassa*, and *Homo sapiens.*[36, 46, 47, 49] MtFASII-deficient yeast are unable to grow on non-fermentable carbon sources, indicating a lack of oxidative phosphorylation (OXPHOS).[13, 14, 22, 36] Additionally, mtFASII mutants exhibit a loss of detectable cytochromes, which are necessary for electron transport chain function.[3, 6, 10, 14, 19, 22, 36] ACP KD in humans and deletion of the MECR homolog *etr1* in yeast resulted in reduced mitochondrial membrane potential, while mitochondria from *cem1* deletion yeast exhibited less oxygen consumption.[14, 46, 48] Respiratory deficiency in mtFASII mutant yeast, mammalian cells, and *N. crassa* translates to hindered cell growth rates, and ACP KD in mammalian cells was shown by MTT assay to reduce mitochondrial viability.[6, 12, 36, 46]

The general respiratory-deficient phenotype seen in mtFASII KDs is further evidenced by dysfunction of specific ETC complexes associated with mtFASII KD. The activities and expression of ETC complexes I and II are disturbed when mtFASII is nonfunctional. ACP KD was observed to elicit a 50% decrease in complex I activity and a 32% decrease in complex II activity.[46] The mtFASII-related loss of ETC function could be related to changes in assembly, expression, and activity of the ETC complexes. In *N. crassa*, assembly of complex I is altered when ACP is knocked down, resulting in a decrease in levels of some protein subunits.[3] Improper complex I assembly in mtFASII mutants could indicate that mtFASII proteins serve structural roles for the ETC.

An interesting connection between mtFASII and OXPHOS is the physical association of ACP with complex I. ACP copurifies with complex I, particularly the complex's peripheral arm.[27, 28] In *B. taurus*, the SDAP subunit of complex I was identified by sequencing to be acyl carrier protein.[32] Despite multiple identifications as a component of complex I, however, ACP has also been identified as a soluble matrix protein.[29, 33] It is likely that ACP has a membrane-bound form and a soluble form. In any case, ACP's close association with complex I suggests that ACP KD could affect complex I function.

In addition to direct influences on OXPHOS, mtFASII mutants exhibit phenotypes that are more loosely related with reduced mitochondrial respiration. Loss of mtDNA is known to result in OXPHOS dysfunction due to loss of mtDNA-encoded ETC subunits. In ACP KD yeast, mtDNA levels decrease.[6] Consistent with problems at the mtDNA level, expression of mtDNA-encoded COX genes is reduced in *etr1* mutants (MECR in humans), while nucleus-encoded COX subunits are not affected.[48] Additionally, mitochondrial RNA is not properly processed in mtFASII mutants, resulting in the accumulation of precursor tRNAs.[9]

Another link between mtFASII and respiratory function is protein lipoylation. One of mtFASII's most well described roles is in the synthesis of octanoate, which is used for lipoic acid synthesis. Several tricarboxylic acid (TCA) cycle enzymes are lipoylated, and this modification is required for their function. ACP KD results in decreased activity of pyruvate dehydrogenase, a lipoylated enzyme.[46]

Though most studies linking mtFASII and mitochondrial respiration were performed in yeast, there is one example of mtFASII mutation in a mammalian system. Deletion of MCAT, the malonyl-CoA transferase in mice, results in respiratory-deficient mitochondria and reduced complex I protein levels. Additionally, these mice have elevated lactate levels, little white adipose tissue, and problems with muscular strength and coordination. In addition to these mitochondrial-disease-like symptoms, MCAT KD mice have reduced protein lipoylation and octanoate synthesis, consistent with phenotypes seen in other mtFASII-deficient organisms.[47]

Mitochondrial morphology

Another consistent phenotype of mtFASII-deficient or –overexpressing cells is alterations in mitochondrial morphology. MtFASII-deficient mitochondria are known to have respiratory deficits, and mitochondria with respiratory deficits often have rudimentary morphology. Consistent with these data, yeast with knockdowns of *htd2* or *etr1*, which have respiratory deficits, also have rudimentary mitochondrial morphology.[3, 6, 10, 19, 22, 50] Additionally, *htd2* mutant yeast exhibit highly branched mitochondria compared to the shorter, thicker mitochondria of wild-type cells, perhaps indicating a deficit in mitochondrial fission.[19, 22]

Overexpression of *htd2* or *etr1* in yeast results in enlarged mitochondria with few or no cristae.[10, 19, 22, 50] In mice, overexpression of MECR in the heart elicited a similar effect—mitochondria were increased in size and number.[51] The molecular mechanism behind the changes in mitochondrial morphology with changes in mtFASII functionality is unknown.

RNA processing

The mtFASII pathway also functionally intersects with mitochondrial RNA processing. The mitochondrial genome (mtDNA) is polycistronic, with tRNAs interspersed between mRNAs and rRNAs.[52] Before translation of the various proteins encoded in mtDNA can occur, tRNAs must be cleaved out of the transcript by endonucleases, thereby releasing free mitochondrial mRNAs and rRNAs. Since tRNAs are interspersed between nearly every mtDNA gene in humans, tRNA processing is critical for mtRNA processing.[53] tRNAs are processed at the 5' end by mitochondrial RNase P (mtRNase P), and at the 3' end by mitochondrial RNase Z (mtRNase Z).[3, 53, 54] Without proper function of mitochondrial RNases, precursor tRNAs accumulate in the mitochondria, preventing the translation of mtDNA-encoded transcripts.[53, 55] Of particular interest is mtRNase P, which displays impaired function upon mutation of any mtFASII gene.[9]

In several species, mtRNase Ps are ribonucleoproteins, containing a protein component and a catalytic RNA component.[3, 19, 53] In yeast, the protein component is encoded in the nuclear genome by RPM2 and the catalytic RNA component is encoded in the mtDNA by RPM1.[3, 53] Interestingly, because RPM1 is encoded by the mtDNA, mtRNase P is required for its maturation, cleaving the 5' end of the downstream tRNA.[3] Defects in yeast mitochondrial RNA processing, then, can result in a positive feedback loop of impaired mtRNase P function.[19]

Despite the presence of catalytic RNAs in the mtRNase Ps of several species, human mtRNase P does not appear to have an essential RNA component; It was originally thought that nuclear RNase P was imported into the mitochondria in human cells.[19] It was later shown, however, that RNase P activity in the mitochondria differs in substrate specificity from nuclear RNase P activity.[54] Human mtRNase P was shown to be nuclease-resistant, and also exhibited protein-like density in a Cs_2SO_4 gradient rather than a ribonucleoprotein-like density.[55, 56] *In vitro* reconstitution of mtRNase P activity using only protein components demonstrated that human mtRNase P is indeed proteinaceous and lacks an RNA component.[55] Human mtRNase P is composed of three nuclear proteins, MRPP1-3, with MRPP3 harboring the catalytic site.[53, 55, 56]

The link between mtFASII and RNA processing was first observed in yeast. A screen of mtRNA processing-deficient yeast strains found that the most severe RNA processing defects were seen with the deletion of any mtFASII gene. Several mitochondrial tRNAs were observed to be improperly processed at the 5' end when any mtFASII gene was knocked down.[9, 48]

The enzymes of the yeast mtFASII pathway and mitochondrial RNA processing have been suggested to be part of a stable supercomplex that also includes the RNA degradosome. In analyzing purified mtRNAse P by liquid chromatography-mass spectrometry (LC-MS), several proteins were found to be associated with mtRNase P, including components of the TCA cycle and translation machinery.[57] MtFASII component Oar1p (KAR in humans) was also identified as a member of the mtRNase P-associated complex, and Htd2p (HSHTD2 in humans) and Mct1p (MCAT in humans) are also physically associated.[57] Deletion of the mtFASII component Oar1p

disrupts the formation of this complex, suggesting that the mtFASII pathway is necessary for complex formation.[53, 57]

Another interesting connection between RNA processing and mtFASII is that HSHTD2, which catalyzes the penultimate step of mtFASII, is bicistronic with RPP14, a component of nuclear RNase P.[3, 19] The RPP14 transcript contains two open reading frames (ORFs): a 5' ORF encoding the RPP14 protein and a 3' ORF encoding HSHTD2.[3, 21] The bicistronic nature of the RPP14 and HSHTD2 locus is notable because very few eukaryotic genes are bicistronic. In fact, only three other bicistronic genes are known to exist in the human genome.[3, 6] The bicistronic arrangement of RPP14 and HSHTD2 is conserved to *Trypanosoma brucei*, indicating that it may have functional importance.[3] In prokaryotes, polycistronic operons typically encode multiple functionally related genes, suggesting a functional link between RNA processing and mtFASII function.[21] It is curious, however, that HSHTD2 is bicistronic with a nuclear RNase P component rather than a mitochondrial RNase P component given the known association between mtFASII function and mitochondrial RNase P activity. Though mtFASII dysfunction is known to disrupt mitochondrial RNA processing, it has not been shown that mtFASII mutation also affects nuclear RNA processing.

Human disease

Mutations in the ACSF3 gene have been identified as the cause of combined malonic and methylmalonic aciduria (CMAMMA). Exome sequencing of CMAMMA patients revealed changes in ACSF3, including nonsense mutations and deletions.[11, 58] As ACSF3 mutant cells show metabolic dysfunction, CMAMMA symptoms are similar to those of mitochondrial diseases and include failure to thrive, acidosis, and neurological symptoms such as memory deficiencies, psychiatric illness, and seizure.[6, 11] Discovery of the genetic basis of CMAMMA demonstrates the importance of mtFASII in human health.

Another potential link between mtFASII and human disease stems from analysis of the human ortholog of yeast Oar1p. Unpublished sequence alignment data from our lab suggests that HADH2/ABAD is a human homolog of yeast Oar1p. ABAD was originally identified as a protein interacting with the Alzheimer's disease (AD)-related protein amyloid β. ABAD co-immunoprecipitates with amyloid β from AD brains, and the two proteins colocalize to the mitochondria. Structural studies of the protein-protein interaction revealed that binding of amyloid β to ABAD results in a distortion of ABAD's NAD-binding site. Preventing the ABAD-amyloid β interaction in cultured mouse neurons resulted in a decrease in cytochrome c release from mitochondria, indicating that the ABAD-amyloid β interaction results in mitochondrial stress. Additionally, ABAD transgenic mouse neurons exhibited greater reactive oxygen species (ROS) levels and DNA fragmentation when ABAD and amyloid β were allowed to interact. Interestingly, mice expressing both amyloid precursor protein and ABAD showed spatial learning deficits when compared to control mice and single-transgene mice. It is not clear whether ABAD's role in mtFASII is causal in the phenotypes observed with ABAD-amyloid β binding.[59]

Bacterial and mitochondrial signaling

Owing to their bacterial origins, mitochondria retain many bacterial characteristics, including the mtFASII pathway. One function of the bacterial FASII pathway is to create fatty acid-based signals used for communication between bacteria. This communication is called quorum sensing, an inter-bacterial signaling mechanism by which bacteria control population-dependent behaviors. Both gram-positive and gram-negative bacteria communicate through quorum sensing, with gram-positive bacteria using small peptides as signals and gram-negative bacteria typically using lipid signaling molecules.

Mitochondria are known to communicate with the nucleus using gram-positive bacteria-like, peptide-based signaling, but the mechanism and purpose of this signaling system are not

fully understood. Despite this gram-positive-like communication system, mitochondria are thought to be derived from gram-negative bacteria. Although gram-negative bacteria typically communicate using lipid molecules, some species are known to use both lipid and peptide signals.[60, 61] Because they are likely derived from gram-negative bacteria, mitochondria might employ a yet-to-be-discovered, lipid-based signaling pathway in addition to the known, peptide-based pathway. Because one function of bacterial fatty acid synthesis is the production of lipid molecules for quorum sensing,[62] it is possible that the mitochondrial equivalent, the mtFASII pathway, is also involved in a quorum sensing-like process.

Quorum sensing

Quorum sensing is a means of communication between bacteria, both within species and between species. Quorum sensing allows bacteria to exhibit population-wide behaviors such as bioluminescence, development of genetic competence, and virulence.[60, 63] In behaving as a population rather than as individuals, the bacteria increase their chance of success at a task, such as, in the case of virulence, at overcoming a host.[64] Quorum sensing was first discovered in the bioluminescent bacteria *Vibrio harveyi* and *Vibrio fischeri*, but the discovery of quorum sensing molecules in other species revealed that quorum sensing is a widespread phenomenon.[64, 65]

Generally, quorum sensing involves secretion and accumulation of a signaling molecule—typically *N*-acyl-homoserine lactones (AHLs) in gram-negative bacteria, and oligopeptides in gram-positive bacteria—in a population-dependent manner.[60, 61] As the bacterial population increases, the concentration of the quorum sensing molecule also increases. When the concentration of the quorum sensing molecule reaches a threshold, quorum sensing receptors activate, leading to enhanced transcription of quorum sensing-related genes, as well as genes linked to population-dependent behaviors.[60]

Quorum sensing in gram-negative bacteria

Quorum sensing in gram-negative bacteria is typically accomplished using AHLs as sensing molecules.[60] AHLs can differ in length of acyl chain and degree of saturation, with acyl chains ranging between four and 14 carbons long.[60, 64, 66, 67] Typically, each gram-negative bacterial species predominantly synthesizes one particular AHL, though other less abundant AHLs may also be present.[65, 68] Additionally, a single bacterial species may use multiple AHL signals for different quorum sensing cascades, so long as the two cascades are specific enough to differentiate between two different types of AHLs.[64, 69]

AHLs are synthesized by AHL synthases using acyl chains produced by the bacterial FASII pathway.[60, 64, 66, 70] AHLs are amphipathic molecules, with a more polar homoserine lactone ring and a hydrophobic acyl chain.[64] The amphipathic nature of AHLs allows them to both diffuse through the cell membrane and remain soluble in the extracellular environment.[60, 64, 65, 71] When the AHL concentration threshold is reached, AHLs bind a receptor, which then acts as a transcription factor for target genes.[60, 65, 72] Using *V. fischeri* as an example, a typical gram-negative bacterial quorum-sensing pathway is described below.

V. fischeri is a bioluminescent, gram-negative bacterium that colonizes host animals, such as squid, that have light-emitting organs.[64] The relationship is symbiotic: the bacteria benefit from the nutrient-rich environment within the host, while the host uses bioluminescence to avoid detection by prey or to attract a mate.[65]

V. fischeri's bioluminescence occurs in a population-dependent manner, with AHL concentration regulating luciferase expression.[64, 73] Two gene products, LuxI and LuxR, largely govern quorum sensing.[65] LuxI is the AHL synthase, using *S*-adenosylmethionine (SAM) and acyl-ACP as substrates.[65, 70, 74] LuxR acts as both the AHL receptor and as a transcription factor for the *luxICDABE* operon.[65, 72] At baseline, the *luxICDABE* operon is expressed at low levels.[65, 75] When the bacterial population density reaches a threshold, the AHL concentration is high

enough to stimulate significant levels of AHL binding to LuxR. Upon AHL binding, LuxR undergoes a conformational change, revealing a DNA-binding domain.[65, 76] The AHL-bound LuxR then binds and stimulates transcription of the *luxICDABE* operon.[72] Because the *luxICDABE* operon encodes the AHL synthase LuxI, LuxR-stimulated transcription starts a positive-feedback loop of AHL synthesis and operon transcription.[65]

Quorum sensing in gram-positive bacteria

Gram-positive bacteria also communicate through quorum sensing, but use oligopeptides as signaling molecules.[60, 63, 65] Because oligopeptides are not amphipathic like AHLs, signal peptides must be actively exported using ATP-binding cassette (ABC) transporters in order to accumulate in the extracellular environment.[60, 63, 65, 77] Quorum sensing peptides have an 18-27 amino acid-long double glycine (GG) leader sequence that is cleaved by the ABC transporter during export from the cell.[60, 61, 77]

Compared to gram-negative bacteria, gram-positive bacteria also have a more complex signaling mechanism for quorum sensing. Rather than having the signal peptide bind a protein that serves as both a receptor and transcription factor, gram-positive bacteria use a two-component signaling system.[63] In this system, the population-dependent accumulation of the quorum sensing peptide activates a histidine kinase receptor at the cell surface to autophosphorylate. The phosphorylation is transferred from the histidine kinase receptor onto a response protein, which binds DNA to promote transcription of target genes.[60, 61, 65, 78] Alternatively, the peptide can be imported and interact with an internal receptor to promote transcription of target genes. Typically, these genes encode the signal peptide itself, the ABC transporter gene, and genes regulating the population-dependent behavior.[61, 63, 78] Using *Bacillus subtilis* as an example, a typical gram-positive quorum sensing pathway is described below.

B. subtilis is a soil bacterium that uses quorum sensing to determine whether to develop genetic competence, which is the ability to take up exogenous DNA, or to sporulate, which occurs during nutrient starvation.[63, 65] There are two separate quorum sensing pathways in *B. subtilis*, one using a cell-surface receptor, and the other involving import of the signal for intracellular effects.

In the histidine kinase-mediated pathway, *B. subtilis* uses the 10 amino acid-long peptide ComX.[63, 79-81] ComX is transcribed in the cell, posttranslationally modified, and then exported.[65, 81, 82] When the extracellular threshold concentration of ComX is reached, ComX binds the ComP histidine kinase receptor.[78, 79, 83] Autophosphorylation of ComP results in phosphorylation of the transcription factor ComA, which stimulates transcription of the *comS* gene.[65, 78, 79, 81, 83-85] The ComS protein prevents proteolysis of ComK, which is a transcription factor promoting the development of genetic competence.[63, 86-90]

B. subtilis employs a second quorum sensing pathway that requires import of the signal peptide.[79] In this pathway, the signaling molecule is competence and sporulation factor (CSF), a pentapeptide cleaved from the PhrC protein.[63, 82, 91] Pre-pro-CSF is secreted from the cell, then cleaved by extracellular peptidase to generate mature CSF, which is imported back into the cell through the Spo0K ABC transporter.[63, 79, 82, 92-94] At low cell densities, CSF promotes ComA phosphorylation by inhibiting the RapC phosphatase, thereby promoting transcription of competence-development genes.[79, 82, 92, 94] CSF concentration rises with cell density; at high concentrations, CSF inhibits transcription of competence development genes through an unknown mechanism.[79, 92, 94] High CSF concentrations not only inhibit development of genetic competence, but also promote sporulation. At high concentrations, CSF inhibits the RapB phosphatase, allowing phosphorylation of the sporulation factor Spo0A, allowing transcription of sporulation-related genes.[79, 82, 91-95]

Quorum sensing crossover: gram-positive characteristics in gram-negative bacteria

Interestingly, the distinctions between the quorum sensing systems of gram-negative and gram-positive bacteria are not concrete. In a search across the genomes of several gram-negative and gram-positive bacteria, some gram-positive quorum sensing characteristics were found in gram-negative bacteria. For instance, multiple gram-negative species were found to have genes resembling those for gram-positive signal peptides.[60, 61] Additionally, genes for gram-positive-like ABC transporters, which contain a peptidase C39 domain to cleave the GG leader sequence of the signal peptide, were found in gram-negative bacterial genomes.[60, 61] A quorum sensing system in which a gram-negative bacterium uses a peptide signal is described below.

The gram-negative bacterium *E. coli* undergoes programmed cell death in a population-dependent manner using the pentapeptide extracellular death factor (EDF) as a signal.[96, 97] EDF is cleaved from the *zwf* and *ygeO* gene products and exported from the cell.[96, 98] When high-density *E. coli* populations experience a stressor such as inhibition of transcription or translation, UV irradiation, or oxidative stress, EDF promotes MazF toxin-mediated programmed cell death.[97-101] MazF is an endoribonuclease, inhibiting protein translation by cleaving single-stranded mRNAs.[97, 99, 102, 103] Under normal conditions, MazF is bound and inhibited by the antitoxin MazE.[97, 99, 101, 103, 104] EDF directly competes with MazE for MazF binding, and because EDF is produced in a population-dependent manner, EDF is more likely to out-compete MazE when *E. coli* populations are dense.[96-98, 105] EDF binding disinhibits MazF, allowing MazF to initiate programmed cell death.[97, 105] Because it is recognized by several bacterial species, EDF can be used by a dense bacterial population to kill off populations of competing species.[97] Additionally, because MazF-mediated cell death occurs subsequent to cell stressors, the pathway serves a quality-control purpose as well.

Bacterial-like signaling in mitochondria: the mitochondrial unfolded protein response (mtUPR)

The mitochondrial genome only encodes 37 genes, and the remaining roughly 1500 genes needed for mitochondrial function are encoded in the nuclear genome (nDNA). Most of the ETC complexes are composed of both mtDNA-encoded and nDNA-encoded proteins, so the balance of proteins encoded by these two genomes must be maintained to prevent accumulation of unassembled proteins. To avoid unfolded protein stress, mitochondria contain their own set of chaperones, including Hsp60 and mtHsp70.[106-108] When proteins fail to fold, or when the amount of unassembled or unfolded proteins exceeds the folding capacity of mitochondrial chaperones, the proteins are degraded by mitochondrial proteases such as Lon protease and ClpP.[106] The degradation of proteins by mitochondrial proteases triggers the mitochondrial unfolded protein response (mtUPR), a retrograde signaling cascade from the mitochondria to the nucleus. The mtUPR alleviates mitochondrial unfolded protein stress by upregulating mitochondrial chaperones and proteases, among other genes.[106, 108-110]

The endoplasmic reticulum (ER) also has its own unfolded protein response (ER-UPR), but it is distinct from the mitochondrial pathway. Mitochondrial stressors such as ethidium bromide treatment or deletion of the ABC transporter HAF-1 do not affect expression of ER-UPR-related genes.[111-113] Likewise, ER stressors such as tunicamycin and thapsigargin do not activate the mtUPR.[113] Additionally, the mtUPR is separate from cytosolic pathways, as heat shock induces cytosolic but not mtHsp70 upregulation, and mitochondrial stress results in upregulation of mitochondrial but not cytosolic Hsp70.[113]

The mtUPR in C. elegans

The mtUPR begins with mitochondrial stress, the most well studied being mitonuclear protein imbalance (Figure 2A). Since several mitochondrial proteins, including four of five ETC complexes, are complexes of mtDNA-encoded and nDNA-encoded proteins, the products of these two genomes must be kept in balance. A change in the expression of either genome

would result in protein complexes failing to form, causing the accumulation of unassembled proteins. For instance, in isolated mitochondria, mtDNA-encoded proteins are synthesized without import of additional nDNA-encoded mitochondrial proteins. As a result, the mtDNA-encoded proteins are left without their nDNA-encoded binding partners, resulting in accumulation of unassembled proteins. Radiolabel tracing of these mtDNA-encoded proteins in *Saccharomyces cerevisiae* found that they were largely degraded and exported from the mitochondria within 30 minutes.[114]

Typically, unfolded mitochondrial proteins are handled by mitochondrial chaperones, such as Hsp60 and mtHsp70.[115] When chaperones are unable to fold proteins, or when proteins are damaged, they are degraded by mitochondrial proteases including ClpP, Lon protease, SPG-7 (paraplegin), and YME1L1. Loss of mitochondrial chaperones induces mtUPR, while loss of mitochondrial proteases prevents mtUPR activation.[106, 110]

Many mitochondrial proteases are ATPase associated with diverse cellular activities (AAA) proteases acting in the inner mitochondrial membrane (i-AAA proteases) or the matrix (m-AAA proteases).[111, 115] MtUPR activation appears to be mediated largely by ClpP, as it is required for upregulation of mtUPR-associated genes.[106, 111, 112, 115] Loss of other mitochondrial proteases results in mitochondrial stress, which promotes mtUPR activation.[110]

Interestingly, respiratory deficiency, a common form of mitochondrial stress, does not clearly activate the mtUPR. Knockdown of ETC subunits does elicit mtUPR activation, but it is not clear if this is from mitochondrial dysfunction or accumulation of unassembled proteins.[110] Knockdown of TCA cycle enzymes, which leads to respiratory dysfunction, does not activate the mtUPR, however.[113] Also, the fact that 92.2% of peptides exported from the mitochondria are from matrix proteins rather than membrane-bound ETC proteins suggests that ETC complex degradation is not the main source of mtUPR activation.[112] Treatment with the uncoupler 2,4 dinitrophenol does not induce the mtUPR despite increased ROS levels, and treatment with the mitochondrial poison paraquat results in upregulation of Hsp60, but not mtHsp70.[113] Lon

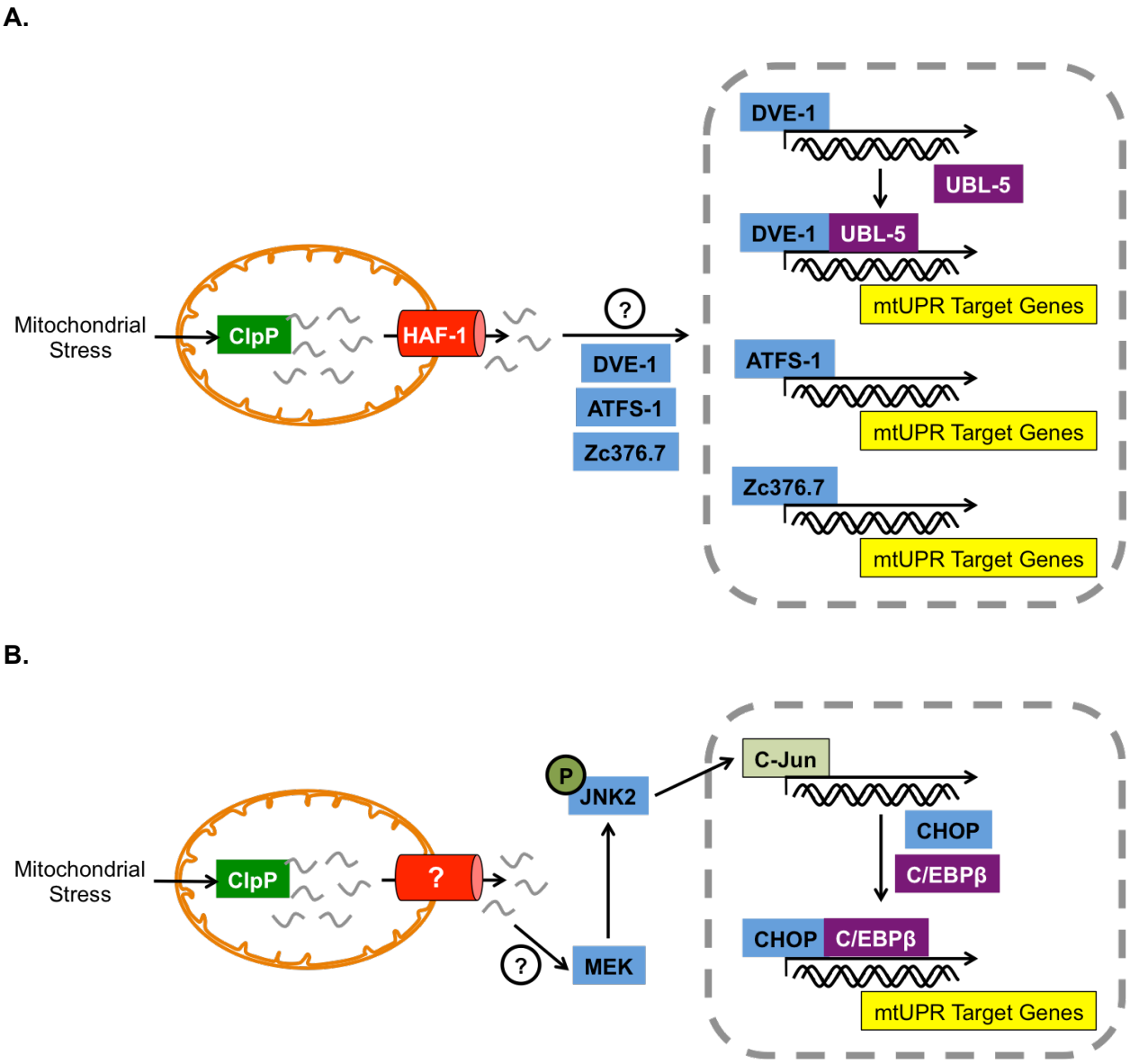

Figure 2. The mitochondrial unfolded protein response.
In A) *C. elegans* and B) mammals. Mitochondrial stress, such as mitonuclear imbalance, results in increased protein degradation by mitochondrial proteases. The resultant peptides are released from the mitochondria and, by an unknown mechanism, activate transcription factors that upregulate a variety of target genes. Adapted from Bernales et al, 2012.[108]

protease, which specifically degrades oxidized proteins, does not induce mtUPR when knocked down, indicating that protein oxidation is not necessarily an mtUPR stimulus.[110, 115]

Once proteins are degraded by mitochondrial proteases, the resultant small peptides are exported from the mitochondria. Peptide efflux from the mitochondria is required for mtUPR activation, and in *C. elegans*, it occurs via the ABC transporter HAF-1.[106, 112] Studies of the mitochondrial secretome show that mitochondria secrete peptides and amino acids within 30 minutes of the onset of mitochondrial stress.[112, 114] The peptides largely originate from matrix proteins, with a very small percentage consisting of mitochondrial membrane proteins.[112] Additionally, the peptides exported during mitochondrial stress are small, typically between six and 20 amino acids long.[112] These peptide lengths are consistent with peptides produced by ClpP: in *C. elegans*, ClpP degrades proteins to 8- to 20-amino acid peptides, while in *E. coli,* ClpP produces 6- to 8-amino acid peptides.[111, 115]

Once peptides are exported from the mitochondria, mtUPR-related transcription factors are activated by an unknown mechanism. There are multiple transcription factors that upregulate mtUPR genes during mitochondrial stress. The first two, DVE-1 and UBL-5, interact to mediate mtUPR-related gene expression. Initially, DVE-1 binds and promotes expression of the UBL-5 gene.[115] During mitochondrial stress, UBL-5 binds DVE-1, and the two proteins mediate upregulation of mtUPR-related genes.[111] Interestingly, HAF-1 mutation does not affect DVE-1 translocation to the nucleus, indicating that there are possibly multiple routes to upregulate mtUPR genes.[112, 115]

Activating transcription factor associated with stress 1 (ATFS-1) has both a mitochondrial targeting sequence and a nuclear localization signal, allowing its movement between the two organelles.[109, 110, 115] Under normal conditions, ATFS-1 is imported into the mitochondria and degraded by Lon protease.[106, 110] During mitochondrial stress, however, ATFS-1 translocates to the nucleus where it promotes upregulation of mtUPR-related genes.[109, 110, 115]

Another transcription factor in *C. elegans*, zc376.7, is also associated with mtUPR activation, but is not well studied. Zc376.7 is similar to mammalian ATF5, which is a stress-

induced transcription factor. Zc376.7 operates in a HAF-1-dependent manner and, like other mtUPR-related transcription factors, translocates to the nucleus during mitochondrial stress.[112]

Regardless of which transcription factor is employed, the mtUPR results in upregulation of genes that increase mitochondrial folding capacity: mitochondrial chaperones, mitochondrial proteases, mitochondrial protein import machinery, and ABC transporters.[110]

The mtUPR in mammals

The mammalian mtUPR pathway appears to function similarly to the *C. elegans* pathway, though the proteins involved differ somewhat. Briefly, mitochondrial stress results in increased proteolysis of mitochondrial proteins, followed by activation of transcription factors, and resulting in upregulation of mitochondrial chaperones and proteases (Figure 2B).[115-117] Many homologs of the mitochondrial proteases and chaperones employed in the *C. elegans* pathway are used in the mammalian pathway. These include AAA proteases such as ClpP and paraplegin, and chaperones such as Hsp60 and mtHsp70.[107, 115]

It has not yet been demonstrated, but it is likely that the mammalian mtUPR involves peptide export from the mitochondria in a way similar to the *C. elegans* mtUPR. In both *S. cerevisiae* and *C. elegans*, small peptides are exported from the mitochondria via ABC transporters, which are also found in mammalian mitochondria.[114, 118]

In *C. elegans*, there appears to be multiple routes to mtUPR activation through multiple transcription factors. In mammalian mtUPR, however, there is only one known route, through CCAAT-enhancer-binding protein homologous protein (CHOP) and CCAAT-enhancer-binding protein β (C/EBPβ).[106, 107, 109] As in *C. elegans*, the link between mitochondrial protein degradation and transcription factor activation is not known in mammals.[108, 115]

Upstream of CHOP, mitogen-activated protein kinase kinase (MEK) is required for mtUPR activation in mammals—its inhibition prevents mtUPR-related changes in gene expression.[119] MEK is known to phosphorylate c-Jun N-terminal kinase 2 (JNK2) during

mitochondrial unfolded protein stress.[109, 115, 119] JNK2 phosphorylation then leads to activation of c-Jun to bind activating protein 1 elements in the promoters for CHOP and C/EBPβ, leading to their upregulation.[108, 109, 115, 119] CHOP and C/EBPβ bind each other during stress and then bind the promoters of mtUPR-responsive genes, promoting their transcription.[106, 107, 109, 119]

Though CHOP is important for mtUPR activation, it is actually upregulated in a variety of conditions, including the ER-UPR, glucose deprivation, and DNA damage.[107] Additionally, CHOP promoter elements are relatively common in the genome.[117] The CHOP element alone, then, is not sufficient for transcription during the mtUPR.[117] For mtUPR-responsive transcription, CHOP elements must also be flanked by two mitochondrial unfolded protein response element (MURE) sites.[108, 109, 117] Though MURE sites are also common in the genome, the coincidence of CHOP and MURE sites in the same promoter is relatively rare, 1.8% of genes.[117] Of the genes whose promoters contain a CHOP element flanked by MURE sites, half are mitochondrial proteins encoded in the nucleus and include mtUPR-responsive genes for mitochondrial proteases, the complex I subunit NDUFB2, endonuclease G, and thioredoxin 2.[109, 117]

Sphingolipids: potential for mitochondrial signaling through lipids

Mitochondria are thought to be derived from a gram-negative bacterium. Since gram-negative bacteria typically participate in quorum signaling using lipid signaling molecules, it is possible that mitochondria might also signal to each other or to other parts of the cell using a lipid signal. While many types of lipids serve structural purposes, such as membrane phospholipids, other lipid molecules may also serve in a signaling capacity. These so-called "bioactive lipids" include sphingolipids, among others.

Sphingolipid structure and synthesis

Sphingolipids are a class of lipid molecules based on a sphingoid backbone. Sphingosine, one of the simplest sphingolipids, is an 18-carbon molecule. Sphingolipids play important roles in both cell membrane structure and organization as well as in cell signaling.

Sphingolipids can be categorized as either simple or complex. Simple sphingolipids include the sphingoid bases sphingosine and sphinganine, as well as ceramides. Sphingoid bases contain an 18-carbon backbone that is unsaturated, as in the case of sphingosine, or saturated, as in the case of sphinganine. Ceramides are composed of sphingosine attached to a fatty acyl chain, which can vary in length. Sphinganine can also be acylated, forming a dihydroceramide. In mammals, complex sphingolipids include sphingomyelins and glycosphingolipids. Sphingomyelins are ceramides linked to a phosphocholine or phosphoethanolamine head group, while glycosphingolipids include ceramides linked to glucose or galactose sugars.

Sphingolipid synthesis begins with the condensation of cytosolic serine and palmitoyl-CoA by serine palmitoyltransferase (SPT) to create 3-ketodihydrosphinganine (Figure 3).[120, 121] There are at least three isoforms of SPT (SPT1-3), all of which have an N-terminal domain in the ER lumen and a catalytic C-terminal domain facing the cytoplasm.[121] 3-ketodihydrosphinganine reductase (KHDR) then reduces 3-ketodihydrosphinganine to sphinganine, a sphingoid base.[120] Like SPT, KHDR is located at the ER, but its active site is in the cytosol.[121] Sphinganine is acylated to dihydroceramide by action of (dihydro)ceramide synthase (CerS), a reaction that requires acyl-CoA and is reversible via ceramidase. There are six CerS isoforms (CerS1-6), each with its own preference for acyl-CoA chain length. Thus, the expression pattern of CerS isoforms determines the prevalence of ceramides with a certain acyl chain length.[121] Dihydroceramide is desaturated by dihydroceramide desaturase to form ceramide, the sphingolipid upon which all complex sphingolipids are based, and from which sphingosine is derived.[120, 121]

Sphingomyelin synthesis occurs largely at the Golgi apparatus and begins with the transfer of a phosphocholine head from phosphatidylcholine onto ceramide, resulting in the release of diacylglycerol, an important signaling molecule.[120, 121] Ceramide can be reformed from sphingomyelin by the action of sphingomyelinases, which results in the release of phosphocholine.[121, 122] Sphingomyelinases appear in three varieties in mammals—acid, neutral,

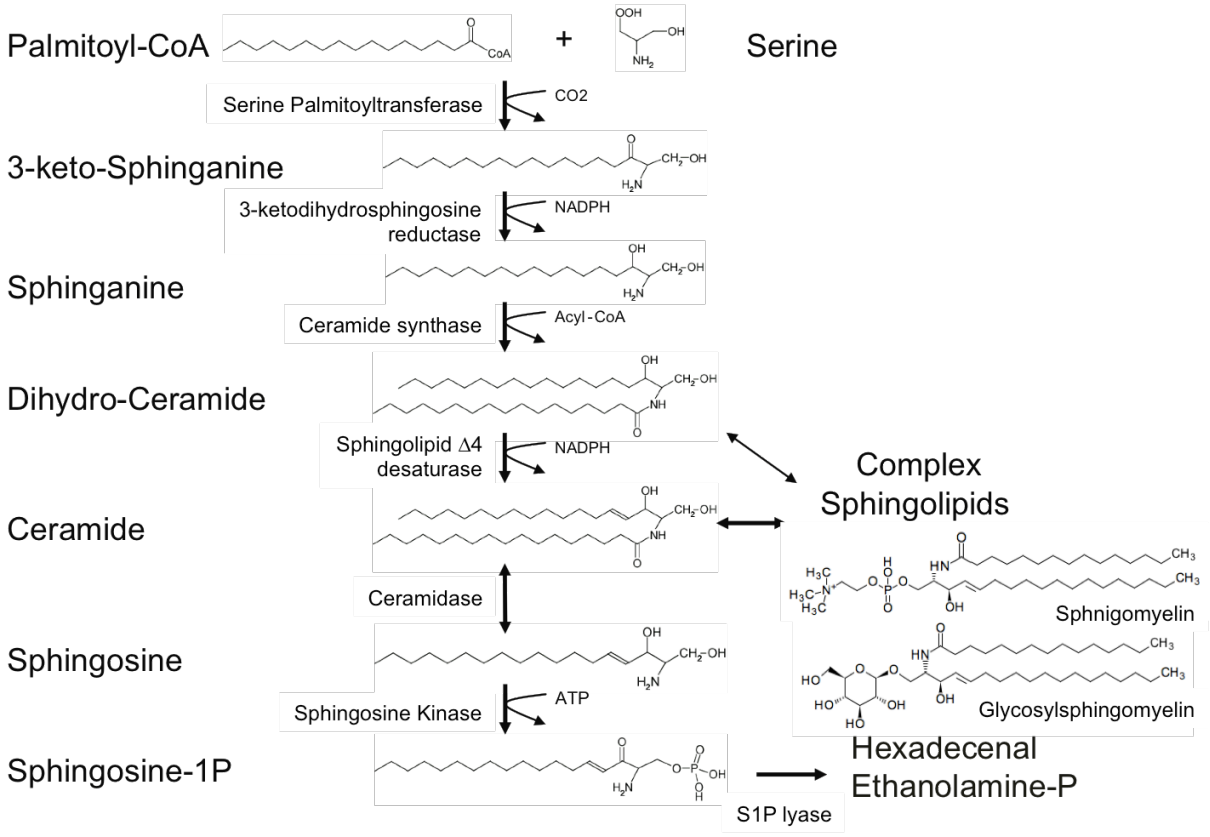

Figure 3. Synthesis and structures of sphingolipids.
Sphingolipid synthesis begins with the condensation of serine and palmitoyl-CoA by SPT. Complex sphingolipids, such as sphingomyelin and glycosylsphingomyelin, are synthesized using ceramide or dihydroceramide as a base. Sphingolipids are ultimately degraded by S1P lyase, producing hexadecenal and phosphoethanolamine. Adapted from Bertea et al, 2010[123] and Kanehisa et al, 2000.[124]

and alkaline—based on the pH at which the enzyme is most active.[121, 122] Sphingomyelinase activity occurs across the cell, as each of the three sphingomyelinases appears in a different subcellular compartment.[121, 122]

Glycosphingolipids can contain galactosyl or glucosyl moieties. Like sphingomyelin, glycosphingolipids are largely formed in the Golgi apparatus.[120] Addition of galactose to ceramide is catalyzed by ceramide galactosyltransferase (CGT), and addition of glucose occurs via ceramide glucosyltransferase. Reversal of galactosylceramide synthesis is catalyzed by

galactosylceramidase, and reversal of glucosylceramide synthesis occurs via glucosylceramidase. In the case of both sphingomyelin and glycosphingolipids, once synthesized in the Golgi apparatus, the lipids move through the secretory pathway to the plasma membrane, where they are involved in a variety of functions, which will be discussed later.[120]

A ceramide with a single glucose or galactose attached is termed a cerebroside. Globosides are glycosphingolipids in which a ceramide is linked to an oligosaccharide. Gangliosides, by contrast, are glycosphingolipids containing an oligosaccharide and sialic acid. Sulfatides are a class of galactosphingolipids containing a sulfur atom, which is added via galactosylceramide sulfotransferase.

While ceramide can be used as a building block upon which larger, more complex sphingolipids are made, ceramide's degradation products are also highly important in the cell. Sphingosine is made through the degradation of ceramide by ceramidases, which occur in acid, neutral, and alkaline forms.[120-122] The breakdown of ceramide into sphingosine also results in the release of a fatty acid. Sphingosine also forms a vital signaling molecule following its phosphorylation by sphingosine kinase to form sphingosine-1-phosphate (S1P).[122] S1P can then be dephosphorylated by lipid phosphate phosphohydrolases and S1P phosphohydrolases.[121] Eventually, all complex sphingolipids are broken back down to ceramide, then to sphingosine and/or S1P. The final event of sphingolipid catabolism occurs when S1P is irreversibly degraded by S1P lyase in the ER into hexedecenal and phosphoethanolamine.[121]

Because of the interconnected pathways that synthesize and degrade sphingolipids at all levels of complexity, there are multiple ways in which ceramide can be synthesized. First, as discussed previously, is the *de novo* pathway, in which ceramide is synthesized largely at the ER by a series of reactions beginning with the condensation of serine and palmitoyl-CoA by SPT.[120] Alternatively, ceramide can be generated via a salvage pathway, which includes the

degradation of more complex sphingolipids into ceramide, as well as the synthesis of ceramide from sphingosine, which is catalyzed by CerS.[122]

Sphingolipids as membrane organizers

Sphingolipids commonly partition into lipid rafts with cholesterol, other highly saturated phospholipids, and certain transmembrane proteins. Sphingolipid acyl chains tend to be more saturated and longer than those of other phospholipids, making the clustering of sphingolipids into rafts more energetically favorable. The high degree of sphingolipid acyl chain saturation enables more dense packing, causing the lipid raft to be less fluid than other parts of the membrane. Also, because of the increased length of raft lipid acyl chains, lipid rafts tend to be a thicker area of the cell membrane.

The changes in membrane fluidity and thickness that comes with the clustering of sphingolipids into lipid rafts help organize the membrane structurally as well as functionally. The decreased fluidity of lipid rafts confines raft proteins to a small area, allowing receptor dimerization, cross-linking, or association with scaffolding proteins. In this way, lipid rafts are important facilitators of signaling cascades. The change in membrane thickness at the border of the lipid raft induces membrane curvature, ultimately resulting in budding of the membrane and endocytosis.

The sphingolipid rheostat

Ceramide, sphingosine, and S1P are interconvertible, as evidenced by the fact that an increase in one of these molecules results in a concomitant decrease in others.[125-128] Because of their interconvertibility and opposing effects with respect to mitochondrial health and apoptosis, the balance between pro-apoptosis ceramide and anti-apoptosis S1P in the mitochondria determines whether or not mitochondria-initiated apoptosis will occur.

Ceramide treatment is anti-proliferative and pro-apoptotic.[129-134] Stressors such as TNFα and radiation increase ceramide concentrations.[122, 133, 135, 136] Additionally, ceramides

accumulate in the mitochondria of apoptotic cells.[122] Within the mitochondria, ceramides inhibit respiration through the electron transport chain, inhibiting complexes I, III, and IV, and consequently elevating ROS levels and reducing oxygen consumption.[122, 137-140] The mechanism by which ceramides inhibit the ETC is not known, but may be due to changes in the phospholipid composition and therefore membrane properties surrounding the ETC complexes.[122] Additionally, ceramides work with the pro-apoptosis protein Bax to form proteolipid pores in the mitochondrial membrane, dissipating the mitochondrial membrane potential and allowing for the release of cytochrome c.[122, 140, 141] Sphingosine, the product of ceramide breakdown, has similar effects on the mitochondria. Sphingosine treatment elicits respiratory impairment, reduction in the mitochondrial membrane potential, cytochrome c release, and ultimately apoptosis.[134, 138, 139, 142]

S1P is associated with not only preventing apoptosis, but also promoting proliferation.[134, 143-145] S1P protects against pro-apoptosis stimuli such as ceramide, irradiation, and TNFα.[125, 127, 130, 131, 134, 144-146] Additionally, S1P inhibits cytochrome c and Smac/DIABLO release and caspase cleavage.[145, 146] S1P levels are increased by a number of growth and pro-survival factors, including platelet-derived growth factor and nerve growth factor.[125, 127, 134, 143, 147] Typically, S1P levels are increased through stimulation of sphingosine kinase (SPHK) function, and in mitochondria, specifically by SPHK2. Loss of SPHK activity and, therefore, S1P, is associated with loss of mitochondrial membrane integrity and increased apoptosis rates.[127, 130, 134, 143, 148-150]

Sphingolipids as intracellular signaling molecules

Not only do sphingolipids support intracellular signaling through the formation of lipid rafts, but sphingolipids themselves often serve as signaling molecules. Ceramide is involved in a several signaling cascades, particularly stress-activated cascades. For instance, JNK stimulates sphingomyelinase activity, resulting in ceramide production,[151] and sphingomyelinase activity is needed for TNFα to signal through the peptidase cathepsin D.[152] Additionally,

ceramide stimulates downstream effects. Ceramide binds and activates proteins such as PP1, PP2A, and PKCζ.[153-155] Through these mediators, ceramide stimulates signaling cascades leading to activation of stress-activated protein kinases such as JNK as well as cell growth arrest and promotion of apoptosis.[131, 156-158]

Much of the research into S1P's signaling properties has been focused on S1P as a ligand for S1P receptors (S1PRs). There are five cell-surface S1PRs, which signal through a variety of G proteins, though all five receptor types signal through $G_{i/o}$.[134, 159, 160] As such, S1PR stimulation is associated with reduced cAMP levels and activation of MAP kinase.[130, 161, 162] S1PR activation is also associated with release of Ca^{2+} from intracellular stores in an IP3-independent manner, leading to activation of Rac and Rho GTPases.[134, 162-164] Interestingly, S1PR-related Ca^{2+} mobilization requires SPHK activity, indicating that intracellular S1P is also required for Ca^{2+} release.[161, 164]

While much of the research on S1P's signaling functions has focused on S1PRs, S1P also acts in a receptor-independent manner. In addition to its role in Ca^{2+} mobilization, intracellular S1P is involved in phosphatidic acid accumulation through activation of phospholipase D and DNA synthesis through p42/p44 MAP kinases, though it is possible that this effect is mediated through Edg receptors.[143, 161, 163, 165-167] Importantly, S1P is involved in regulation of apoptosis.[125, 127, 130, 131, 134, 144-146]

Links between sphingolipids and the mtUPR

Because sphingolipids are important for mitochondrial function and serve as signaling molecules, it is possible that mitochondria could use sphingolipids in a signaling capacity. Interestingly, mitochondrial signaling through the mtUPR is associated with lipid synthesis and signaling, as mtUPR induction upregulates acyl-CoA synthases, acyltransferases, phospholipase A2, SPT, lipoic acid synthase, and sphingomyelin synthase [110].

Another interesting connection between sphingolipids and the mtUPR is prohibitin (PHB). PHB1 and PHB2 interact with components of the m-AAA protease, as they co-elute in HPLC.[168] In addition to the m-AAA protease, the interactome of PHB2 includes the mitochondrial chaperone DNAJC19, inner mitochondrial membrane (IMM) translocases, and subunits of ETC complexes I, III, IV, and V.[169] Prohibitins may act as negative regulators of the m-AAA protease, as prohibitin knockout results in quicker degradation of m-AAA protease substrates.[168] The interaction of prohibitins and the m-AAA protease is required for survival, as knockout of both at the same time, but not of one at a time, results in cell death in *S. cerevisiae*.[168]

Importantly, PHB2 binds S1P, an interaction that is required for PHB2's effects on complex IV assembly and function.[170] Though a definitive link has not been demonstrated, PHB2 is poised to link sphingolipid metabolism with mitochondrial signaling through the mtUPR.

Conclusions

The mtFASII pathway is an independent, intramitochondrial source of fatty acids. While involving the same set of reactions as the cytosolic pathway, mtFASII more closely resembles the bacterial FASII pathway, with each of the pathway's reactions being conducted by a separate enzyme. The exact reason for the conservation of the mtFASII pathway, given that the FASI pathway provides the bulk of the cell's fatty acids, is not fully understood. The mtFASII pathway does have roles in providing octanoate for protein lipoylation, in supporting mitochondrial ETC function and proper morphology, and in mitochondrial RNA processing. Based on work described in the following chapters, mtFASII may also play a role in mitochondrial signaling through lipid and peptide means. It is possible that signaling related to mtFASII is related to bacterial quorum sensing, as both mtFASII-related signaling and quorum sensing employ both lipid and peptide molecules as signals. To investigate the roles of the mtFASII pathway and any potential links to mitochondrial signaling, our work explores the

metabolomic changes associated with altered mtFASII function at both the whole-cell and mitochondrial levels. Additionally, we explore mtFASII's contributions to mitochondrial secretions, or the mitochondrial secretome.

Hypotheses

The mtFASII pathway appears to contribute little to cellular lipid content, yet it is highly conserved. To better understand the role of mtFASII in the cell, we used a variety of methods to characterize the consequences of changes in mtFASII functionality in whole cells, isolated mitochondria, and mitochondrial secretions. We altered mtFASII functionality by knockdown of acyl carrier protein (ACP) or overexpression of mitochondrial trans-2-enoyl-CoA reductase (MECR). As a control for known respiratory deficits in mtFASII knockdowns, we also knocked down a component of complex I of the electron transport chain. In light of the known effects that altering mtFASII pathway function has on cellular respiratory function, we hypothesized that our ACP knockdown cells would exhibit signs of respiratory dysfunction, but that MECR overexpression cells would remain healthy. Based on previous research from our laboratory that suggests a role for the mtFASII pathway in intracellular communication,[25] we believed that altering mtFASII pathway functionality might also have effects on intracellular signaling molecules, though the identities of those molecules were unknown.

CHAPTER II

ALTERING THE MITOCHONDRIAL FATTY ACID SYNTHESIS II (MTFASII) PATHWAY MODULATES CELLULAR METABOLIC STATES AND BIOACTIVE LIPID PROFILES AS REVEALED BY METABOLOMIC PROFILING (CLAY ET AL., 2016)[171]

Abstract

Despite the presence of a cytosolic fatty acid synthesis pathway, mitochondria have retained their own means of creating fatty acids via the mitochondrial fatty acid synthesis (mtFASII) pathway. The reason for its conservation has not yet been elucidated. Therefore, to better understand the role of mtFASII in the cell, we used thin-layer chromatography to characterize the contribution of the mtFASII pathway to the fatty acid composition of selected mitochondrial lipids. Next, we performed metabolomic analysis on HeLa cells in which the mtFASII pathway was either hypofunctional (through knockdown of acyl carrier protein, ACP) or hyperfunctional (through overexpression of mitochondrial enoyl-CoA reductase, MECR). Our results indicate that the mtFASII pathway contributes little to the fatty acid composition of the mitochondrial lipid species examined. Additionally, loss of mtFASII function results in changes in biochemical pathways suggesting alterations in glucose utilization and redox state. To ensure that these results were not simply due to respiratory deficiency, we also analyzed complex I knockdown cells. A lack of correlation between metabolite changes with mtFASII alteration and complex I knockdown indicate that mtFASII has functions outside its role in promoting mitochondrial respiration. Interestingly, levels of bioactive lipids, including lysophospholipids and sphingolipids, directly correlate with mtFASII function, indicating that mtFASII may be involved in the regulation of bioactive lipid levels. Regulation of bioactive lipid levels by mtFASII would indicate the pathway is not only a source of mitochondrial fatty acids, but also serves as an important mediator of intracellular signaling pathways.

Introduction

Mitochondria are cellular organelles with a bacterial evolutionary lineage. Despite the time since their last common ancestor, mitochondria retain many bacterial characteristics. One conserved, bacteria-like feature of mitochondria is their fatty acid synthesis (mtFASII) pathway (Figure 1).[15, 26, 172] Similar to the bacterial fatty acid synthesis pathway, mtFASII synthesizes fatty acids using a series of enzymes, whereas the eukaryotic cytosolic system for fatty acid synthesis (FASI) uses a single multifunctional enzyme, fatty acid synthase. In light of the presence of FASI, the reason for the conservation of the mitochondrial pathway is unknown. Likewise, the complete identities and uses of mtFASII products in mammalian cells are not yet known.

In the mitochondria, fatty acids are synthesized from the precursor molecules malonate, malonyl-CoA, and acetyl-CoA, and their elongation into fatty acids requires ATP and NADPH.[173, 174] The mtFASII pathway is capable of synthesizing fatty acids with acyl chains up to at least 14 carbons long (myristic acid) in mammalian cells, and in other species, mtFASII can synthesize fatty acids up to 16 carbons in length (palmitic acid).[2, 3, 175] The one known destination of mtFASII products is in the creation of lipoic acid. To create lipoic acid, lipoyl synthase uses octanoic acid from the mtFASII pathway and S-adenosyl methionine.[2, 38] Lipoic acid serves as a cofactor for many enzymes, including pyruvate dehydrogenase, α-ketoglutarate dehydrogenase, and the branched chain oxoacid dehydrogenase. Therefore, knockdown of mtFASII components results in reduced cellular lipoic acid content and protein lipoylation levels.[12, 34] Application of exogenous lipoate does not alleviate the effects of mtFASII knockdown on protein lipoylation, indicating that a mitochondrial origin of fatty acids may be required for lipoylation to occur.[46]

Whether through the direct impact of the fatty acids produced, downstream consequences of fatty acid synthesis, or dual roles of mtFASII enzymes, the mtFASII pathway is important for maintaining mitochondrial health and function. Expression of mtFASII proteins in

mammals correlates by tissue with mitochondrial activity, and loss of any mtFASII enzyme in mammals or yeast results in mitochondrial dysfunction.[12, 15, 23] Alteration of mtFASII function by deletion or knockdown of its components results in respiratory deficiency,[14, 22, 34, 36, 46, 176] increased reactive oxygen species (ROS),[46] rudimentary mitochondria with abnormal morphology,[22, 23] and slowed cell growth.[22, 46] In addition, deletion of any mtFASII component in yeast results in impaired mitochondrial tRNA processing by mitochondrial RNaseP.[9, 177]

ACP is integral to mtFASII as the mode of transport for nascent fatty acids between the mtFASII enzymes (Figure 1). To begin the mammalian mtFASII pathway, malonate is transferred to CoA by the acyl-CoA synthetase ACSF3,[12] and then to ACP by malonyltransferase (MCAT).[29, 44, 173, 178] Fatty acids remain bound to ACP by a thioester bond throughout chain elongation.

In addition to a soluble form in the mitochondrial matrix, ACP has been identified as a component of complex I of the electron transport chain (ETC), and is important for the activity of complex I (CI).[27, 29] ACP knockdown in mammals results in decreased expression of several CI subunits, reduced CI assembly, and loss of CI function.[36, 46] The effects of ACP knockdown are consistent with knockdown of other mtFASII genes, as cells exhibit respiratory insufficiency and slowed cell growth.[34, 46] Loss of mitochondrial function is evidenced by a reduced mitochondrial membrane potential and increased presence of ROS.[46]

Mitochondrial enoyl-CoA reductase (MECR), the last enzyme in the mtFASII pathway (Figure 1), is a 2-enoyl thioester reductase that acts as a dimer, with a pocket forming between the two monomers that can accommodate fatty acid chains up to 16 carbons in length.[23, 26] Like other mtFASII proteins, MECR is a mitochondrial matrix protein, and cannot perform its function outside the mitochondria.[23] Upregulation of MECR has been shown to cause activation of the PPARα transcription pathway, either through its role as a coactivator or through increased mtFASII activity.[24, 25]

Given the lingering questions concerning the role of mtFASII in the cell, we sought to identify potential functions of mtFASII through knockdown of ACP (ACP KD), and by promoting mtFASII function through MECR overexpression (MECR OX) in HeLa cells. Here, we demonstrate that the mtFASII pathway contributes little, if anything, to the fatty acid composition of selected mitochondrial lipids. Metabolomics analysis of ACP KD and MECR OX cells revealed the identities of biochemicals altered by mtFASII loss or upregulation, providing insight into the important roles this pathway plays in the cell. We show that altering the mtFASII pathway causes corresponding changes in cellular metabolic state, and a shift between glycolysis and anaerobic respiration. We compare the metabolic profile of ACP KD cells to that of CI KD cells, and demonstrate that changes seen in ACP KD cells are not simply due to respiratory deficiency. Additionally, manipulation of the mtFASII pathway alters cellular levels of bioactive lipids, including lysophospholipids and sphingolipids, pointing to a possible role for mtFASII in lipid signaling and remodeling.

Experimental Procedures

Cell culture conditions and siRNA-mediated RNA knockdown

All cell cultures were maintained at 37 ˚C and 5% CO_2. HeLa cells were plated in 10-cm cell culture dishes (CellTreat) at a density of 1.5×10^5 cells/mL in DMEM + 10% FBS (Mediatech, Gibco). Knockdown of the mtFASII pathway was achieved using Qiagen Flexitube siRNAs specific for the gene for ACP (*NDUFAB1*), and knockdown of CI was achieved using siRNAs against *NDUFS3*. Control cells were transfected with Allstars negative control siRNA (Qiagen). Additionally, as a negative control, cells were transfected with siRNAs specific for *METTL9*, a nuclear gene encoding a mitochondrial protein. HeLa cells were transfected with siRNA using HiPerfect Transfection Reagent (Qiagen). In order to maintain the knockdown, cells were re-transfected after 48 h: cells were trypsinized, resuspended in double their original volume of DMEM + 10% FBS, then plated in a 15-cm dish for an additional 48 h. At 96 h, cells

were harvested by trypsinization and centrifugation. Knockdown efficiency was measured after 96 h using real time quantitative RT-PCR.

MECR plasmid construction

To create the MECR OX plasmid, the entire open reading frame of *Mecr* was amplified from mouse cDNA using primers
5'- CCAGATCTGCCGCCACCATGGTGGTCAGCCAGCGAGTG-3' and
5'-TGGAGAGATCTCATGGTGAGAATCTGCTTCG-3'. The resulting PCR product was cloned into the pCR2.1 vector using the TA cloning kit (Invitrogen) to create pMecr-TA. A FLAG epitope tag was created at the C terminus of *Mecr* by annealing complementary oligonucleotides
5'-GATCCACCATGGATTACAAGGATGACGTACGATAAGA-3' and
5'-GATCTCTTATCGTCGTCATCCTTGTAATCCATGGTG-3' and ligating the resulting product into the pMecr-TA vector that had been digested with BglII, creating pMecr-flagTA. The region encoding MECR-flag was then removed by digestion with EcoRI and BglII, and cloned into pSG5 (Agilent Technologies, Inc), creating a plasmid expressing *Mecr* under the control of the SV40 promoter.

Cell culture conditions and plasmid-mediated MECR overexpression

All cell cultures were maintained at 37˚C and 5% CO_2. HeLa cells were plated in 10-cm cell culture dishes (CellTreat) at a density of 1.5×10^5 cells/mL in DMEM + 10% FBS (Mediatech, Gibco). After 24 h, MECR OX was achieved by transfecting cells with the pSG5 vector with cloned-in MECR under SV40 promoter control. Control cells received an equal amount of empty pSG5 vector (Agilent Technologies, Inc). HeLa cells were transfected using FuGENE transfection reagent (Promega). After an additional 24 h, cells were harvested by trypsinization and centrifugation. MECR OX was confirmed using real-time quantitative RT-PCR.

Real time quantitative RT-PCR

Total RNA was isolated using TRIzol Reagent (Life Technologies) according to manufacturer's protocols. First-strand cDNA was created from total RNA using SuperScript® III First-Strand Synthesis SuperMix for quantitative RT-PCR (Life Technologies). Quantitative RT-PCR was performed using TaqMan Expression Assays (Life Technologies) on the ABI 7900 platform according to manufacturer's protocols.

Western blotting

Whole-cell protein was isolated using RIPA buffer according to manufacturer's protocol (Sigma-Aldrich). Protein was then blotted using 12% Bio-Rad precast gels and PVDF membranes. To indicate protein lipoylation levels, an anti-lipoate antibody was used. To detect levels of electron transport chain proteins, an OXPHOS antibody cocktail (MitoSciences MS604) was used.

Mitochondrial isolation for thin layer chromatography

Mitochondria from HeLa cells were harvested using the MACS Mitochondria Isolation Kit (Miltenyi) according to manufacturer's protocol. Briefly, approximately 10^7 HeLa cells were washed and lysed, then incubated with magnetic beads linked to an anti-TOM22 antibody, which binds the outer surface of the mitochondria. The mitochondria-linked beads were passed through a column in a magnetic field, retaining the beads and mitochondria. Upon removal from the magnetic field, isolated mitochondria were then flushed from the column.

Thin-layer chromatography-gas chromatography

Lipids were extracted using the method of Folch-Lees.[179] Individual lipid classes were separated by thin-layer chromatography using Silica Gel 60 A plates developed in petroleum ether, ethyl ether, acetic acid (80:20:1) and visualized by rhodamine 6G. Phospholipids were scraped from the plates and methylated using BF_3/methanol as previously described.[180] The

methylated fatty acids were extracted and analyzed by gas chromatography. Gas chromatographic analyses were carried out on an Agilent 7890A gas chromatograph equipped with flame ionization detectors, a capillary column (SP2380, 0.25 mm × 30 m, 0.25 μm film, Supelco, Bellefonte, PA). Helium was used as a carrier gas. The oven temperature was programmed from 160°C to 230°C at 4°C/min. Fatty acid methyl esters were identified by comparing the retention times to those of known standards. Inclusion of dipentadecanoyl phosphatidylcholine (C15:0) in the samples permitted quantitation of total phospholipid in the sample.

Metabolomics

Sample preparation and metabolic profiling

Sample preparation and metabolic profiling were performed on samples of 5×10^6 HeLa cells. The untargeted metabolic profiling platform employed for this analysis was performed by Metabolon (Durham, NC) and combined three independent platforms: ultrahigh performance liquid chromatography/tandem mass spectrometry (UHLC/MS/MS) optimized for basic species, UHLC/MS/MS optimized for acidic species, and gas chromatography/mass spectrometry (GC/MS). Samples were processed as previously described.[181-184] Cells were homogenized in a minimum volume of water, and 100 μL was withdrawn for subsequent analyses. Using an automated liquid handler (Hamilton LabStar, Salt Lake City, UT), protein was precipitated from the homogenized cells with methanol that contained four standards to report on extraction efficiency. The resulting supernatant was split into equal aliquots for analysis on the three platforms. Aliquots, dried under nitrogen and vacuum-desiccated, were subsequently either reconstituted in 50 μL 0.1% formic acid in water (acidic conditions) or in 50 μL 6.5 mM ammonium bicarbonate in water, pH 8 (basic conditions) for the two UHLC/MS/MS analyses, or derivatized to a final volume of 50 μL for GC/MS analysis using equal parts bistrimethyl-silyl-trifluoroacetamide and solvent mixture acetonitrile:dichloromethane:cyclohexane (5:4:1) with

5% triethylamine at 60°C for one hour. In addition, three types of controls were analyzed in concert with the experimental samples: samples generated from pooled experimental samples served as technical replicates throughout the data set, extracted water samples served as process blanks, and a cocktail of standards spiked into every analyzed sample allowed instrument performance monitoring.

For UHLC/MS/MS analysis, aliquots were separated using a Waters Acquity UPLC (Waters, Millford, MA) and analyzed using a linear trap quadrupole (LTQ) mass spectrometer (Thermo Fisher Scientific, Inc., Waltham, MA), which consisted of an electrospray ionization (ESI) source and linear ion-trap (LIT) mass analyzer. The MS instrument scanned 99 to 1000 *m/z* and alternated between MS and MS^2 scans using dynamic exclusion with approximately 6 scans per second. Derivatized samples for GC/MS were separated on a 5% phenyldimethyl silicone column with helium as the carrier gas and a temperature ramp from 60°C to 340°C, and then analyzed on a Thermo-Finnigan Trace DSQ MS (Thermo Fisher Scientific, Inc.) operated at unit mass resolving power with electron impact ionization and a 50 to 750 atomic mass unit scan range.

Metabolite identification and data analysis

Metabolites were identified by automated comparison of the ion features in the experimental samples to a reference library of chemical standard entries that included retention time, mass-to-charge ratio (*m/z*), preferred adducts, and in-source fragments as well as associated MS spectra, and curated by visual inspection for quality control using software developed at Metabolon.[185]

Experimental samples and controls were randomized across a one-day platform run. Any missing values were assumed to be below the limits of detection. Therefore, for statistical analyses and data display purposes, these values were imputed with the compound minimum (minimum value imputation). Statistical analysis of log-transformed data was performed using

"R" version 2.14 (http://cran.r-project.org/), which is a freely available, open-source software package. Welch's t-tests were performed to compare data between experimental groups. Multiple comparisons were accounted for by estimating the false discovery rate (FDR) using q-values.[186] Metabolites were deemed significantly changed when $p \leq 0.05$, and metabolites were considered to have trending changes when $0.05 < p < 0.10$.

Glucose assay

Cell culture media content was assayed using a Beckman glucose analyzer (Beckman Instruments, Fullerton, CA), which is accurate to 450 mg/dL. The assay used was the glucose oxidase method.[187] The reaction sequence is

(1) ß-D-glucose + O_2 $\xrightarrow{\text{glucose oxidase}}$ gluconic acid + H_2O_2

(2) H_2O_2 + ethanol $\xrightarrow{\text{catalase}}$ acetaldehyde + H_2O

(3) $H_2O_2 + 2H^+ + 2I^-$ $\xrightarrow{\text{molybdate}}$ $I_2 + H_2O$

In this assay, glucose concentrations are proportional to oxygen consumption rates. Media glucose concentrations were determined by comparing the samples' oxygen consumption rate to that of a standard solution. Each sample was measured four times, using 10 µL of sample per reading.

Lactate assay

Levels of lactate in the medium of ACP KD and MECR OX cells and controls were measured using the Lactate Colorimetric Assay Kit (Biovision) at 96 h (ACP KD) or 24 h (MECR OX) after transfection. At least three independent samples of each cell state (ACP KD, MECR OX, or control) were assayed in triplicate.

Sphingolipid analysis using liquid chromatography-tandem mass spectrometry (LC-MS/MS)

Sphingolipid extraction from HeLa cells

Sphingolipid extraction was carried out as previously described.[188] Samples were first spiked with a set of sphingolipid standards, and then underwent single-phase lipid extraction using ethyl acetate:iso-propanol:water at a ratio of 60:30:10 by volume. After extraction, samples were dried under nitrogen gas and resuspended in 150 µL 1 mM ammonium formate in methanol + 0.2% formic acid.

Liquid chromatography-tandem mass spectrometry for sphingolipid levels

LC-MS/MS was performed as previously described.[188] Briefly, samples were analyzed by LC-MS/MS using an Agilent-1100 (Agilent Technologies) HPLC pump equipped with an Agilent-1100 (Agilent Technologies) autosampler, and a Thermo Finnigan TSQ 7000 (Thermo Fisher Scientific) triple quadrupole mass spectrometer with an Electrospray Ion Source (ESI) and syringe pump. LC was carried out using a Spectra C8SR column (Peeke Scientific, Redwood City, CA), 150 × 3.0 mm with a 3-mm particle size. Samples underwent a full scan using tandem mass spectrometry, and sphingolipids were identified by their decomposition signatures. Data was processed using the instrument's data handling software.

ELISA for sphingosine-1-phosphate

Sphingosine-1-phosphate (S1P) levels were determined in ACP KD cells (96 h) using the S1P ELISA Kit (Echelon Biosciences) according to manufacturer's protocol. Protein concentrations in each sample were first determined using BSA protein assay (Bio-Rad) according to manufacturer's protocol. Samples were assayed in triplicate using 40 µg protein per well.

Results

The goal of this study was to explore the cellular role of the fatty acids produced by the mtFASII pathway. To accomplish this, siRNA was used to knockdown the expression of the gene encoding ACP (*NDUFAB1*) (Figure 4A). Knockdown of *NDUFAB1* resulted in defective lipoylation of proteins, consistent with defects in the mtFASII pathway (Figure 4B). Western blot analysis with an antibody cocktail for several proteins involved in oxidative phosphorylation showed decreased levels of UQCRC of complex III, MTCOI of complex IV, SDH3 of complex II, and NDUFB8 of CI, but not ATP5A of complex V (Figure 4C). This result is consistent with selective loss of OXPHOS enzyme subunits in the mtFASII knockout mice.[47] To evaluate the contribution of the mtFASII pathway to the fatty acid profile of mitochondria, lipids were extracted from mitochondria isolated from control and ACP KD cells. Individual lipid classes were isolated by TLC, and the fatty acid side chain lengths were determined by gas chromatography. No changes in fatty acid composition were observed in neutral phospholipids, triglycerides, or free fatty acids (Figure 5).

The lack of changes in the major pools of fatty acids in mitochondrial polar lipids, triglycerides, and free fatty acids suggested that determining the role of mtFASII products in the cell required a more agnostic approach. To this end, we performed an untargeted metabolomics study of cells with downregulated or upregulated mtFASII function. Downregulation was again achieved by knockdown of the gene encoding ACP, while upregulation was achieved by overexpressing the gene encoding MECR, a system that has been previously characterized.[25] Additionally, to distinguish between phenotypes due ACP KD and phenotypes due to respiratory deficiency, NDUFS3, a subunit of CI of the ETC, was knocked down (CI KD). For ACP KD and MECR OX, six independent samples from each condition were extracted and analyzed using a combination of three independent platforms: UHLC/MS/MS optimized for basic species,

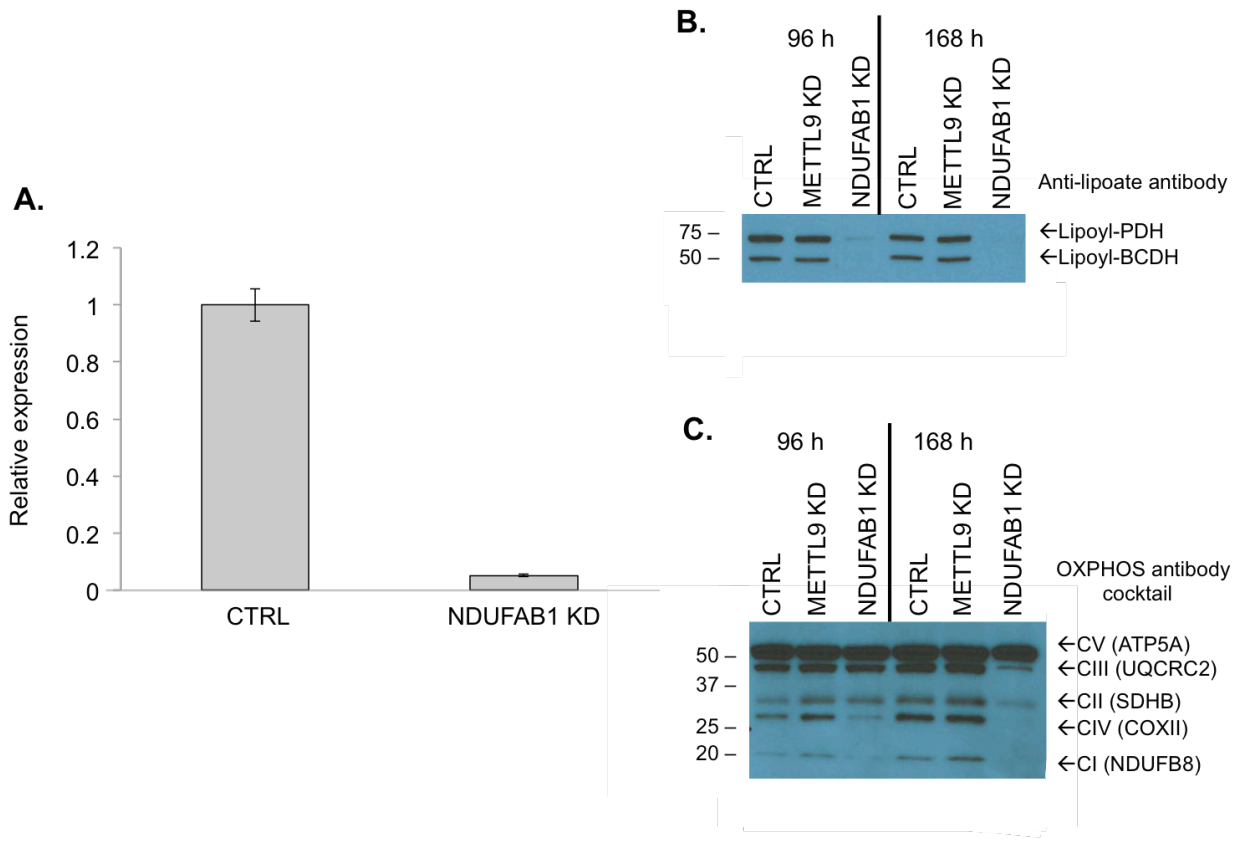

Figure 4. Characterization of ACP KD.
A) Relative expression of ACP in control siRNA-treated and ACP siRNA-treated cells as measured by Taqman assay. B) Representative western blot using anti-lipoate antibody to compare protein from control siRNA-treated, negative control METTL9 siRNA-treated, and ACP siRNA-treated cells at 96 h and 168 h. C) Representative western blot using OXPHOS antibody cocktail to compare protein from control siRNA-treated, negative control METTL9 siRNA-treated, and ACP siRNA-treated cells at 96 h and 168 h. Data courtesy of A. Parl.

UHLC/MS/MS optimized for acidic species, and GC/MS. For CI KD samples, five independent samples were extracted and analyzed in the same manner as ACP KD and MECR OX cells. For ACP KD and MECR OX, a total of 296 biochemicals were measured by these three independent platforms; for CI KD, 435 biochemicals were measured. A total of 115 biochemicals were significantly altered ($p \leq 0.05$) in ACP KD, and levels of 57 biochemicals were altered in the MECR OX cells (Table 1). Of the biochemicals that were significantly altered in both

upregulation and downregulation of the mtFASII pathway, 29 were altered in opposite directions, and seven were altered in the same direction, supporting the idea that the two model

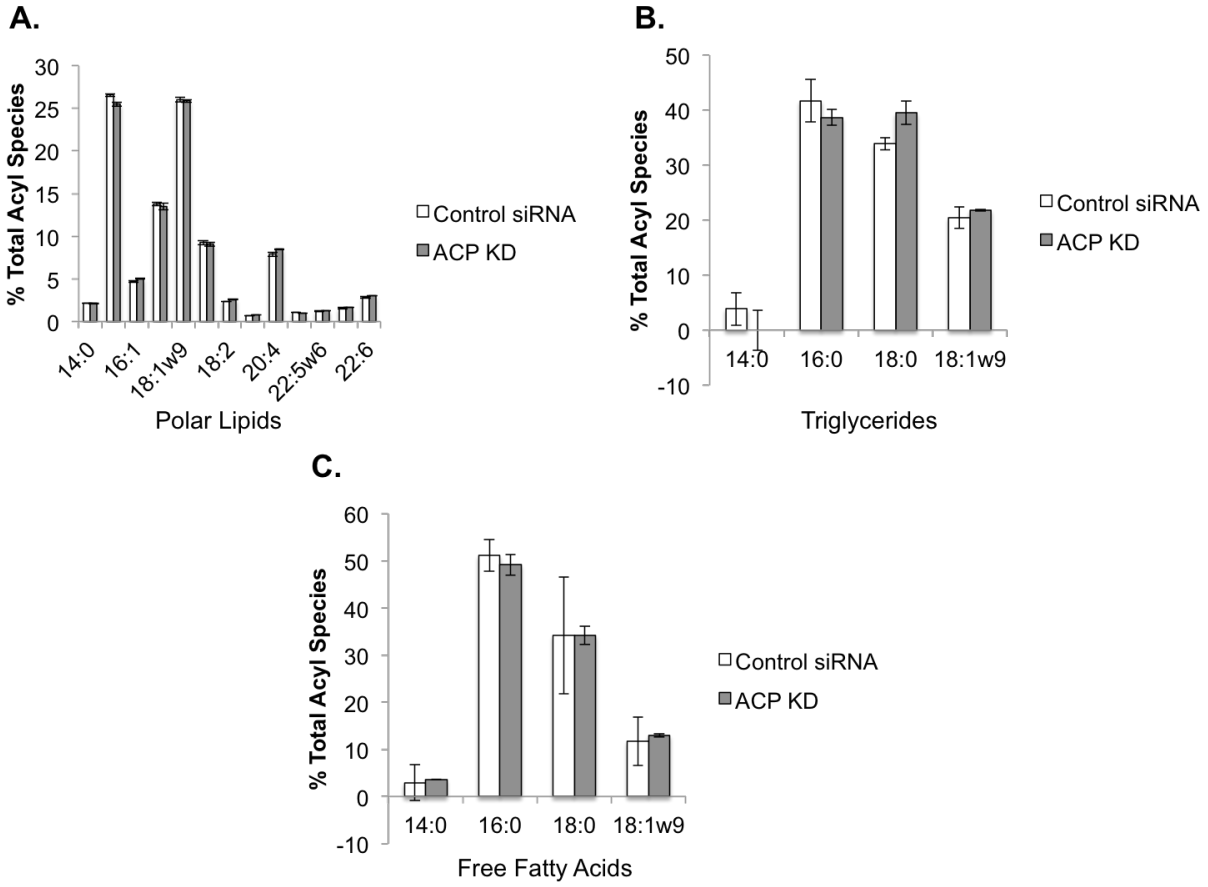

Figure 5. ACP KD does not alter the overall fatty acid composition of selected mitochondrial lipids.
Lipids from isolated mitochondria were analyzed by TLC, and the fatty acid side chain levels are expressed as µg lipid. n=2, * $p<0.05$.

systems are regulating mtFASII in opposite directions. For CI KD, 15 metabolites were changed in the same direction as those in ACP KD, and four were changed in the same direction as MECR OX, suggesting that CI KD more closely aligns phenotypically with ACP KD. In order to interpret the biochemical changes observed in both experimental conditions, these data were

analyzed in the context of biological pathways. Descriptions of these pathways and interpretations of the changes are discussed below.

	ACP KD/ Control	MECR OX/ Control	CI KD/ Control
Total Biochemicals, p≤0.05	115	57	132
Biochemicals Increased	57	33	92
Biochemicals Decreased	58	24	40
Total Biochemicals, 0.05≤p≤0.1	28	24	35
Biochemicals Increased	18	12	25
Biochemicals Decreased	10	12	10

Table 1. Significantly altered biochemical detected by metabolomics analysis.
The total number of biochemicals that reached or neared significance for ACP KD, MECR OX, and CI KD conditions are presented.

Glycolysis and sorbitol pathways

Levels of molecules in both the glycolysis and sorbitol pathways were changed as a result of mtFASII dysregulation (Figure 6). Intermediates in the glycolysis pathway, including glucose 6-phosphate and 3-phosphoglycerate, as well as the end product lactate were significantly reduced in ACP KD cells. Reflecting dysfunction of overall cell metabolism, glycolysis metabolites were also downregulated in CI KD cells, with reductions in phosphoenoylpyruvate, 3-phosphoglycerate, and an isobar including fructose 1,6-diphosphate, glucose 1,6-diphosphate, myo-inositol 1,4 and 1,3-diphosphate. Intermediates in the sorbitol (or polyol) pathway, including sorbitol and fructose, were at decreased levels in ACP KD cells, and fructose levels were increased in MECR OX cells. These results suggest that ACP KD cells are using glycolysis instead of oxidative phosphorylation, and as such are depleting glucose in the medium. Although not statistically significant, the intracellular glucose levels were down almost two-fold in ACP KD, and up almost two-fold in the MECR OX cells, supporting this idea.

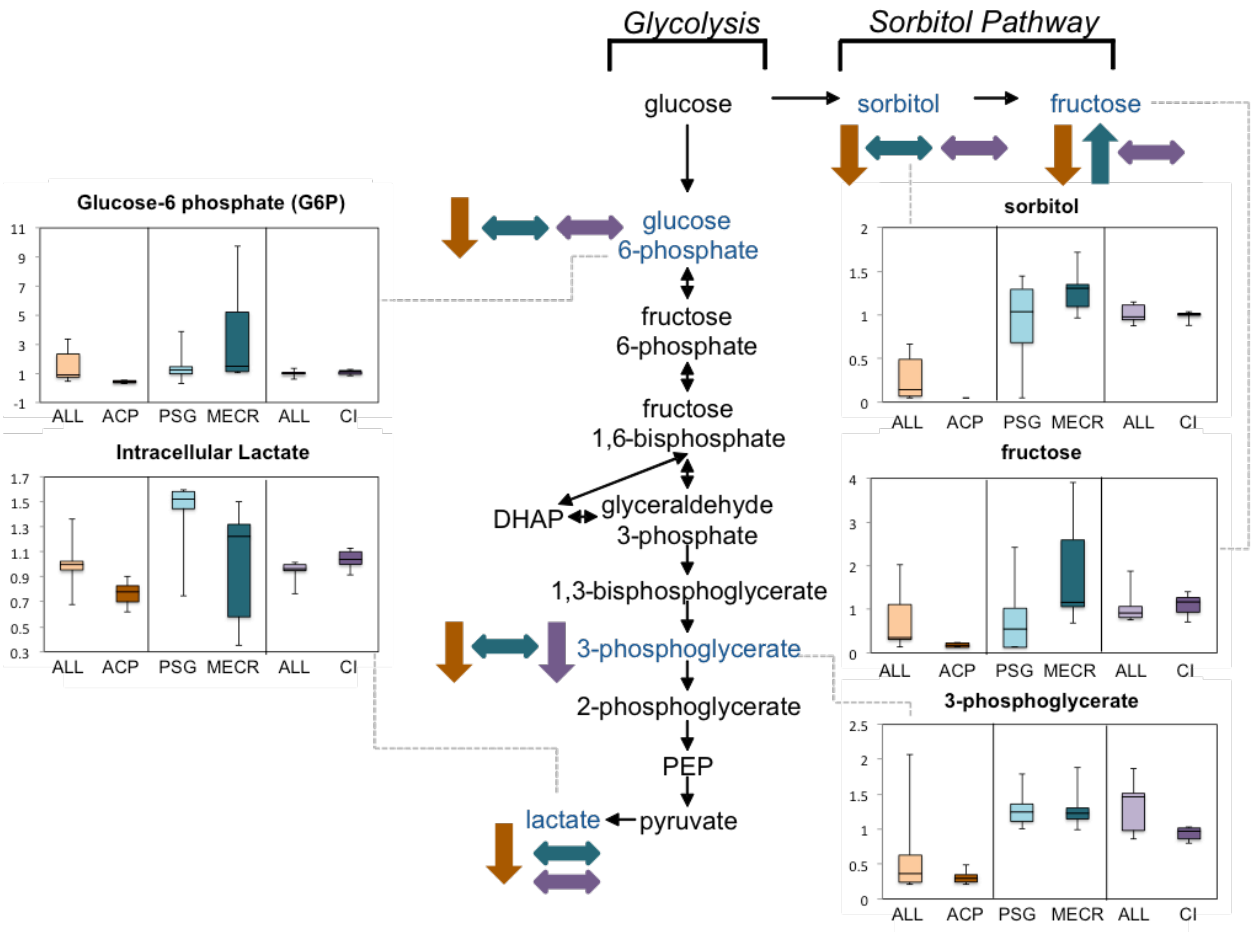

Figure 6. Glycolysis and the sorbitol pathway are significantly altered by changes in mtFASII function.

Glycolysis intermediates that were assayed are indicated with arrows and a corresponding box plot. Y-axes for box plots indicate scaled intensity, except where indicated otherwise. Box blot error bars represent the maximum and minimum of the data distribution. Direction of change compared to control in ACP KD is indicated by brown arrows, direction of change relative to control in MECR OX is indicated by blue arrows, and direction of change relative to control in CI KD is indicated by purple arrows. In box plots, metabolite levels are shown for ACP KD cells, MECR OX cells, and CI KD cells, and their respective controls. For each ACP KD and MECR OX box, n=6; for CI KD boxes, n=5.

Glucose levels were measured in the medium after 96 hours of knockdown of ACP, and lactate levels were measured in the medium after 96 hours of knockdown of ACP or 24 hours of upregulation of MECR. Extracellular glucose levels were significantly reduced in ACP KD media, confirming the depletion of glucose by glycolysis in ACP KD cells (Figure 7A). In

addition, while intracellular lactate was significantly decreased in ACP KD cells, there was a nonsignificant trend toward increased extracellular lactate levels in the medium of ACP KD cells (Figure 7B). Extracellular lactate was not altered in MECR OX cells.

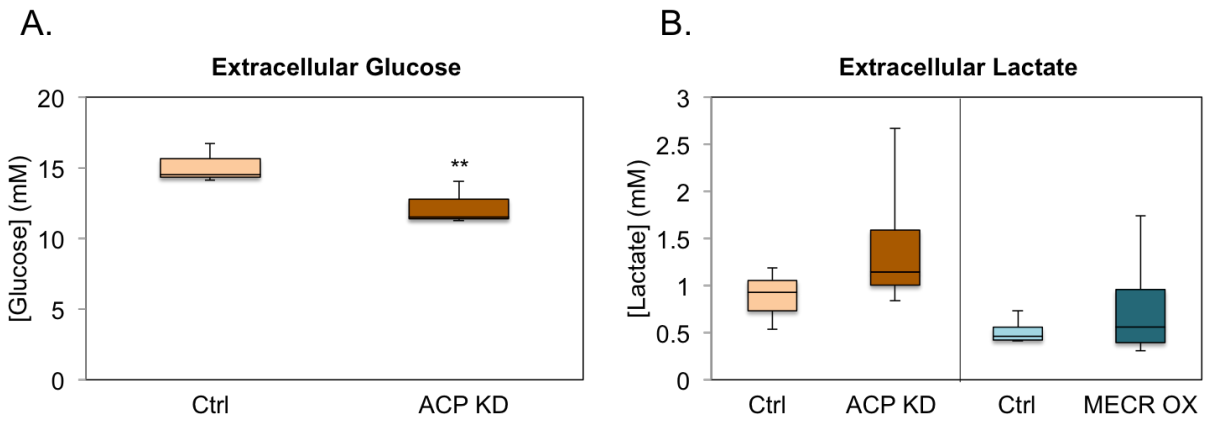

Figure 7. Cell culture media glucose and lactate levels are altered by changes in mtFASII.
A) Glucose levels in cell culture media were examined using the glucose oxidase method after 96 h ACP KD. Glucose concentration is expressed as mg/dL. n=3, *p<0.05; **p<0.01.
B) Extracellular lactate was measured in cell culture media using a colorimetric lactate assay (Biovision). n=4. Changes in both conditions are not significant.

Tricarboxylic acid (TCA) cycle and amino acid anaplerosis

In ACP KD cells, levels of several TCA cycle intermediates, including citrate, succinate, and fumarate, were significantly elevated. In CI KD cells, several TCA cycle intermediates were at reduced levels, reflecting the overall respiratory deficiency of CI KD cells. Correspondingly, levels of several amino acids were decreased (Figure 8). Specifically, levels of several glucogenic (asparagine, aspartate, valine, threonine, methionine, glutamine, and histidine) and glucogenic/ketogenic (tyrosine, phenylalanine, and isoleucine) amino acids were significantly reduced in ACP KD cells, suggesting that amino acid anaplerosis is compensating for defects in the TCA cycle, which are likely due to loss of mtFASII-related protein lipoylation.

Pentose phosphate pathway

Levels of many intermediates in the pentose phosphate pathway (PPP) were decreased in ACP KD cells, and most of these were increased in the MECR OX cells (Figure 9). In CI KD, PPP intermediates were downregulated despite an increase in the levels of ribose and its

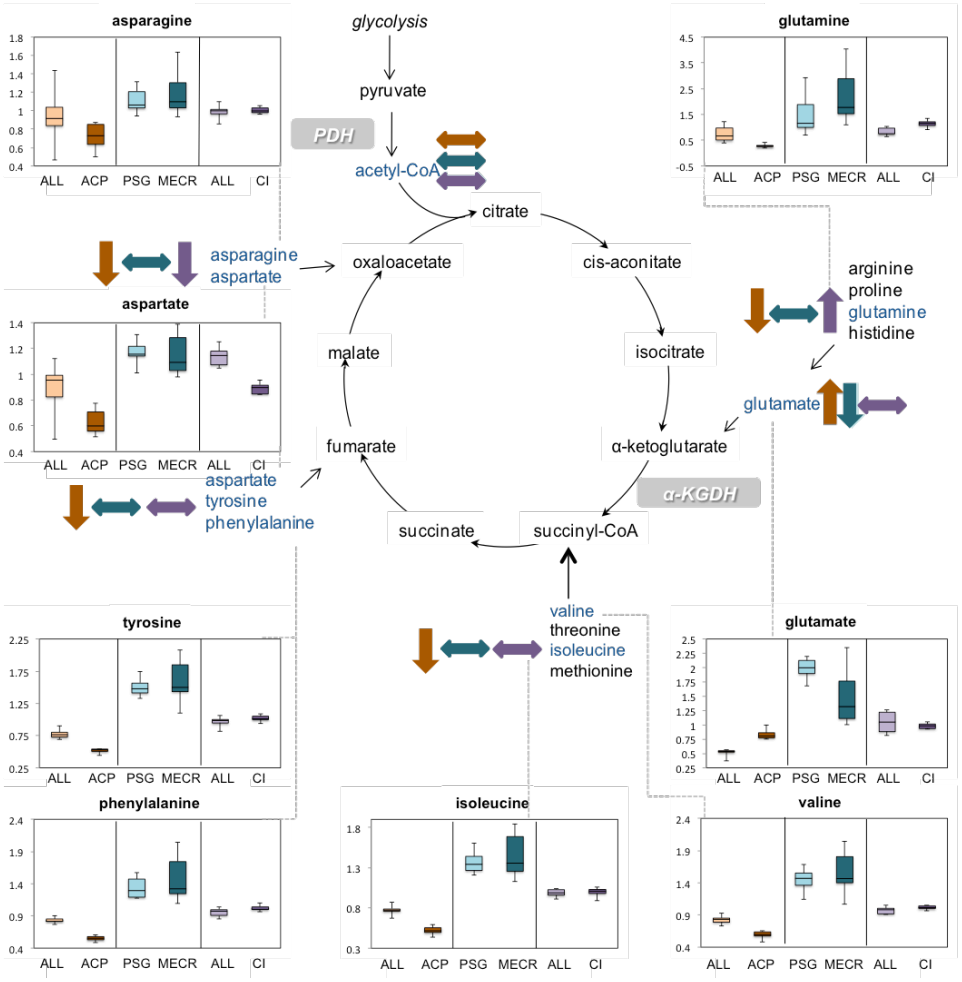

Figure 8. Amino acids used in amino acid anaplerosis are largely depleted in ACP KD and CI KD.

Amino acid anaplerosis intermediates that were assayed are indicated with arrows and a corresponding box plot. Y-axes for box plots indicate scaled intensity. Box blot error bars represent the maximum and minimum of the data distribution. Direction of change compared to control in ACP KD is indicated by brown arrows, direction of change relative to control in MECR OX is indicated by blue arrows, and direction of change relative to control in CI KD is indicated by purple arrows. In box plots, metabolite levels are shown for ACP KD cells, MECR OX cells,

and CI KD cells, and their respective controls. For each ACP KD and MECR OX box, n=6; for CI KD boxes, n=5.
derivatives. Like glycolysis, the PPP oxidizes of glucose, but glucose oxidation is used to synthesize five-carbon sugars. Molecules from both the first part of the pathway that creates reducing equivalents (NADPH), and the second part of the pathway that makes five-carbon sugars were changed in the mtFASII KD and OX cells.

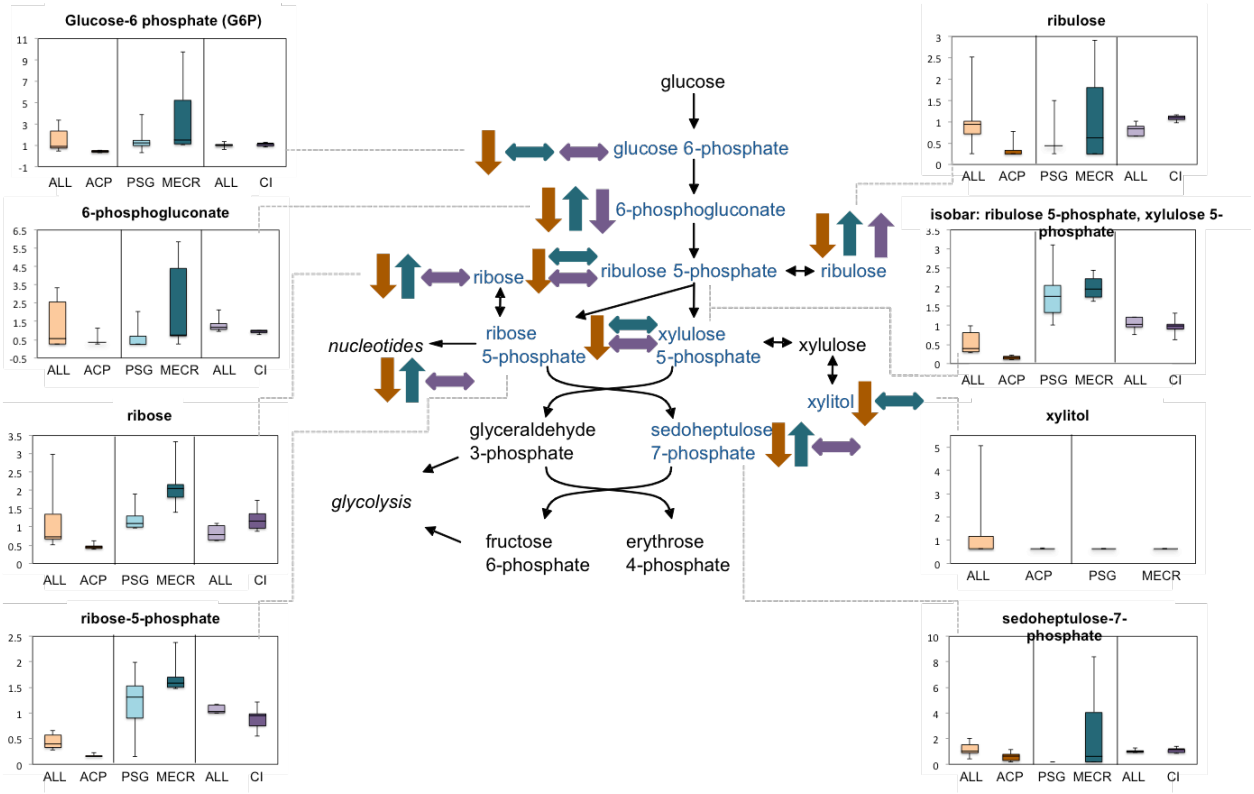

Figure 9. Pentose phosphate pathway metabolites are reduced in ACP KD and CI KD, and are elevated in MECR OX.
Pentose phosphate pathway intermediates that were assayed are indicated with arrows and a corresponding box plot. Y-axes for box plots indicate scaled intensity. Box blot error bars represent the maximum and minimum of the data distribution. Direction of change compared to control in ACP KD is indicated by brown arrows, direction of change relative to control in MECR OX is indicated by blue arrows, and direction of change relative to control in CI KD is indicated by purple arrows. In box plots, metabolite levels are shown for ACP KD cells, MECR OX cells, and CI KD cells, and their respective controls. For each ACP KD and MECR OX box, n=6; for CI KD boxes, n=5.

Redox status: γ-glutamyl cycle

Many of the intermediates in the γ-glutamyl cycle were also changed in opposite directions in ACP KD and MECR OX cells (Figure 10). Glutamate and γ-glutamyl-linked amino acids, including γ-glutamyl-cysteine, were increased in ACP KD and CI KD and decreased in MECR OX. In addition, 5-oxoproline, cysteine, and cysteine-glutathione disulfide were all increased in ACP KD and CI KD cells. These metabolites are intermediates in the synthesis of glutathione (GSH), which plays a key role in cellular defenses against oxidative stress. While intermediates in GSH synthesis were increased significantly, levels of reduced GSH were slightly increased in ACP KD cells. Because GSH levels are dictated by a balance between synthesis of reduced GSH and oxidation to glutathione disulfide (GSSG), we also examined the ratio of GSH to GSSG. The GSH/GSSG ratio was significantly different when mtFASII is altered (Figure 11). An increase in the GSH/GSSG ratio in ACP KD cells compared to control indicates a more reduced environment, while a decrease in the ratio in MECR OX compared to control cells suggests a more oxidizing environment.

Polyamine synthesis

In ACP KD cells, levels of the polyamines spermidine and spermine were elevated, whereas in MECR OX, spermidine levels were reduced while spermine levels were unchanged. CI KD had no effect on polyamine metabolism (Figure 12).

Bioactive lipid metabolism

ACP KD and MECR OX resulted in significant changes in the levels of specific phospholipids that were not measured in the initial TLC-GC experiments, namely lysophospholipids and sphingolipids. Lysophospholipids measured in this study included acyl-glycerophosphocholines, acyl-glycerophosphoinositols, and acyl-glycerophosphoethanolamines.

Several side chain length forms of acyl-glycerophosphocholines and

acyl-glycerophosphoethanolamines are changed, but acyl-glycerophosphoinositols were

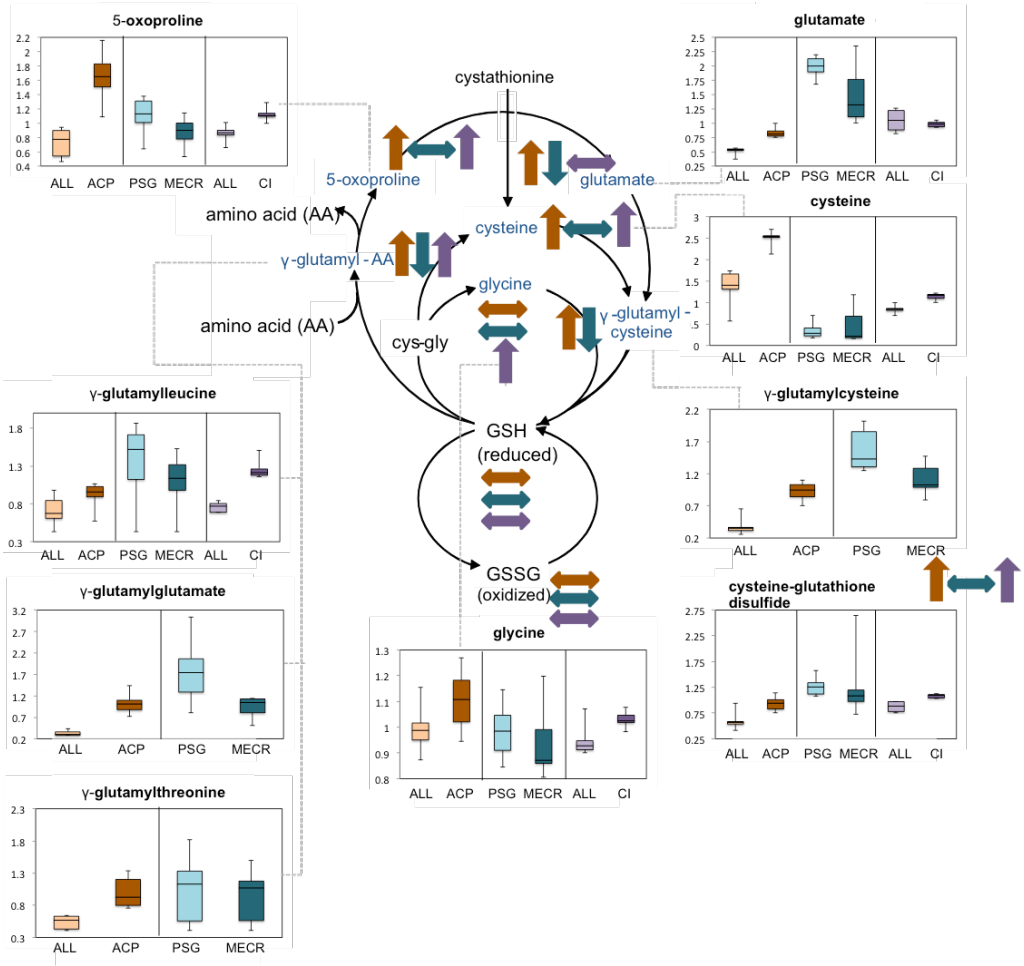

Figure 10. Markers of oxidative stress are altered with changes in mtFASII function and CI KD.

Intermediates of the γ-glutamyl cycle that were assayed are indicated with arrows and a corresponding box plot. Y-axes for box plots indicate scaled intensity. Box blot error bars represent the maximum and minimum of the data distribution. Direction of change compared to control in ACP KD is indicated by brown arrows, direction of change relative to control in MECR OX is indicated by blue arrows, and direction of change relative to control in CI KD is indicated by purple arrows. In box plots, metabolite levels are shown for ACP KD cells, MECR OX cells, and CI KD cells, and their respective controls. For each ACP KD and MECR OX box, n=6; for CI KD boxes, n=5.

unchanged. These lysophospholipids were strikingly diminished in the cells with mtFASII knockdown, and increased at least two-fold when MECR was overexpressed (Figure 13 and Table 2). In CI KD, lysophospholipids showed a scattered pattern of changes, with roughly equal numbers of lysophospholipids upregulated, downregulated, or unchanged. Sphinganine and sphingosine levels were decreased in ACP KD, but increased in MECR OX cells (Figure 14). In addition, palmitoylcarnitine, a precursor of the palmitoyl-CoA required for production of sphingolipids, was significantly reduced 11-fold in ACP KD cells. By contrast, CI KD cells showed no change in sphingosine or sphinganine levels, indicating that sphingolipid alterations are specific to the mtFASII pathway, as opposed to mtFASII-related respiratory deficiency.

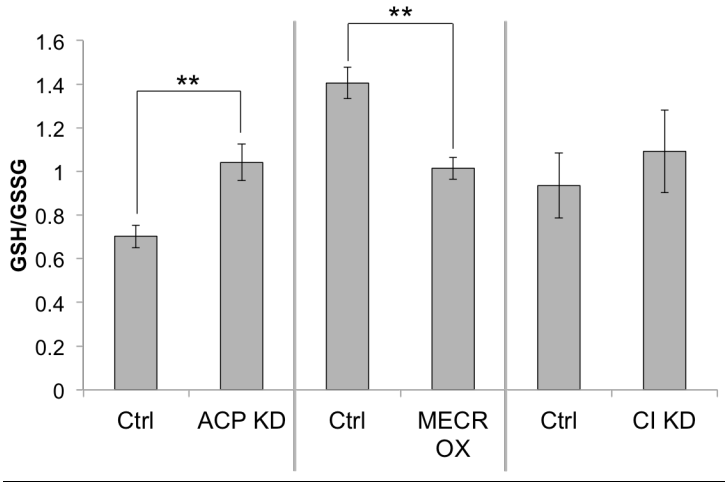

Figure 11. GSH/GSSG ratios are altered by changes in mtFASII function.
GSH/GSSG ratios were calculated from metabolomics data. For ACP KD and MECR OX, n=6. For CI KD, n=5. **p<0.01.

Because our metabolomics analysis does not cover a wide range of sphingolipid species, we investigated additional sphingolipids, namely ceramides and S1P. LC-MS/MS analysis of ceramide levels shows that ACP KD cells do not upregulate ceramide levels despite

the increased presence of γ-glutamyl cycle ROS markers (Figure 15). S1P, a bioactive lipid signaling molecule, created by the phosphorylation of sphingosine, was measured by ELISA. S1P was increased over two-fold in ACP KD cells (Figure 16), suggesting that sphingosine is down in ACP KD cells because it is being converted into S1P.

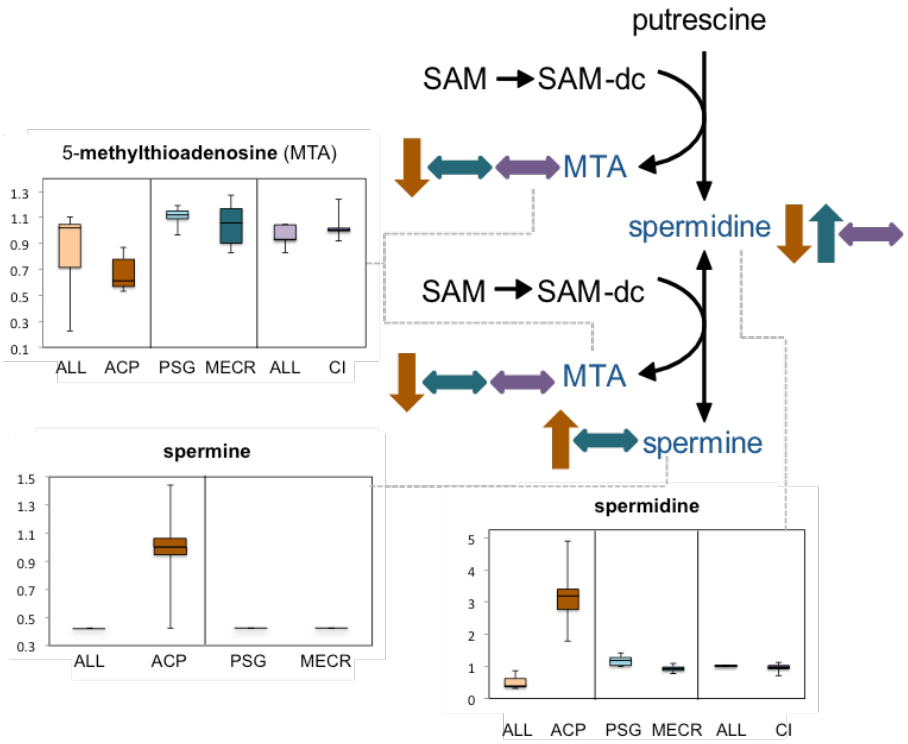

Figure 12. ACP KD results in upregulation of the polyamine synthesis pathway. Polyamine synthesis pathway intermediates that were assayed are indicated with arrows and a corresponding box plot. Y-axes for box plots indicate scaled intensity. Box blot error bars represent the maximum and minimum of the data distribution. Direction of change compared to control in ACP KD is indicated by brown arrows, direction of change relative to control in MECR OX is indicated by blue arrows, and direction of change relative to control in CI KD is indicated by purple arrows. In box plots, metabolite levels are shown for ACP KD cells, MECR OX cells, and CI KD cells, and their respective controls. For each ACP KD and MECR OX box, n=6; for CI KD boxes, n=5.

Discussion

While it is clear that mitochondria can synthesize fatty acids, questions remain about how disruption of the mtFASII pathway causes the extensive array of observed phenotypes. A lack of change in the fatty acid profiles of polar lipids, triglycerides, and free fatty acids in ACP KD mitochondria indicates that the mtFASII pathway is likely not a major contributor to mitochondrial fatty acid composition. If the mtFASII pathway is not an important contributor to mitochondrial membrane lipid composition, we reasoned that perhaps the pathway plays other roles in the cell. For this reason, we took a broad approach, using metabolomics in whole cells with altered mtFASII function to investigate the roles of the mtFASII pathway in the cell. Pathway analysis of the biochemicals changed upon altering mtFASII function links the mtFASII pathway to a general switch in energy metabolism, redox state, polyamine levels, and bioactive lipid levels.

Manipulation of mtFASII function elicits changes in several pathways that reveal a common theme of altered glucose utilization. Intermediates in glycolysis, the sorbitol pathway, amino acid anaplerosis, and the PPP are all changed in a way that suggests increased glucose utilization with knockdown of the mtFASII pathway, and decreased glucose utilization with increased function of the pathway. Correspondingly, we find that extracellular glucose is decreased and extracellular lactate is increased in ACP KD, both of which point to increased glycolysis. This is consistent with previous work, as knockdown of any mtFASII component in yeast or mammalian cells leads to defects in oxidative phosphorylation and subsequent increased reliance on glycolysis.[14, 22, 46, 47] Additionally, these changes are each consistent with a respiratory-deficient phenotype, as they are also seen in CI KD cells.

Another glucose-responsive pathway, the TCA cycle, is also altered by changes in mtFASII function. The intermediates in the TCA cycle, however, are increased in ACP KD, and levels of acetyl-CoA remain the same. Since a lack of mtFASII would be expected to interfere

with the TCA cycle by decreased lipoylation of pyruvate dehydrogenase and α-ketoglutarate dehydrogenase, the increased levels of these intermediates suggests that a compensatory mechanism is in place. Amino acid stores are decreased in ACP KD cells, likely indicating that increased amino acid anaplerosis replenishes TCA cycle metabolite levels in response to depleted glucose level or dysfunctional TCA cycle enzymes.[189]

Changes in all of the above-mentioned glucose responsive pathways are limited mainly to decreased intermediates in ACP KD cells with very few changes observed in MECR OX cells. PPP intermediates, however, are upregulated in MECR OX cells as well as decreased in ACP KD cells. The PPP generates much of the NADPH in the cell, and is also an essential source of metabolites important to several biosynthetic pathways.[190] The rate-limiting enzyme of PPP, glucose-6-phosphate dehydrogenase (G6PD), exhibits increased activity with reductions in the NADPH/NADP ratio.[190, 191] In MECR OX cells, enhanced mtFASII function could increase NADPH consumption, lowering the NADPH/NADP ratio, thereby increasing G6PD activity and PPP flux. Though mtFASII is not the cell's main consumer of NADPH, ACP KD could ostensibly elevate NADPH levels, which would increase the NADPH/NADP ratio, causing a decrease in G6PD activity. However, the PPP is also suppressed in CI KD cells, indicating that PPP changes seen in ACP KD could be due to respiratory deficiency.

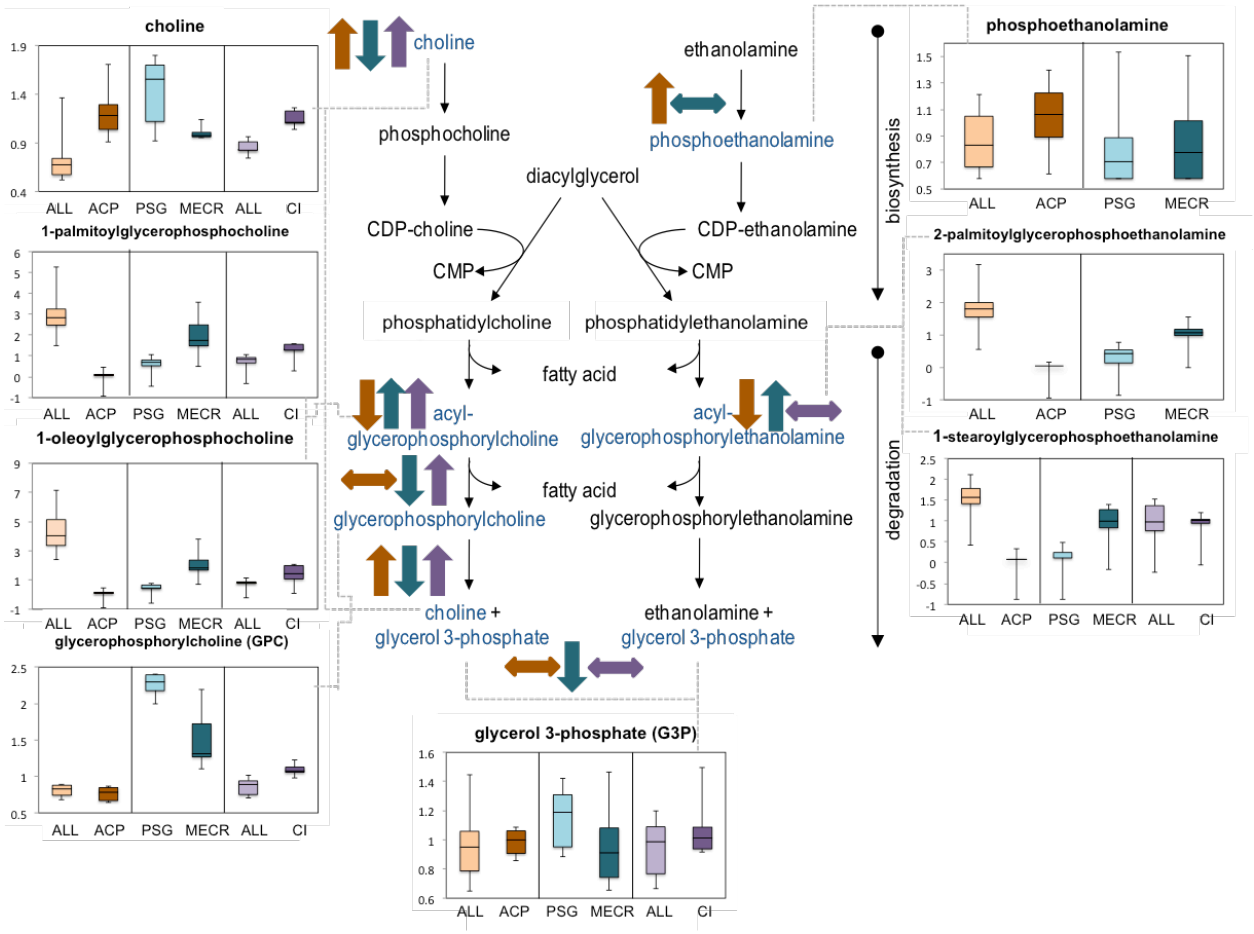

Figure 13. Lipid homeostasis is altered by ACP KD and MECR OX.
Lipid synthesis and degradation intermediates that were assayed are indicated with arrows and a corresponding box plot. Y-axes for box plots indicate scaled intensity. Box blot error bars represent the maximum and minimum of the data distribution. Direction of changed compared to control in ACP KD is indicated by brown arrows, direction of change relative to control in MECR OX is indicated by blue arrows, and direction of change relative to control in CI KD is indicated by purple arrows. In box plots, metabolite levels are shown for ACP KD cells, MECR OX cells, and CI KD cells, and their respective controls. For each ACP KD and MECR OX box, n=6; for CI KD boxes, n=5.

Lysophospholipid	ACP KD/ Control	MECR OX/ Control	CI KD/ Control
1-arachidonoylglycerophosphoethanolamine	0.98	1.37	**0.83**
1-myristoylglycerophosphocholine	0.24	3.16	-
1-oleoylglycerophosphocholine	0.04	4.33	**1.75**
1-oleoylglycerophosphoethanolamine	1.26	2.36	0.79
1-oleoylglycerophosphoinositol	**1.67**	2.23	**0.55**
1-palmitoleoylglycerophosphocholine	0.11	2.08	0.95
1-palmitoylglycerophosphocholine	0.05	3.08	**1.59**
1-palmitoylglycerophosphoethanolamine	1.14	1.57	0.87
1-palmitoylglycerophosphoinositol	**1.5**	**2.6**	**0.6**
1-palmitoylplasmenylethanolamine	1.05	1.17	0.81
1-stearoylglycerophosphocholine	0.10	2.80	**1.87**
1-stearoylglycerophosphoethanolamine	0.10	4.97	0.91
1-stearoylglycerophosphoglycerol	1.61	1.30	0.92
1-stearoylglycerophosphoinositol	1.38	2.18	**0.71**
2-arachidonoylglycerophosphocholine	0.09	3.19	-
2-arachidonoylglycerophosphoethanolamine	0.04	2.49	-
2-docosahexaenoylglycerophosphocholine	0.21	1.59	-
2-docosahexaenoylglycerophosphoethanolamine	0.05	2.56	-
2-docosapentaenoylglycerophosphocholine	0.16	3.38	-
2-docosapentaenoylglycerophosphoethanolamine	0.04	2.46	-
2-linoleoylglycerophosphocholine	0.28	2.80	-
2-myristoylglycerophosphocholine	0.06	2.25	-
2-oleoylglycerophosphocholine	0.02	3.99	-
2-oleoylglycerophosphoethanolamine	0.03	2.88	-
2-oleoylglycerophosphoinositol	1.47	2.19	-
2-palmitoleoylglycerophosphocholine	0.03	3.52	1.12
2-palmitoleoylglycerophosphoethanolamine	0.12	3.57	-
2-palmitoylglycerophosphocholine	0.02	3.17	**1.3**
2-palmitoylglycerophosphoethanolamine	0.04	2.96	-

Table 2. Alteration of mtFASII results in changed lysophospholipid levels.
All lysophospholipids assayed are presented with their corresponding levels in ACP KD or MECR OX, each normalized to its own control. Dark green boxes indicate significant downregulation, and red boxes indicate significant upregulation. Light green boxes indicate trending downregulation, and pink boxes indicate trending upregulation. Metabolite levels were deemed significant when $p<0.05$. Trending changes occurred when fold changes were $0.05<p<0.1$.

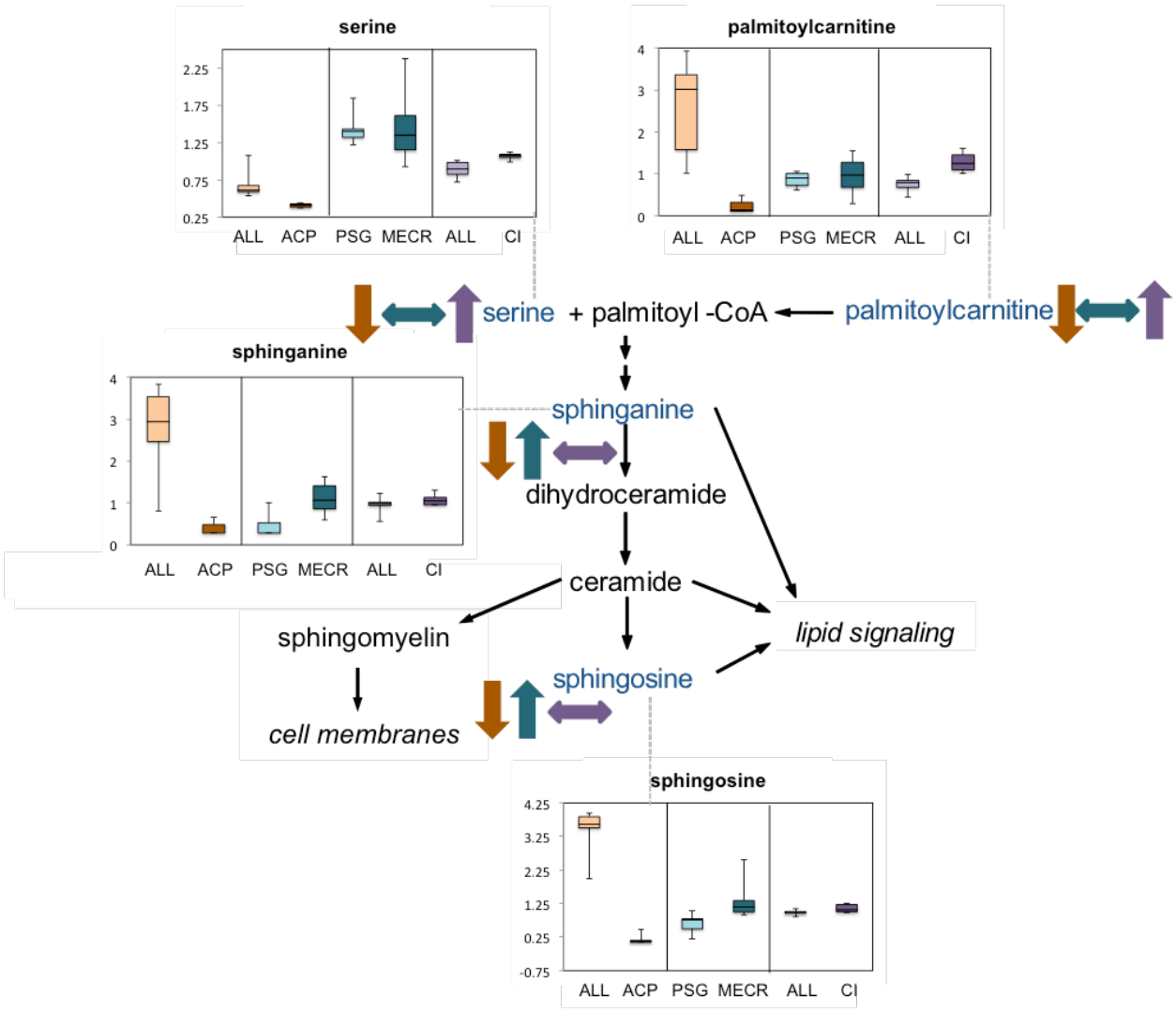

Figure 14. Sphingolipid synthesis metabolites are downregulated in ACP KD and largely upregulated in MECR OX.

Sphingolipid synthesis pathway intermediates that were assayed are indicated with arrows and a corresponding box plot. Y-axes for box plots indicate scaled intensity. Box blot error bars represent the maximum and minimum of the data distribution. Direction of change compared to control in ACP KD is indicated by brown arrows, direction of change relative to control in MECR OX is indicated by blue arrows, and direction of change relative to control in CI KD is indicated by purple arrows. In box plots, metabolite levels are shown for ACP KD cells, MECR OX cells, and CI KD cells, and their respective controls. For each ACP KD and MECR OX box, n=6; for CI KD boxes, n=5.

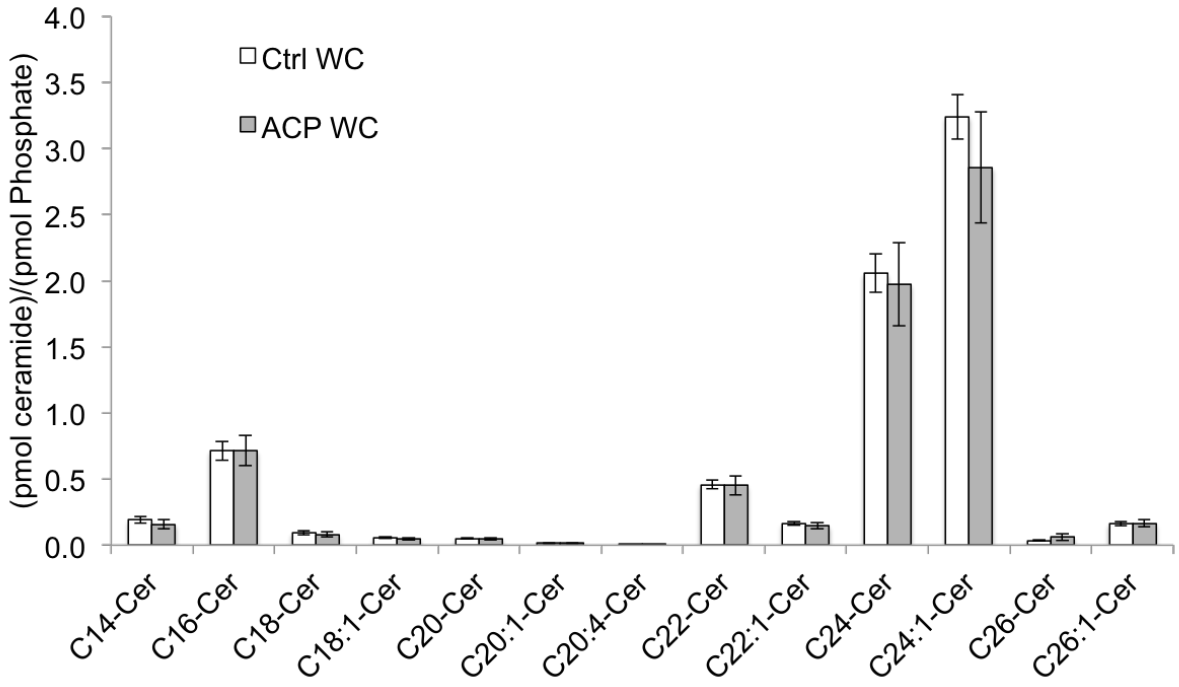

Figure 15. ACP KD does not elevate ceramide levels despite ROS induction.
Control (white) and ACP KD (grey) whole cells were analyzed for various ceramides by LC-MS/MS. Ceramide levels are expressed as the pmol concentration of the ceramide normalized to sample phosphate levels. n=3, and * indicates $p<0.05$.

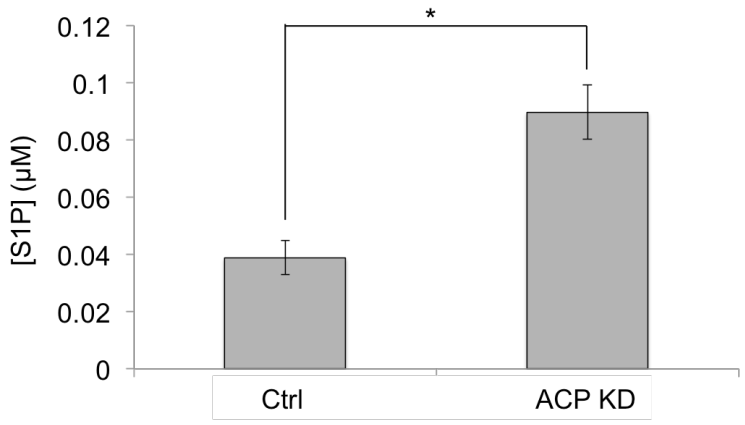

Figure 16. S1P levels are increased in ACP KD cells.
S1P levels were measured by ELISA of 40 μg protein, and are expressed in μM concentrations. n=3, and *$p<0.05$.

Gamma-glutamyl cycle intermediates show an opposite pattern to the PPP intermediates and are upregulated in ACP KD and CI KD cells and decreased in MECR OX cells. In general, increases in γ-glutamyl cycle metabolites are correlated with oxidative stress levels. Alternatively, elevated γ-glutamyl amino acids may reflect the increased need for amino acid transport due to anaplerotic contribution to the TCA cycle. In MECR OX cells, however, several GSH synthesis metabolites are at decreased levels, indicating that the cells have decreased oxidative stress, perhaps due to increased levels of the antioxidant and mtFASII product lipoic acid. GSH and GSSG, the most abundant markers of the pathway, appear relatively unchanged in ACP KD cells, although it is possible that changes in these molecules were masked by their conversion to other molecular species or their export from the cell.[192-194] The closely related molecule, cysteine-glutathione disulfide is retained in the cell, its levels are proportional to redox status,[192, 195, 196] and it is increased in ACP KD and CI KD cells. Surprisingly, the most widely used indicator of oxidative stress, the GSH/GSSG ratio, is higher in ACP KD cells, indicating a more reduced environment, and down in MECR OX cells, suggesting a more oxidizing environment. This suggests that although the γ-glutamyl cycle is upregulated by mtFASII dysfunction, the increased pools of NADPH caused by decreases in mtFASII activity promote the reduction of GSSG to GSH, creating a more reducing environment, and that the opposite is happening with improved mtFASII function.

Levels of the polyamines spermine and spermidine are increased in ACP KD and CI KD cells, and spermidine is decreased in MECR OX cells. An increase in ROS could be responsible for increased polyamine levels in ACP KD and CI KD cells. During oxidative stress, polyamines prevent DNA nicking and protein carbonylation, enhancing cell survival.[197, 198] Ornithine decarboxylase (ODC) and spermidine/spermine-N^1-acetyltransferase (SSAT), enzymes involved in the synthesis and degradation of polyamines, respectively, are upregulated in both expression and activity during oxidative stress.[197, 199] The upregulation of ODC, however, outpaces that of SSAT, resulting in polyamine accumulation during oxidative stress.[197, 199]

Alternatively, changes in polyamine levels could be in response to the mitochondrial RNA processing defects in mtFASII KD cells,[3, 9] since polyamines bind to RNA and are important in RNA processing and expression.[200, 201]

The most striking changes observed in ACP KD and MECR OX were in bioactive lipid levels, including lysophospholipids and sphingolipids. Levels of both classes of bioactive lipids were directly correlated with mtFASII activity, with 20 of 31 assayed species showing significant differences in both directions of mtFASII change, and an additional four species showing significant changes in one condition. Lysophospholipids that responded to changes in mtFASII function are species of phosphatidylethanolamine and phosphatidylcholine containing a single acyl chain. Lysophospholipids are often the products of phospholipid remodeling or breakdown, but can also be synthesized directly in the cytosol via acylation of glycerol-3-phosphate by glycerol-3-phosphate acyltransferase (GPAT), or in the mitochondria by mitochondrial glycerol-3-phosphate acyltransferase (GPAM).[202-204] In contrast to the robust lysophospholipid changes seen in ACP KD and MECR OX, CI KD cells show no consistent pattern in lysophospholipid regulation. Of the 29 lysophospholipids examined in CI KD cells, five were increased, nine were decreased, and 15 were unchanged. The lack of similarity in lysophospholipid profiles between CI KD cells and either ACP KD or MECR OX cells indicates that lysophospholipid changes in ACP KD and MECR OX are possibly due to the mtFASII pathway itself, rather than a respiratory deficient phenotype.

The mtFASII pathway is known to affect lysophospholipid levels, as ACP knockdown in the fungi *N. crassa* resulted in elevated mitochondrial membrane lysophospholipid levels.[36] The loss of lysophospholipids in ACP KD cells, together with increased choline and phosphoethanolamine levels, suggest that the canonical pathway for generation of the phospholipids phosphatidylethanolamine and phosphatidylcholine is not completely functional. Suppression of the PPP in ACP KD cells would lead to a reduction in PPP-mediated synthesis of cytidine diphosphate (CDP), a molecule used in the canonical phospholipid synthesis

pathway. ACP KD-related suppression of the PPP would decrease cytidine diphosphate (CDP) levels. Hence, loss of mtFASII might lead to loss of the canonical pathway for synthesis of phosphatidylethanolamine and phosphatidylcholine and the compensatory conversion of lysophospholipids into phospholipids. This correlates also with the increase in both PPP and lysophospholipids in the MECR OX cells. Taken together, these data suggest a model where mtFASII function alters the NADPH/NADP ratio, which alters flux through the PPP, rendering downstream effects on CDP levels, the canonical phospholipid synthesis pathway, and lysophospholipid levels.

Sphingolipids, the second class of bioactive lipids assayed, are lipids derived from the condensation of serine and palmitoyl-CoA and are characterized by an 18-carbon backbone. Our data indicate that levels of sphingolipids and their precursors are reduced in ACP KD and increased in MECR OX, but unchanged in CI KD. Sphingolipids are important determinants of cell survival, as ceramides and sphingosine promote growth arrest and apoptosis, while S1P promotes proliferation and survival.[122, 139-141, 205, 206] We analyzed ceramide levels in ACP KD cells and found no change despite ROS induction.

Sphingosine and S1P are interconvertible through specific kinases and phosphatases; because of this interconvertibility and opposite signaling functions, the relative levels of sphingosine and S1P are important markers of cell or organelle health. In ACP KD cells, sphingosine levels are decreased, while S1P levels are increased. These changes could be a result of the cell compensating for damage caused by respiratory deficiency and increased oxidative stress, but further analysis is necessary to understand the mechanisms underlying changes in sphingolipid levels under altered mtFASII function.

The role mtFASII plays in the mitochondria and the cell is not entirely clear. The present study provides insight into the specific molecules and pathways affected by changes in mtFASII function and demonstrates that they are not all simply the result of respiratory changes. Our data regarding metabolic states in cells with reduced mtFASII function is consistent with

previously published research and provides an in-depth look at the root of mitochondrial dysfunction upon loss of ACP. We demonstrate that mtFASII hyperfunction through MECR OX may actually bolster mitochondrial health, as it appears that MECR OX cells have an improved redox state compared to control cells. The observation that there is an important connection between mtFASII function and bioactive lipid levels is intriguing, but the mechanism behind this relationship awaits further investigation.

CHAPTER III

CHANGES IN THE MITOCHONDRIAL FATTY ACID SYNTHESIS II (MTFASII) PATHWAY ALTER METABOLISM AND DIPEPTIDE PRODUCTION IN ISOLATED MITOCHONDRIA

Abstract

The mitochondrial fatty acid synthesis II (mtFASII) pathway is a conserved, bacterial-like means of fatty acid production within the mitochondria. Though effects of the mtFASII pathway on respiration and protein lipoylation are documented, the role of mtFASII in the mitochondria is not fully characterized. For this reason, we analyzed mitochondria isolated from mtFASII hypofunctional cells (through acyl-carrier protein knockdown) and mtFASII hyperfunctional cells (through mitochondrial enoyl-2-CoA reductase overexpression) using metabolomics, liquid chromatography-mass spectrometry, and ELISA. We found that loss of mtFASII function disturbs metabolism at the mitochondrial level. Interestingly, altering mtFASII function affects mitochondrial dipeptide content, indicating a potential role for the mtFASII pathway in mitochondrial signaling through the mitochondrial unfolded protein response. Disruption of mtFASII also alters the sphingosine:sphingosine-1-phosphate ratio, pointing to an additional role of mtFASII in sphingolipid-mediated signaling. Additionally, metabolomic comparison between mitochondria from cells with changes in mtFASII function to mitochondria from complex I knockout cells indicates that changes seen after altering mtFASII function are not simply due to respiratory dysfunction.

Introduction

Mitochondria are cellular organelles that originated from a symbiotic relationship between an anaerobic proto-eukaryote and an aerobic proto-prokaryote. Because of the mitochondria's bacterial origins, many of its characteristics remain bacterial-like. One such characteristic is the presence of a mitochondrial fatty acid synthesis II (mtFASII) pathway that,

like bacterial fatty acid synthesis II (FASII) pathways, relies on a sequence of separate enzymes to catalyze each step of the pathway.[3] The cytosolic fatty acid synthesis I (FASI) pathway, by contrast, uses a large, multifunctional enzyme to catalyze all steps of fatty acid synthesis.[1, 3]

The mtFASII pathway synthesizes fatty acids in the mitochondrial matrix, starting with malonate or malonyl-CoA, and consuming ATP and NADPH.[3, 173] In mammals, mtFASII has been demonstrated to synthesize fatty acids up to 14 carbons in length (myristic acid), whereas in plants, mtFASII is known to synthesize up to 16-carbon fatty acids (palmitic acid).[2, 3, 32, 38]

While the mtFASII pathway is conserved in eukaryotic species, the reason for mtFASII's conservation is unclear. One known function of the mtFASII pathway is in the synthesis of lipoic acid. Octanoic acid synthesized by mtFASII is a precursor for mitochondrial lipoic acid, and knockdown of mtFASII components results in reduced protein lipoylation.[3, 4, 6, 9, 10, 19, 34, 46, 47] This effect has metabolic consequences, as multiple tricarboxylic acid (TCA) cycle enzymes require lipoylation for function.[46]

In addition to its effects on the TCA cycle, mtFASII is also important for electron transport chain function (ETC) and mitochondrial health—knockdown of any mtFASII component results in respiratory deficiency, increased production of reactive oxygen species (ROS), and altered mitochondrial morphology.[3, 6, 10, 19, 22, 23, 46, 48] Interestingly, mtFASII function also impacts mitochondrial tRNA processing, as deletion of any mtFASII component results in impaired mitochondrial tRNA processing by mitochondrial RNase P.[9]

Acyl carrier protein (ACP) is a central component of the mtFASII pathway. ACP binds nascent fatty acids and shuttles them among the various mtFASII pathway enzymes. Like other mtFASII knockdowns, ACP knockdown (KD) results in loss of protein lipoylation, respiratory deficiency, and reduced cell growth.[3, 6, 34, 36, 46] In addition to its role in mtFASII, ACP is a putative component of complex I (CI) of the ETC, and ACP KD results in reduced CI assembly and function.[3, 27, 28, 32, 46]

The consequences of overexpressing mtFASII components are not as well studied as mtFASII knockdowns. The mtFASII protein mitochondrial enoyl-CoA reductase (MECR), however, has been overexpressed in mouse heart.[3, 19] MECR catalyzes the last step in the mtFASII pathway, and, like other mtFASII proteins, is a mitochondrial matrix protein.[51] Mice with overexpressed MECR in cardiac tissue exhibited impaired heart function, disorganized myofibrils, and enlarged mitochondria. Additionally, these mice had reduced NADH/NAD^+ ratios and an inability to increase oxidative phosphorylation (OXPHOS) capacity when workload was increased.[3]

Previous work from our lab used metabolomics to investigate the effects of altering mtFASII on whole cells (Chapter II). We found a number of biochemical changes associated with respiratory deficiency, as well as with altered bioactive lipid regulation. In order to understand the effects of mtFASII alteration at the mitochondrial level, we analyzed mitochondria isolated from ACP KD and MECR overexpression (OX) HeLa cells using a multiple techniques, including metabolomics and liquid chromatography-tandem mass spectrometry (LC-MS/MS). To understand the role of respiratory dysfunction in mtFASII alteration phenotypes, we also analyzed mitochondria isolated from CI KD cells. We show that knockdown of the mtFASII pathway suppresses TCA cycle function and alters NAD metabolism and bioactive sphingolipid levels. We also show that metabolomic changes seen in ACP KD mitochondria do not completely align with those of CI KD mitochondria, indicating that the ACP KD phenotype is not simply due to respiratory dysfunction.

Experimental Procedures

Cell culture conditions and siRNA-mediated RNA knockdown of ACP and complex I

HeLa cells were plated in 10-cm cell culture dishes (CellTreat) at a density of 1.5×10^5 cells/mL in DMEM + 10% FBS (Mediatech, Gibco). Knockdown of the mtFASII pathway and complex I of the ETC was achieved using Qiagen Flexitube siRNAs specific for the

genes for ACP (*NDUFAB1*) and NDUFS3, respectively; control cells were transfected with Allstars negative control siRNA (Qiagen). HeLa cells were transfected with siRNA using HiPerfect Transfection Reagent (Qiagen). After 48 h, cells were trypsinized, resuspended in double their original volume of DMEM + 10% FBS, then plated in a 15-cm dish for an additional 48 h. At 96 h, cells were harvested by trypsinization and centrifugation. Knockdown efficiency was measured after 96 h using real-time quantitative RT-PCR.

Overexpression of MECR

Plasmid construction

To create the MECR OX plasmid, the entire open reading frame of *Mecr* was amplified from mouse cDNA using primers
5'- CCAGATCTGCCGCCACCATGGTGGTCAGCCAGCGAGTG-3' and
5'-TGGAGAGATCTCATGGTGAGAATCTGCTTCG-3'. The resulting PCR product was cloned into the pCR2.1 vector using the TA cloning kit (Invitrogen) to create pMecr-TA. A FLAG epitope tag was created at the C terminus of *Mecr* by annealing complementary oligonucleotides
5'-GATCCACCATGGATTACAAGGATGACGTACGATAAGA-3' and
5'-GATCTCTTATCGTCGTCATCCTTGTAATCCATGGTG-3' and ligating the resulting product into the pMecr-TA vector that had been digested with BglII, creating pMecr-flagTA. The region encoding MECR-flag was then removed by digestion with EcoRI and BglII and cloned into pSG5 (Agilent Technologies, Inc), creating a plasmid expressing *Mecr* under the control of the SV40 promoter.

Cell culture conditions and plasmid-mediated MECR overexpression

HeLa cells were plated in 10-cm cell culture dishes (CellTreat) at a density of 1.5×10^5 cells/mL in DMEM + 10% FBS (Mediatech, Gibco). After 24 h, MECR OX was achieved by transfecting cells with the pSG5 vector with cloned-in MECR under SV40 promoter

control; control cells received an equal amount of empty pSG5 vector (Agilent Technologies, Inc). HeLa cells were transfected using FuGENE transfection reagent (Promega). After an additional 24 h, cells were harvested by trypsinization and centrifugation. MECR OX was confirmed using real-time quantitative RT-PCR.

Real-time quantitative RT-PCR

Total RNA was isolated using TRIzol Reagent (Life Technologies) according to manufacturer's protocols. First-strand cDNA was created from total RNA using SuperScript® III First-Strand Synthesis SuperMix for quantitative RT-PCR (Life Technologies). Quantitative RT-PCR was performed using TaqMan Expression Assays (Life Technologies) on the ABI 7900 platform according to manufacturer's protocols.

Mitochondrial isolation

Mitochondria from HeLa cells were harvested using the MACS Mitochondria Isolation Kit (Miltenyi) according to manufacturer's protocol. Briefly, approximately 10^7 HeLa cells were washed, lysed, and incubated magnetic beads linked to an anti-TOM22 antibody, which binds the outer surface of the mitochondria. The mitochondria-linked beads were passed through a column in a magnetic field, retaining the beads and mitochondria. Upon removal from the magnetic field, isolated mitochondria were then flushed from the column.

Western blotting

Mitochondrial protein was isolated by lysing mitochondria with five freeze-thaw cycles in liquid nitrogen. Whole-cell protein was isolated using RIPA buffer according to manufacturer's protocol (Sigma-Aldrich). Mitochondrial and whole-cell protein was blotted using Bio-Rad precast gels and PVDF membranes. Mitochondrial protein was assayed by direct application of isolated mitochondria into the loading buffer. To indicate the presence of ER contamination, an

antibody against FACLS4 was used (Santa Cruz), and an anti-PDH antibody (Santa Cruz) was used for protein normalization.

Sample preparation and metabolic profiling of mitochondria

The non-targeted metabolic profiling platform employed for this analysis combined four independent platforms: ultrahigh performance liquid chromatography/tandem mass spectrometry (UHPLC/MS/MS) optimized for basic species, UHPLC/MS/MS optimized for acidic species, UHPLC/MS/MS optimized for polar species, and gas chromatography/mass spectrometry (GC/MS). Sample preparation was carried out as described previously.[184, 207, 208] Briefly, an automated liquid handler (Hamilton LabStar, Salt Lake City, UT) was used to add methanol containing recovery standards to the experimental samples to facilitate protein precipitation. Following centrifugation, the supernatants were split into five aliquots for analysis on the four platforms, with one aliquot retained as a spare. All aliquots were dried under nitrogen and vacuum-desiccated. The samples were subsequently reconstituted in 50 µL 0.1% formic acid in water (acidic conditions) or in 50 µL 6.5 mM ammonium bicarbonate in water, pH 8 (basic conditions) for the UHPLC/MS/MS analyses or derivatized to a final volume of 50 µL for GC/MS analysis using equal parts bistrimethyl-silyl-trifluoroacetamide and solvent mixture acetonitrile:dichloromethane:cyclohexane (5:4:1) with 5% triethylamine at 60°C for one hour. In addition, three types of controls were analyzed in concert with the experimental samples: aliquots of a “client matrix” (formed by pooling a small amount of each experimental sample) served as technical replicates throughout the data set, extracted water samples served as process blanks, and a cocktail of standards spiked into every analyzed sample allowed instrument performance monitoring. Experimental samples and controls were randomized across all platform run days.

For the UHPLC/MS/MS analysis, aliquots were separated using a Waters Acquity UPLC (Waters, Millford, MA) and analyzed using a Q-Exactive high resolution/accurate mass

spectrometer (Thermo Fisher Scientific, Inc., Waltham, MA), which consisted of an electrospray ionization (ESI) source and Orbitrap mass analyzer. Derivatized samples for GC/MS were separated on a 5% phenyldimethyl silicone column with helium as the carrier gas and a temperature ramp from 60°C to 340°C and then analyzed on a Thermo-Finnigan Trace DSQ MS (Thermo Fisher Scientific, Inc.) operated at unit mass resolving power with electron impact ionization and a 50 to 750 atomic mass unit scan range.

Metabolites were identified by automated comparison of the ion features in the experimental samples to a reference library of chemical standard entries that included retention time, molecular weight (*m/z*), preferred adducts, and in-source fragments as well as associated MS spectra, and were curated by visual inspection for quality control using software developed at Metabolon.[185] For data display purposes and statistical analysis, each biochemical was rescaled to set the median equal to one. In addition, any missing values were assumed to be below the limits of detection and these values were imputed with the compound minimum (minimum value imputation). Following median scaling and imputation of missing values, statistical analysis of log-transformed data was performed using "R" (http://cran.r-project.org/), which is a freely available, open-source software package. Biochemicals that differed significantly between the experimental groups were determined in t-tests and/or a two-way ANOVA test. P-values ≤0.05 were considered statistically significant and p-values <0.10 were reported as trends. Multiple comparisons were accounted for by estimating the false discovery rate (FDR) using q-values.[186]

Sphingolipid analysis using liquid chromatography-tandem mass spectrometry (LC-MS/MS)

Sphingolipid extraction from whole cells and mitochondria

Sphingolipid extraction was carried out as previously described.[188] Samples were first spiked with a set of sphingolipid standards and then underwent single-phase lipid extraction using ethyl acetate:iso-propanol:water at a ratio of 60:30:10 by volume.[188] After extraction,

samples were dried under nitrogen gas and resuspended in 150 µL 1 mM ammonium formate in methanol + 0.2% formic acid.

Liquid chromatography-mass spectrometry for sphingolipid levels

LC-MS/MS was performed as previously described.[188] Briefly, samples were analyzed by LC-MS/MS using an Agilent-1100 (Agilent Technologies) HPLC pump equipped with an Agilent-1100 (Agilent Technologies) autosampler, and a Thermo Finnigan TSQ 7000 (Thermo Fisher Scientific) triple quadrupole mass spectrometer with an electrospray ion source (ESI) and syringe pump. LC was carried out using a Spectra C8SR column (Peeke Scientific, Redwood City, CA), 150 × 3.0 mm with a 3-mm particle size. Samples underwent a full scan using tandem mass spectrometry, and sphingolipids were identified by their decomposition signatures. Data was processed using the instrument's data handling software.

Results

Mitochondrial isolation removes ER contamination

Often, mitochondrial preparations are contaminated with ER protein, as the two organelles are directly apposed. To ensure complete mitochondrial purity, we blotted using the ER marker FASCL4 and assayed three sample types: whole HeLa cells, crude HeLa cell mitochondrial preparations, and HeLa cell mitochondria isolated using the Miltenyi Mitochondrial Isolation Kit (Figure 17). For normalization purposes, samples were also blotted using an anti-pyruvate dehydrogenase (PDH) antibody. Only the mitochondria isolated using the Miltenyi Mitochondrial Isolation Kit were free from ER contamination. For this reason, all subsequent mitochondrial isolations were carried out using this kit.

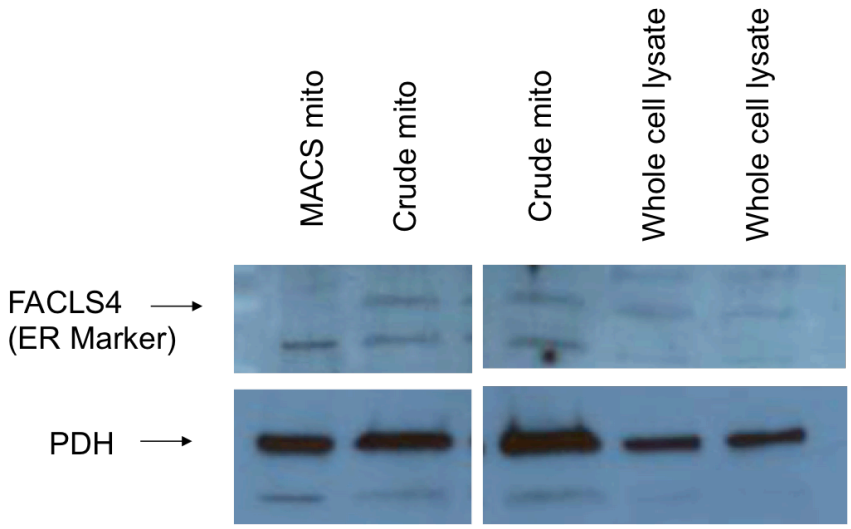

Figure 17. Mitochondrial isolation with anti-TOM22-linked beads removes ER contamination.
Mitochondria from HeLa cells were harvested using the Miltenyi MACS Mitochondria Isolation Kit ("MACS mito") or using the standard cell fractionation kit from MitoSciences ("Crude mito"), both according to manufacturer's protocol. To indicate the presence of ER contamination, an antibody against FACLS4 was used, and anti-PDH antibody was used for normalization.

Metabolomic profiling

To gain a broad view of the mitochondrial changes associated with alterations in mtFASII function, we analyzed isolated mitochondria from ACP KD, CI KD, and MECR OX cells using metabolomics. For each condition, five independent samples were extracted and analyzed using a combination of four independent platforms: UHLC/MS/MS optimized for basic species, UHLC/MS/MS optimized for polar species, UHLC/MS/MS optimized for acidic species, and GC/MS. Of the 316 metabolites analyzed, 46 were significantly altered ($p \leq 0.05$) in ACP KD, 32 in CI KD, and eight in MECR OX mitochondria (Table 3). The biochemicals analyzed in our metabolomics study were organized into pathways, which are discussed below.

	ACP KD/ Control	CI KD/ Control	MECR OX/ Control
Total Biochemicals, p≤0.05	46	32	8
Biochemicals Increased	23	27	2
Biochemicals Decreased	23	5	6
Total Biochemicals, 0.05≤p≤0.1	20	20	13
Biochemicals Increased	16	19	5
Biochemicals Decreased	4	1	8

Table 3. Significantly altered biochemicals.
The total number of biochemicals that reached or neared significance for ACP KD, CI KD, and MECR OX mitochondria are presented.

Tricarboxylic acid (TCA) cycle and amino acid anaplerosis in mitochondria

Metabolomics analysis of isolated HeLa cell mitochondria indicate that the levels of several TCA cycle intermediates are decreased in ACP KD (Figure 18). Levels of amino acid precursors of TCA cycle intermediates asparagine and aspartate were also reduced.

Nicotinamide metabolism in mitochondria

Levels of metabolites involved in nicotinamide metabolism were measured using metabolomics (Figure 19). While the *de novo* pathway of NAD^+ synthesis appears relatively unchanged, the salvage pathway of NAD^+ synthesis is significantly upregulated in ACP KD, whose metabolites include nicotinamide, nicotinamide ribonculeoside, and NAD^+.

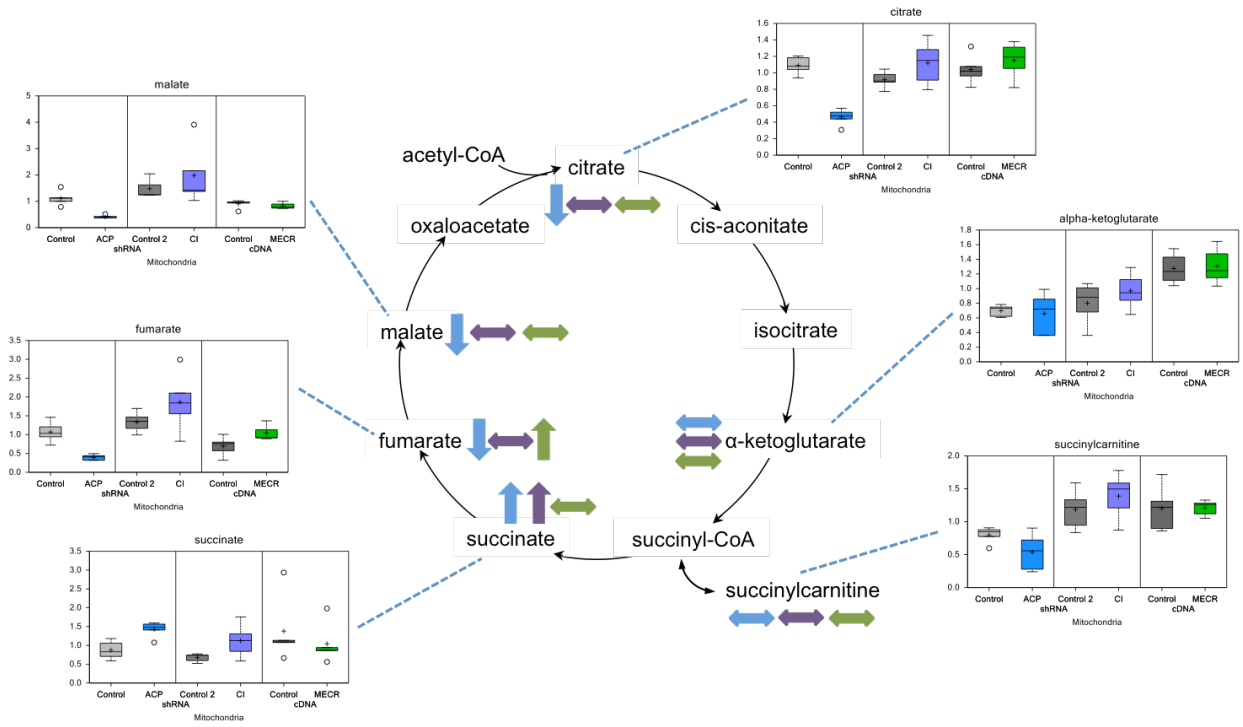

Figure 18. TCA cycle intermediates are altered by changes in mtFASII function.
TCA cycle intermediates that were assayed are indicated with arrows and a corresponding box plot. Y-axes for box plots indicate scaled intensity. Box blot error bars represent the maximum and minimum of the data distribution. Direction of change compared to control in ACP KD is indicated by blue arrows, direction of change relative to control in CI KD is indicated by purple arrows, and direction of change relative to control in MECR OX is indicated by green arrows. In box plots, metabolite levels are shown for ACP KD mitochondria, CI KD mitochondria, and MECR OX mitochondria, and their respective controls. For each box, n=5.

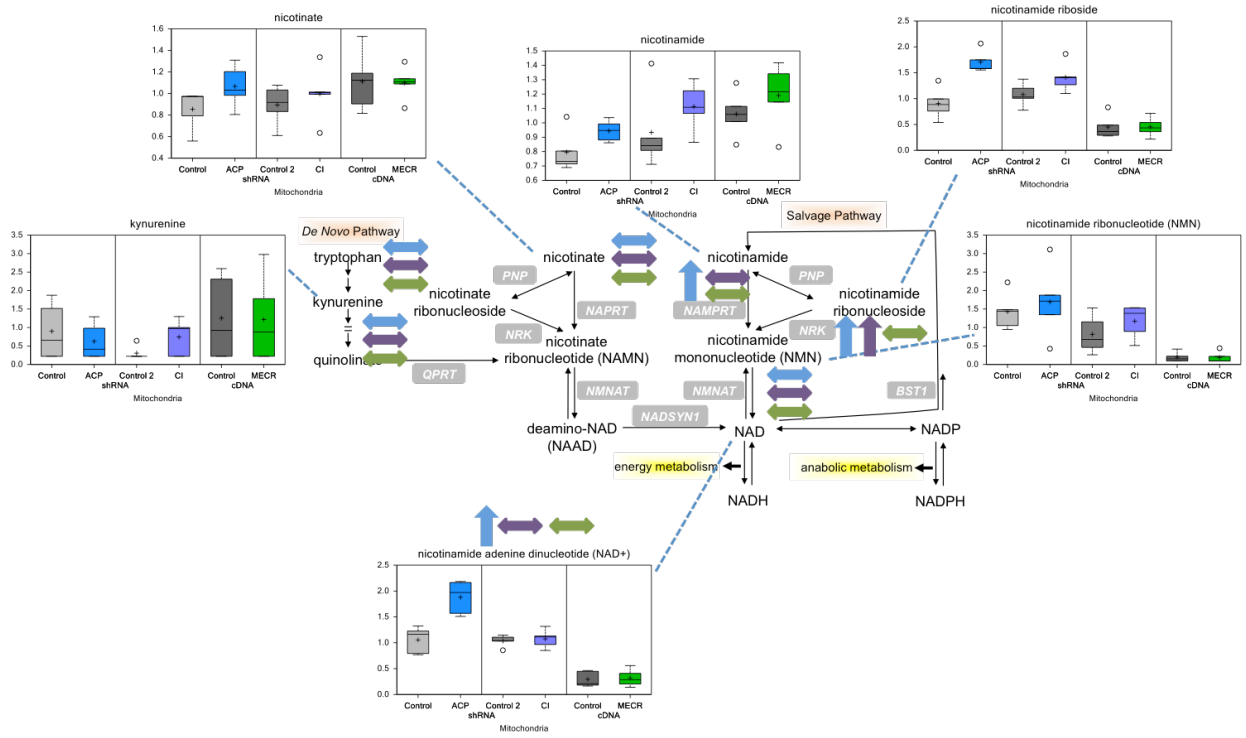

Figure 19. Alterations in mtFASII function affect nicotinamide metabolism in isolated mitochondria.

Nicotinamide metabolism intermediates that were assayed are indicated with arrows and a corresponding box plot. Y-axes for box plots indicate scaled intensity. Box blot error bars represent the maximum and minimum of the data distribution. Direction of change compared to control in ACP KD is indicated by blue arrows, direction of change relative to control in CI KD is indicated by purple arrows, and direction of change relative to control in MECR OX is indicated by green arrows. In box plots, metabolite levels are shown for ACP KD mitochondria, CI KD mitochondria, and MECR OX mitochondria, and their respective controls. For each box, n=5.

Sphingolipid levels in mitochondria

In our previous metabolomics study (Chapter II), we found significant changes in whole-cell sphingolipid regulation with alterations in mtFASII function. We explored whether the sphingolipid changes we saw at the whole-cell level also occurred at the mitochondrial level. LC-MS/MS measurement of whole-cell and mitochondrial sphingolipid levels revealed that the sphingosine:sphingosine-1-phosphate (S1P) ratio is higher in wild-type mitochondria compared to whole cells (Figure 20). However, in ACP KD, the mitochondria's increased sphingosine:S1P

ratio is more pronounced, though not significantly, than that of wild type (Figure 21). The sphingosine:S1P ratio serves as a measure of organelle health, and the increased

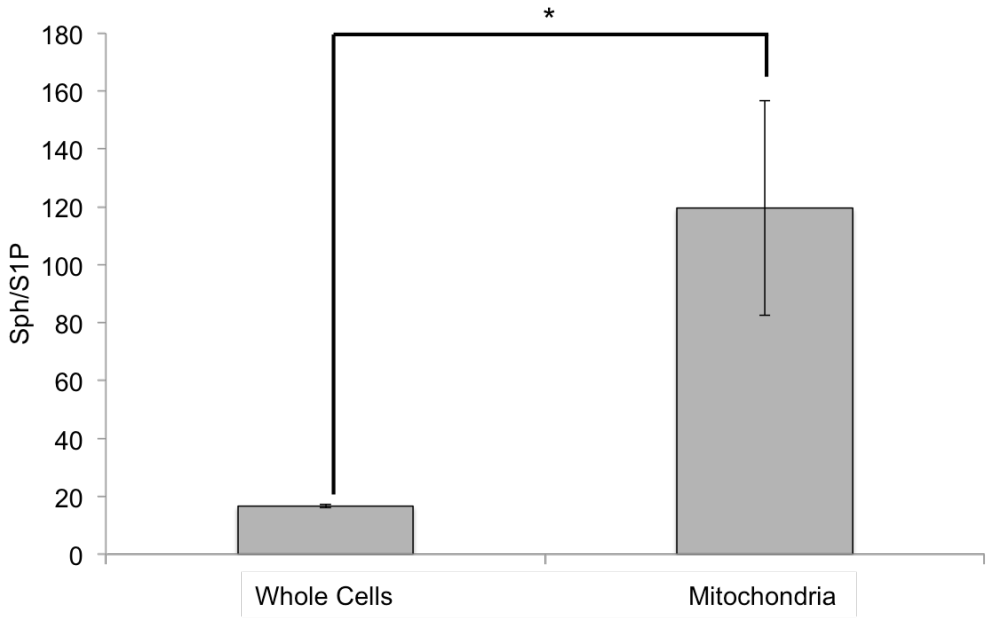

Figure 20. The sphingosine:S1P ratio is increased in mitochondria compared to whole cells.
Sphingosine and S1P levels in wild-type whole HeLa cells were measured using LC-MS/MS, and are expressed as a ratio of their pmol concentrations. n=3, *$p<0.05$.

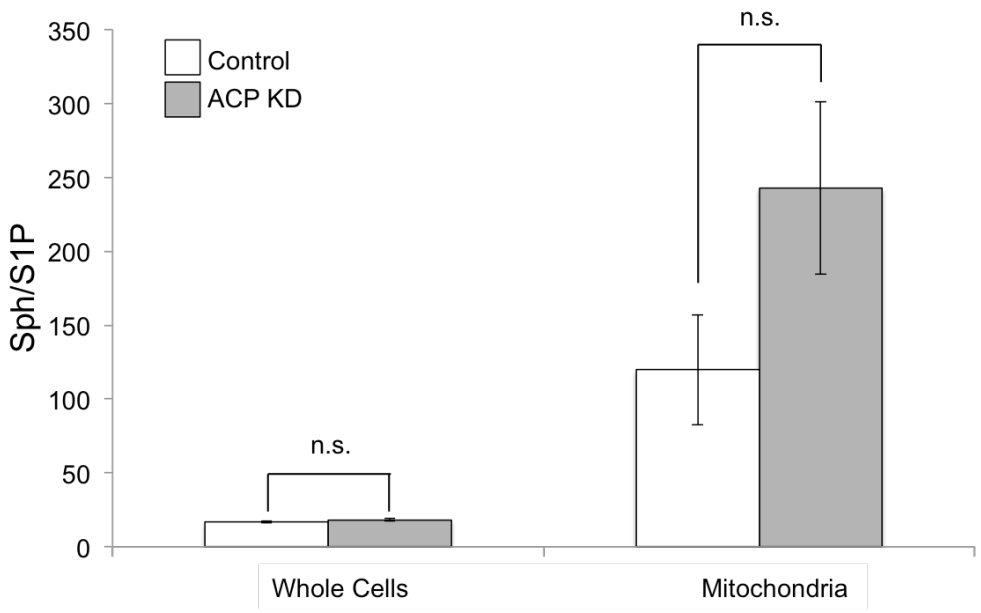

Figure 21. ACP KD increases the sphingosine:S1P ratio in mitochondria but not whole cells.
Sphingosine and S1P levels were measured using LC-MS/MS, and are expressed as a ratio of their pmol concentrations. n=3, *p<0.05, n.s.=nonsignificant

sphingosine:S1P ratio in ACP KD mitochondria is indicative of poor mitochondrial health.

Next, we used LC-MS/MS to measure ceramide levels in control and ACP KD mitochondria and found that ceramide levels are unchanged in ACP KD mitochondria (Figure 22). In the present dataset, only one γ-glutamyl-amino acid, γ-glutamylglutamate, was assessed. Though nonsignificant, γ-glutamylglutamate levels in ACP KD mitochondria were increased more than two fold, suggesting that ROS may be increased in ACP KD mitochondria as they were in whole ACP KD cells.

Presence of dipeptides in mitochondria

Metabolomics analysis of HeLa cell mitochondria determined that ACP KD mitochondria have increased levels of dipeptides, while MECR OX mitochondria have reduced dipeptide levels (Table 4). This phenomenon is not likely due to ETC dysfunction, as dipeptide levels are

oppositely regulated by up- or downregulation of the mtFASII pathway, and dipeptide levels are unaffected by CI KD.

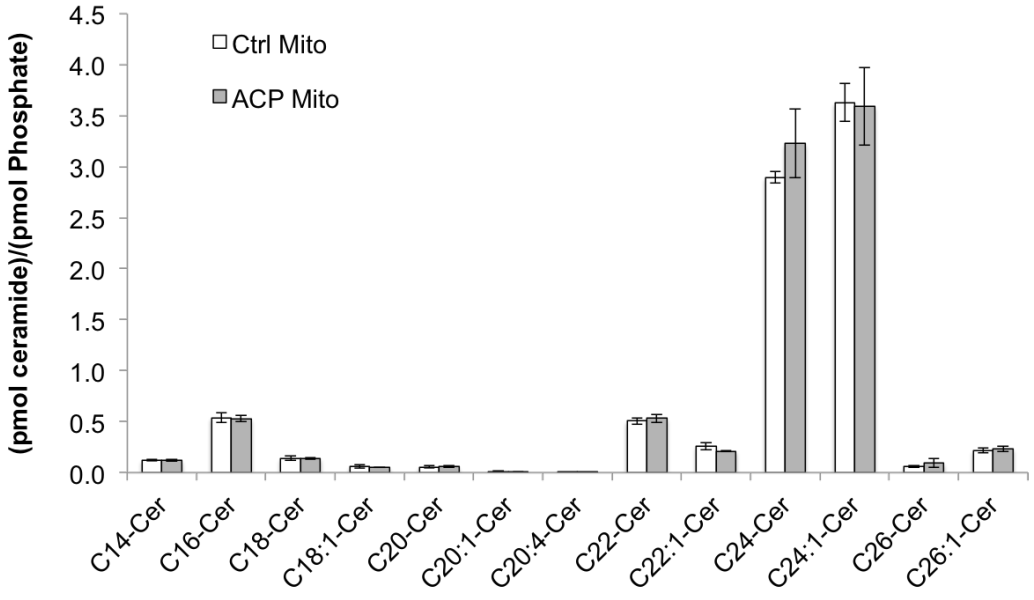

Figure 22. ACP KD does not alter levels of mitochondrial ceramides.
Ceramides from isolated control and ACP KD mitochondria were analyzed by LC-MS/MS, and individual ceramide species are presented as a ratio with intramitochondrial phosphate levels. n=2, *$p<0.05$.

Biochemical Name	ACP KD/ Control	CI KD/ Control	MECR OX/ Control
alanylleucine	3.39	1.10	1.00
glycylleucine	1.53	1.11	**0.77**
glycylvaline	1.43	**1.25**	0.57
isoleucylglycine	**1.27**	1.13	0.81
leucylglycine	1.90	1.13	**0.72**
lysylleucine	1.55	1.19	1.05
phenylalanylalanine	1.50	1.16	0.80
phenylalanylglycine	1.58	1.09	**0.70**
prolylglycine	1.17	1.46	0.85
threonylphenylalanine	1.56	1.18	0.76
tryptophylglycine	1.71	1.10	0.89
valylglutamine	1.99	1.17	0.82
valylglycine	1.68	1.11	**0.76**
valylleucine	1.75	1.19	0.77

Table 4. Dipeptide levels inversely correlate with mtFASII function.
All dipeptides assayed by metabolomics are presented with their corresponding levels in ACP KD, CI KD, or MECR OX, each normalized to its own control. Dark green boxes indicate significant downregulation, and red boxes indicate significant upregulation. Light green boxes indicate trending downregulation, and pink boxes indicate trending upregulation. Metabolite levels were deemed significant when $p<0.05$. Trending changes occurred when fold changes were $0.05<p<0.1$.

Discussion

The mtFASII pathway is highly conserved, yet its role beyond the synthesis of fatty acids is not fully understood. Knockdown of any mtFASII component results in respiratory deficiency, and previous research from our lab indicates that the mtFASII pathway may be involved in mitochondrial-nuclear communication.[25] In a previous study of mtFASII knockdown or overexpression in whole cells, we identified a respiratory-deficient phenotype in mtFASII KD cells, as is seen in other work (Chapter II).[3, 6, 10, 13, 14, 19, 22, 36, 46-49] Additionally, our previous work showed that alteration of mtFASII resulted in a concomitant change in whole-cell bioactive lipid regulation (Chapter II). In order to better understand the phenotypes observed with changes in mtFASII functionality, we investigated the effects of ACP KD and MECR OX in isolated mitochondria.

Because the mitochondria and ER are so closely apposed, we sought to ensure that our mitochondrial preparations were free from ER contamination. Using a marker for the mitochondrial associated ER membrane, FASCL4, we showed that our mitochondrial isolation technique is free of ER protein.

Consistent with previous research, including work from our lab, the current dataset indicates that ACP KD suppresses of the TCA cycle. ACP KD resulted in reduced levels of TCA cycle intermediates citrate, malate, and fumarate. This result could arise multiple ways. First, the mtFASII pathway is a known source of lipoate for protein lipoylation, and several TCA cycle enzymes require lipoylation for proper function.[2, 12, 34, 38] Secondly, respiratory deficiency elicited by ACP KD may result in increased reliance on glucose for energy, as opposed to oxidative phosphorylation. In this case, gluconeogenesis rates would increase, requiring cataplerosis of TCA cycle intermediates. Because the MECR OX phenotype is less pronounced compared to that of ACP KD, MECR OX mitochondria showed only one change in the TCA cycle—MECR OX results in increased fumarate levels. This data point may indicate an overall increase in TCA cycle activity. It is possible that increased mtFASII function through MECR OX results in increased TCA cycle activity and a subsequent increase in TCA cycle intermediate levels. Though CI KD should result in respiratory deficiency at the level of the ETC, no changes were seen in TCA cycle metabolite levels in CI KD mitochondria. This lack of change could have several causes, including differences in knockdown efficiency between ACP KD and CI KD or differences in the severity of the respiratory deficiency elicited by ACP KD and the specific CI KD used in this study.

ACP KD mitochondria showed increased NAD^+ salvage pathway activity with increased levels of NAD^+, nicotinamide, and nicotinamide ribonucleoside. Nicotinamide synthesis occurs in two separate pathways. The *de novo* pathway synthesizes NAD^+ from dietary tryptophan, whereas the salvage pathway synthesizes NAD^+ using a series of largely reversible reactions involving molecules closely related to NAD^+, including nicotinamide, nicotinamide

mononucleotide, and nicotinamide ribonucleoside.[209] The rate-limiting enzyme in both pathways is nicotinamide mononucleotide adenylyltransferase (NMNAT), which has nuclear, cytosolic, and mitochondrial isoforms.[210, 211]

Potentially because *de novo* NAD^+ synthesis largely occurs in the cytosol, *de novo* pathway metabolites are unchanged in mitochondria of any treatment group. In light of the cell's depressed respiratory state in ACP KD, it is likely that elevated NAD^+ levels in ACP KD mitochondria are the result of reduced NADH levels. Because of the interconvertability between NAD^+ and the other molecules in the salvage pathway, increased salvage pathway metabolites may reflect elevated NAD^+ levels. Another potential cause of increased NAD^+ levels in ACP KD mitochondria is suppression of the TCA cycle. One product of the TCA cycle is NADH. Given the reduced TCA cycle metabolite levels seen in ACP KD mitochondria, less NADH is being produced, resulting in a rise in NAD^+ levels. A third potential route for increased NAD^+ levels is through elevated ROS levels. CSSG and γ-glutamylglutamate, markers of increased reactive oxygen species, are elevated in ACP KD mitochondria, indicating the presence of increased ROS levels. ROS detoxification consumes NADPH, raising NADP levels. NADP can subsequently be converted to NAD^+ by mitochondrial transhydrogenase;[209, 211] elevated NADP levels, then, can translate to increased NAD^+ levels.

In previous work from our lab, we found that ACP KD had a significant impact on cellular sphingolipid levels (Chapter II). To identify if whole-cell changes in sphingolipid levels are also seen at the mitochondrial level, we assayed for sphingolipids in isolated mitochondria using LC-MS/MS. Similar to results at the whole-cell level, mitochondrial ceramide levels are not affected by ACP KD. However, when we investigated sphingosine:S1P ratios in control whole HeLa cells compared to isolated control-cell mitochondria, we found that mitochondria have higher sphingosine:S1P ratios compared to the whole cell. Thus, what occurs at the whole-cell level may not be representative of what occurs at the mitochondrial level. We also found that ACP KD results in a nonsignificantly increased sphingosine:S1P ratio in the mitochondria. S1P

is an important anti-apoptosis signal, as it inhibits synthesis of pro-apoptosis ceramides through ceramide synthase 2 (CerS2).[121] Normally, elevated S1P levels would indicate that the mitochondria are in good health. However, S1P exists in a balance with pro-apoptosis sphingosine. Sphingosine promotes apoptosis by inhibiting ceramide breakdown through alkaline ceramidase 3, leading to inhibition of the ETC and increased outer mitochondrial membrane permeability.[121, 141] Because the sphingosine:S1P ratio in ACP KD mitochondria is increased, it is likely that the increased S1P levels seen in ACP KD mitochondria are overshadowed by an even larger increase in sphingosine levels. Overall, the lack of expected change in ceramide levels in ACP KD mitochondria along with the ACP KD-related changes in sphingosine:S1P ratios indicate a role for mtFASII in sphingolipid regulation or sphingolipid signaling.

The most interesting changes in the current dataset were among dipeptides. Dipeptides were at increased levels in ACP KD mitochondria, and decreased in MECR OX mitochondria. CI KD mitochondria showed no clear pattern of regulation. Of the 14 dipeptides assayed, 12 were increased in ACP KD mitochondria, five were decreased in MECR OX, and two were increased in CI KD. One possible cause for changes in dipeptide levels is alterations in protein degradation. In *Arabidopsis thaliana*, induction of oxidative stress activates mitochondrial proteases, resulting in degradation of specific mitochondrial proteins, including components of CI and ATP synthase, as well as TCA cycle enzymes aconitase and fumarase.[212] ACP KD mitochondria likely have increased ROS levels, which translate to mitochondrial protein damage. Protein damage then triggers activity of mitochondrial proteases, resulting in protein degradation into small peptides.

Mitochondrial proteolysis has recently been shown to initiate the mitochondrial unfolded protein response (mtUPR), a retrograde signaling mechanism from the mitochondria to the nucleus. The mtUPR can be triggered by a variety of circumstances, including accumulation of unfolded proteins in the mitochondria and unbalanced levels of mitochondria-encoded and

nucleus-encoded mitochondrial genes.[106, 108, 109, 115] In mammals, mitochondrial peptides are exported into the cytosol and, by an unknown mechanism, activate the transcription factors CCAAT-enhancer-binding protein homologous protein (CHOP) and CCAAT-enhancer-binding protein β (C/EBPβ).[106-109] The end result of the mtUPR is upregulation of nuclear genes encoding mitochondrial chaperones and proteases, resulting in reduction of stress on the mitochondria.[106, 109, 110] In the case of ACP KD, it is possible that elevated ROS could induce the mtUPR, though ROS-mediated induction of the mtUPR has not been clearly demonstrated.[113] Other methods of mtUPR activation such as mitonuclear protein imbalance were not assayed in this study, though mtFASII components are known to affect mitochondrial tRNA processing, which could affect mitonuclear protein balance.[3, 9, 19, 57]

While the complete nature of mtFASII's role in the cell is not yet understood, this study has provided useful insight into the pathway's effects at the level of the mitochondria. Many of our observations are consistent with previous research, including work from our own lab (Chapter II). These new data demonstrate that many of the metabolite changes in ACP KD mitochondria are not simply due to respiratory deficiency, as these changes were not seen in mitochondria with deficient complex I of the ETC. Additionally, this study provides novel insight into a potential role for mtFASII in the mtUPR, with ACP KD resulting in increased mitochondrial dipeptide levels. In light of the potential role of the mtFASII pathway in signaling through both lipids and the mtUPR, our next study will explore the contents of mitochondrial secretions, or the mitochondrial secretome.

CHAPTER IV

CHARACTERIZATION OF THE MITOCHONDRIAL SECRETOME AND THE CONTRIBUTION OF THE MITOCHONDRIAL FATTY ACID SYNTHESIS II (MTFASII) PATHWAY TO ITS CONTENTS

Abstract

Because nearly all mitochondrial genes are encoded in the nuclear genome, mitochondria must be able to communicate with the nucleus to regulate expression of mitochondrial genes based on need. Previous work from our lab has indicated that the mitochondrial fatty acid synthesis II (mtFASII) pathway may have a role in mitochondrial signaling through both lipid- and peptide-mediated signaling. For this reason, we investigated the contents of mitochondrial secretions, or the mitochondrial secretome, and how the secretome's contents are altered by disruption of the mtFASII pathway or knockout of complex I of the electron transport chain. We found that the mitochondrial secretome may contain bioactive lipids and small peptides, and that knockdown of the mtFASII pathway results in increased levels of dipeptides, among other metabolites, in the mitochondrial secretome. These data indicate that the mtFASII pathway may have a role in mitochondrial signaling in a manner not linked to mtFASII's effects on the electron transport chain.

Introduction

Mitochondria are cellular organelles that were originally derived from a symbiotic relationship between an aerobic proto-prokaryote and an anaerobic proto-eukaryote. As such, mitochondria maintain several bacterial-like traits, including a double membrane and a circular, polycistronic genome. Additionally, mitochondria retain a bacterial-like fatty acid synthesis pathway, the mitochondrial fatty acid synthesis II (mtFASII) pathway. Like the bacterial fatty acid synthesis II (FASII) pathway, mtFASII employs a series of enzymes, each catalyzing a different

step of fatty acid synthesis. Eukaryotes also contain a cytosolic fatty acid synthesis I (FASI) pathway which is catalyzed by a single, multi-functional enzyme, FASN.[1] Because FASN generates the vast majority of the cell's fatty acids, the reason for mtFASII's conservation is unclear. Likewise, the end-use of many mtFASII products is not known.

One mtFASII product, octanoate, is known to contribute to lipoic acid synthesis: radiolabeled tracers have tracked individual carbon atoms from the mtFASII pathway to lipoic acid.[2, 38, 44, 45] Also, loss of mtFASII function abolishes mitochondrial protein lipoylation.[3, 4, 6, 9, 10, 19, 34, 46, 47] Lipoic acid is important for mitochondrial respiration, as multiple tricarboxylic acid (TCA) cycle enzymes require lipoylation for function.[46] Though a major product of the mtFASII pathway, octanoate is not the pathway's only product.[2, 3, 38] In mammals, the mtFASII pathway synthesizes fatty acids up to 14 carbons long, while in plants, up to 16-carbon fatty acids have been observed.[2, 3, 32, 38] Additionally, the mtFASII pathway has apparent roles outside lipoic acid synthesis, as the pathway is vital for assembly of complex I of the electron transport chain (ETC) as well as mitochondrial tRNA processing, both through unknown mechanisms.

Our lab recently identified that the mtFASII pathway may have roles in mitochondrial signaling through bioactive lipids, small peptides, or both (Chapters II and III). Because the vast majority of mitochondrial proteins are encoded in the nuclear genome, mitochondria must be able to signal their needs to the nucleus. Knockdown of the mtFASII component acyl carrier protein (ACP) in whole HeLa cells resulted in reduced bioactive lipid levels, including lysophospholipids and sphingolipids (Chapter II). In isolated mitochondria, ACP knockdown resulted in increased dipeptide levels (Chapter III). Though no retrograde signaling pathway involving bioactive lipids has been identified, mitochondria are known to use peptides to signal to the nucleus during the mitochondrial unfolded protein response (mtUPR), resulting in the upregulation of mitochondrial chaperones and proteases. Additionally, work from our lab has shown that the mtFASII pathway is capable of mediating mitochondrial-nuclear communication via the PPAR pathway.[25]

To further explore the role of the mtFASII pathway in mitochondrial signaling, we characterized mitochondrial secretions, or the mitochondrial secretome. For the mitochondria to communicate with the nucleus, mitochondria must secrete a signaling molecule, the identity of which has not been fully characterized. To investigate whether the mitochondrial secretome contains potential signaling molecules, we used liquid chromatography-mass spectrometry (LC-MS) and metabolomics. Additionally, we used metabolomics to assess the impact of loss of mtFASII or complex I function on the secretome's composition. We show that mitochondria are secreting substances consistent with both bioactive lipids and small peptides, and that loss of mtFASII or complex I function alters the secretome makeup.

Experimental Procedures

Cell culture conditions and shRNA knockdown of ACP and complex I

HeLa cells were plated in 10-cm cell culture dishes (CellTreat) at a density of 1.5×10^5 cells/mL in DMEM + 10% FBS (Mediatech, Gibco). Knockdown of the mtFASII pathway and complex I of the ETC was achieved using Qiagen Flexitube siRNAs specific for the genes for ACP (*NDUFAB1*) and the complex I component (*NDUFS3*), respectively; control cells were transfected with Allstars negative control siRNA (Qiagen). HeLa cells were transfected with siRNA using HiPerfect Transfection Reagent (Qiagen). After 48 h, cells were trypsinized, resuspended in double their original volume of DMEM + 10% FBS, retransfected, then plated in a 15-cm dish for an additional 48 h. At 96 h, cells were harvested by trypsinization and centrifugation. Knockdown efficiency was measured after 96 h using real time quantitative RT-PCR.

Real time quantitative RT-PCR

Total RNA was isolated using TRIzol Reagent (Life Technologies) according to manufacturer's protocols. First-strand cDNA was created from total RNA using SuperScript® III

First-Strand Synthesis SuperMix for quantitative RT-PCR (Life Technologies). Quantitative RT-PCR was performed using TaqMan Expression Assays (Life Technologies) on the ABI 7900 platform according to manufacturer's protocols.

Mitochondrial isolation

Mitochondria from HeLa cells were harvested using the MACS Mitochondria Isolation Kit (Miltenyi) according to manufacturer's protocol. Briefly, approximately 10^7 HeLa cells were washed, lysed, and incubated with magnetic beads linked to an anti-TOM22 antibody, which binds the outer surface of the mitochondria. The mitochondria-bound beads were passed through a column in a magnetic field, retaining the beads and mitochondria. Upon removal from the magnetic field, isolated mitochondria were then flushed from the column.

Citrate synthase assay

Mitochondria isolated using the MACS Mitochondria Isolation Kit (Miltenyi) were examined for intactness using a citrate synthase assay kit (Sigma-Aldrich) according to manufacturer's instructions. Citrate synthase is a TCA cycle enzyme, and its reaction product, CoA-SH, reacts with a 5,5'-dithiobis-(2-nitrobenzoic acid) (DTNB) supplied in the assay, resulting in the production of 5-thio-2-nitrobenzoic acid (TNB). TNB absorbs light at 412 nm, so TNB production and, thus, the rate of citrate synthase activity, can be monitored using a spectrophotometer.

Briefly, isolated mitochondria from approximately 10^7 HeLa cells were incubated for 0 minutes or 6 hours, then were separated into two equal aliquots, one in which mitochondria were left intact, and one in which mitochondria were lysed. Because citrate synthase activity is restricted to the mitochondrial matrix, inner mitochondrial membrane intactness can be assessed by comparing the citrate synthase activity in a sample of intact mitochondria to that of a sample of lysed mitochondria.

Mitochondrial secretome collection

Isolated mitochondria were suspended in 200 µL buffer containing 100 mM 3-(N-morpholino)propanesulfonic acid (MOPS, pH 7.1), 2 mM dithiothreitol (DTT), 4.5 mM nicotinamide adenine dinucleotide (NAD), 4.5 mM nicotinamide adenine dinucleotide phosphate (NADP), 5 mM adenosine triphosphate (ATP), 2 mM $MgCl_2$, 4 mM coenzyme A (CoA), and 20 µL malonate.[2] Upon suspension in reaction buffer, samples were immediately separated into two 100-µL aliquots, one for a zero-minute incubation time, and one for a 90-minute incubation time. The zero-minute incubation time samples were immediately centrifuged to pellet mitochondria. The 90-minute incubation time samples were kept at 37˚C for 90 min, followed by pelleting the mitochondria by centrifugation. Immediately after centrifugation, the supernatant was isolated from the mitochondrial pellet and stored at -70˚C until they were used for downstream analysis.

Comparison of changed biochemicals by LC-MS

Sample preparation

Lipids were extracted from mitochondrial secretomes using a modified Folch extraction.[179] First, samples were spiked with a standard cocktail containing equal amounts 17:0 lysophosphatidylcholine, 17:0 phosphatidylcholine, and 1,2,3-triheptadecanoyl-glycerol, all diluted in methanol. Mitochondrial lysates and secretomes were combined with two volumes chloroform and methanol + standards. Samples were shaken vigorously and then phase-separated by centrifugation. The lower, lipid-containing layer was removed and combined with an additional volume of chloroform, followed by shaking and centrifugation. This process was repeated twice. Lipid samples were further purified by undergoing the same phase-separation process with 0.25 volumes 1 M KCl, then with 0.25 volumes water. Next, samples were dried down under nitrogen gas, then reconstituted in 50 µL methanol + 0.1% formic acid.

Liquid chromatography-mass spectrometry (LC-MS)

LC-MS was performed at the Vanderbilt University Mass Spectrometry Core as described in Ehrmann et al., 2013.[213] Briefly, samples were analyzed by LC-MS using a Waters Acquity UPLC (Waters Corp.) instrument linked to a Waters Synapt Q-TOF mass spectrometer (Waters Corp.). LC was carried out using a Waters Symmetry Shield 300TM C18 3.5 µm reverse phase column, 2.1 × 100 mm (Waters Corp.) using a binary solvent manager. MS analysis involved a full scan in positive ion mode, with the instrument set to the parameters listed in Table 5. MassLynx V4.1 SCN639 software (Waters Corp.) was used for data collection and quality control. Comparison of spectra across treatment groups and identification of potential metabolites was performed using XCMS Online (Scripps).

Mode	Positive
Desolvation Gas (N_2)	800 l/h, 350˚C
Capillary Voltage	2.25 kV
Sampling Cone Voltage	40 V
Extraction Cone Voltage	4 V
Source Temperature	125˚C
Nominal Mass Resolution	10,000 [(peak width at half height)$^{-1}$ × m/z]
Scan Speed	2 s
Mass Range	500-3,000 m/z

Table 5. Mass spectrometer settings for replication of metabolomics using LC-MS/MS.

Sample preparation and metabolic profiling of mitochondrial secretomes

The non-targeted metabolic profiling platform employed for this analysis combined four independent platforms: ultrahigh performance liquid chromatography/tandem mass spectrometry (UHPLC/MS/MS) optimized for basic species, UHPLC/MS/MS optimized for acidic species, UHPLC/MS/MS optimized for polar species, and gas chromatography/mass

spectrometry (GC/MS). Sample preparation was carried out as described previously.[184, 207, 208] Briefly, an automated liquid handler (Hamilton LabStar, Salt Lake City, UT) was used to add methanol containing recovery standards to the experimental samples to facilitate protein precipitation. Following centrifugation, the supernatants were split into five aliquots for analysis on the four platforms, with one aliquot retained as a spare. All aliquots were dried under nitrogen and vacuum-desiccated. The samples were subsequently reconstituted in 50 µL 0.1% formic acid in water (acidic conditions) or in 50 µL 6.5 mM ammonium bicarbonate in water, pH 8 (basic conditions) for the UHPLC/MS/MS analyses or derivatized to a final volume of 50 µL for GC/MS analysis using equal parts bistrimethyl-silyl-trifluoroacetamide and solvent mixture acetonitrile:dichloromethane:cyclohexane (5:4:1) with 5% triethylamine at 60°C for one hour. In addition, three types of controls were analyzed in concert with the experimental samples: aliquots of a "client matrix" (formed by pooling a small amount of each experimental sample) served as technical replicates throughout the data set, extracted water samples served as process blanks, and a cocktail of standards spiked into every analyzed sample allowed instrument performance monitoring. Experimental samples and controls were randomized across all platform run days.

For the UHLC/MS/MS analysis, aliquots were separated using a Waters Acquity UPLC (Waters, Millford, MA) and analyzed using a Q-Exactive high resolution/accurate mass spectrometer (Thermo Fisher Scientific, Inc., Waltham, MA), which consisted of an electrospray ionization (ESI) source and Orbitrap mass analyzer. Derivatized samples for GC/MS were separated on a 5% phenyldimethyl silicone column with helium as the carrier gas and a temperature ramp from 60°C to 340°C and then analyzed on a Thermo-Finnigan Trace DSQ MS (Thermo Fisher Scientific, Inc.) operated at unit mass resolving power with electron impact ionization and a 50-750 atomic mass unit scan range.

Metabolites were identified by automated comparison of the ion features in the experimental samples to a reference library of chemical standard entries that included retention

time, molecular weight (*m/z*), preferred adducts, and in-source fragments as well as associated MS spectra, and were curated by visual inspection for quality control using software developed at Metabolon.[185]

For data display purposes and statistical analysis, each biochemical was rescaled to set the median equal to 1. In addition, any missing values were assumed to be below the limits of detection and these values were imputed with the compound minimum (minimum value imputation). Following median scaling and imputation of missing values, statistical analysis of log-transformed data was performed using "R" (http://cran.r-project.org/), which is a freely available, open-source software package. Biochemicals that differed significantly between the experimental groups were determined in t-tests and/or a two-way ANOVA test. P-values ≤0.05 were considered statistically significant, and p-values <0.10 were reported as trends. Multiple comparisons were accounted for by estimating the false discovery rate (FDR) using q-values.[186]

ELISA for sphingosine-1-phosphate

Sphingosine-1-phosphate (S1P) levels were determined in HeLa cells using the S1P ELISA Kit (Echelon Biosciences) according to manufacturer's protocol. Protein concentrations in each sample were first determined using BSA protein assay (Bio-Rad) according to manufacturer's protocol. 40 µg protein was used for each well in triplicate per sample.

Results

Citrate synthase assay for mitochondrial intactness

To ensure that isolated mitochondria were intact and, therefore, usable in subsequent assays, we compared citrate synthase activity in samples of lysed mitochondria to that of mitochondria that were not lysed after incubation in mitochondrial secretion assay buffer for 0 minutes or 6 hours. Because citrate synthase is a TCA cycle enzyme, its activity should be restricted to the mitochondrial matrix. For this reason, citrate synthase activity would be higher

in lysed mitochondria compared to intact mitochondria. In the citrate synthase assay kit (Sigma-Aldrich) used, rates of citrate synthase activity are measured by observing the production rate of a yellow dye.

This mitochondrial intactness assay indicated that, after 6 hours of incubation in mitochondrial secretion assay buffer, the percent of mitochondria that were ruptured rose from 19.0% at 0 minutes to 29.5% at 6 hours (Figure 23). These data indicate that mitochondria isolated in our laboratory are largely intact, even after several hours.

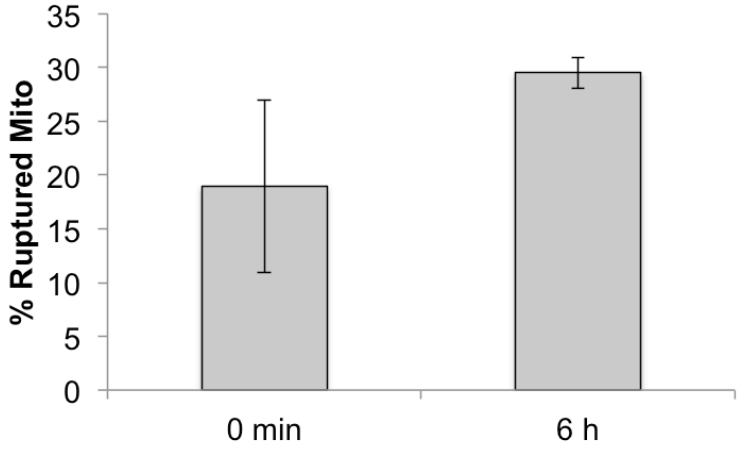

Figure 23. Isolated mitochondria remain largely intact.
Isolated mitochondria were measured for intactness after 0 minutes or 6 hours of culture in mitochondrial secretion assay buffer. n=2.

LC-MS analysis of mitochondrial secretome biochemicals

In light of the roughly 1500 mitochondrial genes housed in the nuclear genome, mitochondria and the nucleus must communicate in order to coordinate gene expression. For the mitochondria to communicate with the nucleus, mitochondria might be expected to secrete a signaling molecule, the identity of which has not been fully characterized. To determine if we could detect molecules secreted by the mitochondria, we performed pilot LC-MS experiments

on isolated mitochondria. Mitochondria from normal and ACP KD cells were incubated in a mitochondrial secretion assay buffer[2] for zero or 90 minutes. We then separated the mitochondria from the assay buffer by centrifugation, and analyzed the assay buffer's contents using LC-MS.

Comparing control-mitochondrial secretomes between zero and 90 minutes, our analysis yielded 33 metabolites for which $p<0.01$ and the fold change >2 (Figure 24). All but one of these metabolites was upregulated at 90 minutes compared to zero minutes. We attempted to identify these metabolites using XCMS online, but there was an average of 18.4 possible identities for each metabolite, leaving us unable to make a positive identification for any one metabolite. However, 14 of these secreted metabolites had a possible match with bioactive lipids, and 11 had potential matches with small peptides.

Metabolomic profiling

Our analysis of the mitochondrial secretome using LC-MS provided preliminary evidence that mitochondria secrete a number of lipid-soluble substances. To gain a more specific understanding of the secretome's contents, we used metabolomic analysis. To assess the secretome's contents at baseline, we analyzed secretomes collected from control siRNA-treated cells. To investigate mtFASII-related changes in secretome contents, we also analyzed secretomes collected from ACP siRNA-treated and CI siRNA-treated mitochondria using four independent platforms: UHPLC/MS/MS optimized for basic species, UHPLC/MS/MS optimized for acidic species, UHPLC/MS/MS optimized for polar species, and GC/MS. 106 biochemicals were analyzed in all conditions (Control siRNA, ACP siRNA, and CI siRNA) at zero-minute and 90-minute time points. Control siRNA-treated secretomes contained 66 significantly upregulated biochemicals and four downregulated biochemicals, while ACP KD secretomes contains 63 upregulated biochemicals and one downregulated biochemical, and CI KD secretomes contained 60 upregulated biochemicals and four downregulated biochemicals (Table 6).

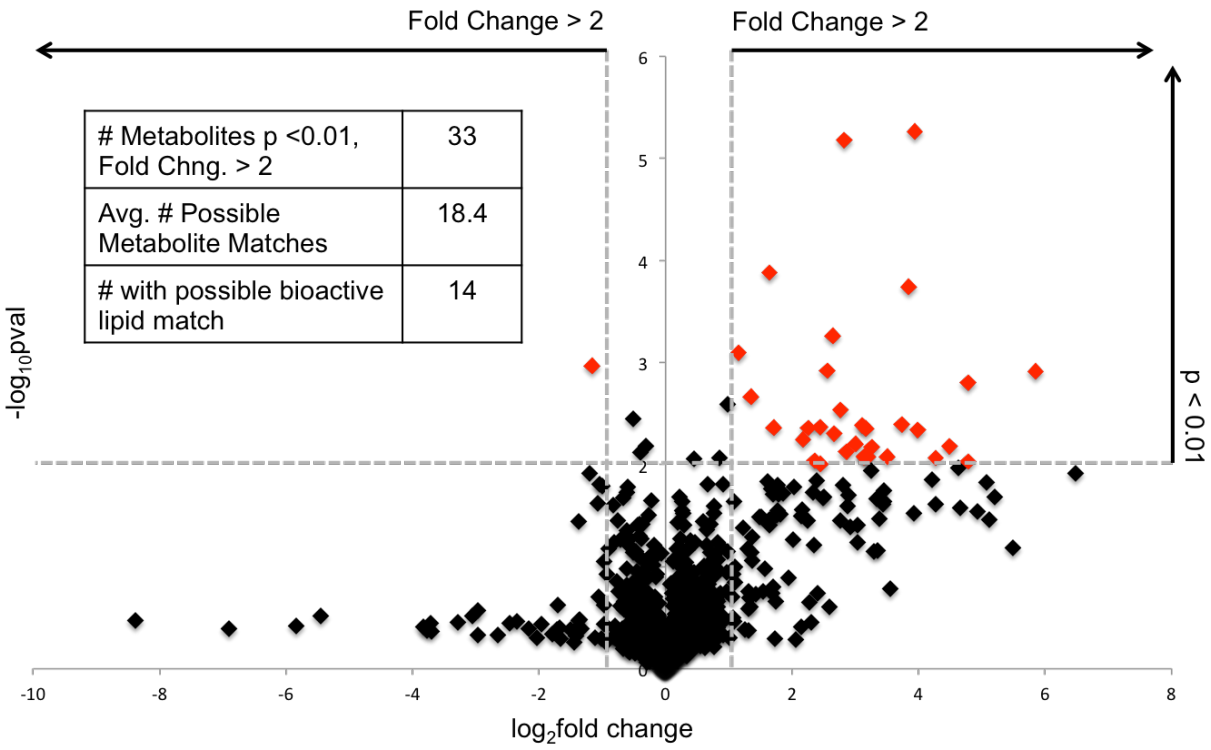

Figure 24. Mitochondria secrete a number of substances.
The mitochondrial secretome was analyzed after 0 minutes and 90 minutes incubation by LC-MS. Scans were aligned and metabolites identified using XCMS Online. Metabolites are presented in a volcano plot. Horizontal gray lines indicate the cutoff for statistically significantly changed metabolites (p<0.01). Vertical gray lines indicate the cutoff for metabolites changed more than two-fold. Metabolites for which p<0.01 and fold change >2 are indicated in red. n=3.

	Control siRNA 0 min vs 90 min	ACP KD 0 min vs 90 min	CI KD 0 min vs 90 min
Total Biochemicals, p≤0.05	70	64	64
Biochemicals Increased	66	63	60
Biochemicals Decreased	4	1	4
Total Biochemicals, 0.05≤p≤0.1	10	11	9
Biochemicals Increased	8	11	8
Biochemicals Decreased	2	0	1

Table 6. Significantly altered biochemicals.
The total number of biochemicals that reached or neared significance when comparing zero-minute to 90-minute time points for Control, ACP KD, and CI KD secretomes are presented.

Metabolomic analysis of control mitochondrial secretomes

To further characterize the contents of the mitochondrial secretome, we performed metabolomics on mitochondrial secretomes collected from control shRNA-treated mitochondria. Control mitochondria secreted a number of substances, including metabolites related to energy production pathways such as glycolysis and the TCA cycle. Additionally, control mitochondrial secretomes contained several amino acids, dipeptides, and metabolites related to nucleotide metabolism.

In addition to molecules whose levels increase with time during the mitochondrial secretion assay, the levels of some molecules decrease, indicating absorption into the mitochondria. These molecules include malonate, NAD+, and phosphopantetheine.

Metabolomic analysis of ACP KD and CI KD mitochondrial secretomes

When using metabolomics to compare zero-minute and 90-minute time point secretomes, several trends became apparent among ACP KD and CI KD mitochondrial secretomes (Table 7). Compared to control, ACP KD mitochondria trended toward increased secretion of amino acids, dipeptides, lysophospholipids, glycerol-3-phosphate, and AMP. ACP KD mitochondria trended toward secretion of lower amounts of spermidine, sphingosine, and ADP. In CI KD mitochondria, only lysophospholipid secretion showed a trend toward increased levels; secretion of amino acids, spermidine, and ADP trended toward decreased levels compared to control. Though ACP KD and CI KD resulted in similar changes in secretion of spermidine, lysophospholipids, and ADP, the other metabolites that were changed in ACP KD were not changed in CI KD. This lack of correlation between ACP KD and CI KD secretomes indicates that the ACP KD phenotype is not solely due to CI dysfunction.

ACP KD secretome vs. Control siRNA secretome	CI KD secretome vs. Control siRNA secretome
Increased amino acid secretion	**Decreased amino acid secretion**
Reduced spermidine secretion	**Reduced spermidine secretion**
Increased secretion of 5/7 dipeptides analyzed	Increased secretion of 3/7 dipeptides analyzed and decreased secretion of 1/7 dipeptides analyzed
Increased lysophospholipid secretion	**Increased lysophospholipid secretion**
Decreased sphingosine secretion	No change in sphingosine secretion
Increased G3P secretion	No change in G3P secretion
Increased AMP secretion	No change in AMP secretion
Decreased ADP secretion	**Decreased ADP secretion**

Table 7. Heatmap of pathway trends in ACP KD secretomes and CI KD secretomes compared to their respective controls.
Red boxes indicate increasing trends and green boxes indicate decreasing trends.

Sphingosine-1-phosphate (S1P) ELISA

Because our previous studies have implicated the mtFASII pathway in sphingolipid regulation, we investigated whether changes in mtFASII function would affect mitochondrial secretion of S1P. S1P concentrations in control and ACP KD mitochondrial secretomes were measured using an S1P ELISA. Though secretion of one type of bioactive lipid, lysophospholipids, showed a trend toward increased levels in ACP KD secretomes, levels of S1P secretion were unchanged (Figure 25).

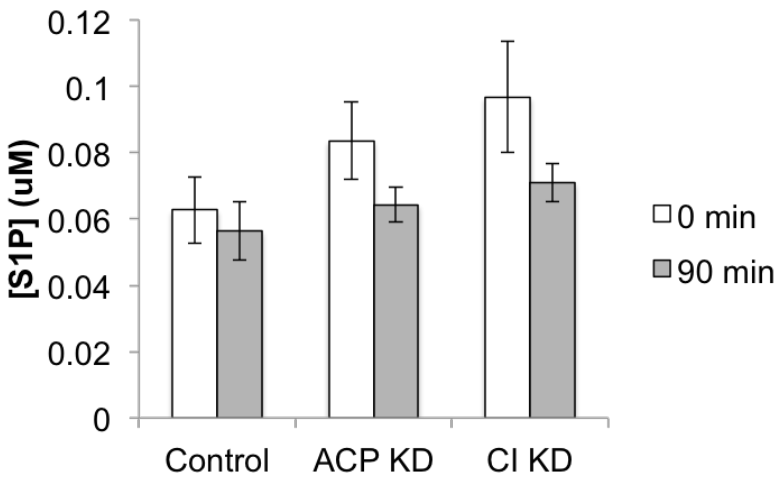

Figure 25. ACP KD and CI KD do not alter mitochondrial secretion of S1P.
S1P levels were determined in mitochondrial secretomes using the S1P ELISA Kit (Echelon Biosciences) according to manufacturer's protocol. Protein concentrations in each sample were first determined using BSA protein assay (Bio-Rad) according to manufacturer's protocol. 40 µg protein was used for each well in triplicate per sample. n=3, *p<0.05.

Discussion

Previous data from our lab indicate that the mtFASII pathway may be involved in mitochondrial signaling through bioactive lipids and small peptides (Chapters II and III). In order to signal to other parts of the cell, we hypothesize that mitochondrial signaling molecules are secreted from the mitochondria. To gain a better understanding of what mitochondria secrete and how the mtFASII pathway might be involved, we performed a number of experiments on isolated mitochondrial secretions, or the mitochondrial secretome. We first cultured isolated mitochondria and then isolated the supernatants after zero-minute and 90-minute cultures. By comparing the levels of individual substances between the 90- and zero-minute time points, we were able to assess the types of molecules secreted by mitochondria and how the contents of the mitochondrial secretome changes with ACP KD or CI KD.

To investigate whether wild-type mitochondria secrete lipid molecules that might serve as signaling molecules, we performed LC-MS on lipid extracts from the secretomes of wild-type

mitochondria. We found that mitochondria secrete a number of substances, but because of technical limitations we were unable to narrow down the observed changes to individual metabolites. However, of the 33 metabolites that were most significantly changed in our analysis, 14 were potential matches for bioactive lipids and 11 were potential matches for small peptides.

Next, to further characterize the mitochondrial secretome in wild-type conditions, we used metabolomics to assess the contents of mitochondrial secretomes from scrambled siRNA-treated cells. Our data indicate that, at baseline, mitochondria secrete substances from a number of energy-related pathways, including glycolysis and TCA cycle intermediates. Being metabolites of mitochondria-related pathways, their secretion from the mitochondria is not unexpected. Consistent with our LC-MS data, our metabolomics analysis revealed that mitochondria also secrete lipid molecules, including sphingosine and substances related to lipid metabolism such as lysophospholipids, choline, and glycerophosphocholine.

Additionally, both our metabolomics analysis and LC-MS data indicate that mitochondria secrete small peptides. Amino acids and dipeptides were secreted from mitochondria isolated from scrambled shRNA-treated cells. In our LC-MS data, though secretomes underwent lipid extraction, several metabolites were potentially matched to small peptides. The lipid extraction procedure we performed for the LC-MS experiments used chloroform as the lipophilic phase of the extraction mixture. Thus, in order for molecules to separate into the lipophilic phase, they must have partition coefficients equal to or greater than that of chloroform. Several of the peptides that were potential matches for secretome components were sufficiently lipophilic to be included in the lipid fraction, and therefore appear in the LC-MS data. Our LC-MS data, then, appears to confirm the metabolomics data, indicating that peptide secretion from mitochondria is constitutive. This notion is consistent with previous research describing constitutive proteolysis within the mitochondria.[110, 214]

Interestingly, the levels of some molecules examined in our metabolomics analysis were reduced with time in the mitochondrial secretome, indicating that these molecules are absorbed by mitochondria over time. These molecules included components of the mitochondrial secretion assay buffer, such as malonate, which is known to be imported into the mitochondria, likely through the oxaloacetate carrier.[215] NAD^+, another component of the mitochondrial secretion assay buffer, and phosphopantetheine were also imported into the mitochondria over time, likely due to their use in the mitochondria by the mtFASII pathway, among other pathways.

Having characterized the mitochondrial secretome at baseline, we also sought out how loss of mtFASII function through ACP KD alters the contents of the mitochondrial secretome. Additionally, to confirm that changes in ACP KD secretomes were not simply due to respiratory deficiency, we isolated mitochondrial secretomes from CI KD cells. Compared to control secretomes, ACP KD and CI KD secretomes contained less ADP, while AMP levels were increased in the ACP KD secretome. Reduced ADP levels and increased AMP levels could be indicative of respiratory deficiency in ACP KD and CI KD cells, as the electron transport chain is not sufficiently able to maintain levels of high-energy phosphates.

ACP KD secretomes also displayed reduced sphingosine levels. This is consistent with previous data that showed decreased sphingosine levels in ACP KD cells and a slight reduction in ACP KD mitochondria. S1P secretion levels, as measured by ELISA, however, were unchanged in ACP KD and CI KD, indicating that S1P is not the mitochondrial signaling molecule. In all conditions (Control, ACP KD, and CI KD), we determined that S1P was not significantly secreted nor absorbed by mitochondria (Figure 25). Thus, effects of S1P are likely intramitochondrial, rather than S1P itself serving as a signaling molecule.

ACP KD and CI KD mitochondria both secrete more lysophospholipids compared to control. In previous data from our lab, ACP KD whole cells contained fewer lysophospholipids, while some lysophospholipids were at increased levels in isolated ACP KD and CI KD mitochondria. Because both ACP KD and CI KD affect mitochondrial pathways, it is possible

that ACP KD and CI KD have different effects on lysophospholipids at the mitochondrial level than what appears at the whole-cell level.

In addition to lysophospholipids, ACP KD mitochondria tended to secrete higher levels of dipeptides, with five of the seven dipeptides tested being elevated by more than 20%, though the increase is not statistically significant. Increased dipeptide secretion is consistent with our previous work, in which we found significantly increased dipeptide levels within isolated ACP KD mitochondria (Chapter III). While increased nonspecific proteolysis is a possible explanation for the increased dipeptide secretion in ACP KD mitochondria, a more interesting explanation could be that ACP KD results in activation of the mitochondrial unfolded protein response (mtUPR). The mtUPR is a mitochondrial signaling pathway in which the mitochondria signal to the nucleus using small peptides, resulting in the transcription of genes that reduce unfolded protein stress in the mitochondria.[106, 108-110, 115] The full mechanism by which the mtUPR works in mammals has not yet been elucidated, but the pathway can be triggered by imbalance between nuclear- and mitochondrial-encoded proteins in the mitochondria, as well as increased levels of damaged proteins.[106, 107, 109] Unpublished RNAseq data from our lab shows that several mtUPR-related genes are upregulated in ACP KD, providing further evidence of mtUPR induction (data not shown). In the case of ACP KD, respiratory deficiency results in elevated ROS marker levels (Chapter II), which could lead to protein damage and, thus, increased protein-folding stress in the mitochondria. However, this same phenomenon would occur in CI KD, where mtUPR induction is not seen. It is also possible that RNA processing defects in ACP KD mitochondria results in mitonuclear protein imbalance, triggering the mtUPR [9].

Another interesting possibility involves the observed link between the mtFASII pathway, mitochondrial tRNA processing, and mitochondrial protein synthesis pathways. An investigation of mitochondrial RNaseP and RNaseZ, which process precursor mitochondrial tRNAs into mature tRNAs, found a physical association between these enzymes and proteins involved in multiple other mitochondrial functions, including the mitochondrial degradosome, the mtFASII

pathway, the TCA cycle, and mitochondrial protein translation machinery, into a supercomplex of 136 proteins.[57] In *oar1* deletion mutant yeast, this supercomplex is absent, indicating that the mtFASII pathway is a vital support for other mitochondrial functions. Importantly, the inclusion of mitochondrial tRNA processing and protein synthesis machinery in this supercomplex provides a potential link between the mtFASII pathway and triggering of the mtUPR: loss of mtFASII function disrupts the supercomplex, thereby altering the ability of tRNA processing and protein synthesis to occur normally, potentially leading to the induction of the mtUPR.

Though not entirely elucidated, our work brings to light some of the consequences of altering the mtFASII pathway and confirms previous research that the mtFASII pathway is linked to activation of the mtUPR. We demonstrated that mitochondria secrete a number of substances, including apparently constitutive secretion of bioactive lipids and small peptides from control mitochondria. We showed that loss of mtFASII pathway function results in further increases in lysophospholipids and dipeptides, indicating a potential link between mtFASII function and regulation of bioactive lipids and the mtUPR. Additionally, in comparing the contents of ACP KD secretomes to those of CI KD, we demonstrated that the changes seen in ACP KD secretomes are not simply due to respiratory deficiency. While our investigation of the mitochondrial secretome provides novel insight into a little-explored component of mitochondrial function, further research is needed in order to fully understand the mechanisms of mitochondrial signaling and the exact role of the mtFASII pathway in its regulation.

CHAPTER V

CONCLUSIONS AND FUTURE DIRECTIONS

Summary and Discussion

Consistent with the literature on the mitochondrial fatty acid synthesis II (mtFASII) pathway, we found that perturbation of its function results in respiratory changes. Glycolysis and the TCA cycle were consistently impaired by acyl carrier protein knockdown (ACP KD) in both whole cells and isolated mitochondria. ACP is a putative component of complex I (CI),[3, 27, 28, 32] and its knockdown is known to result in impaired electron transport chain (ETC) function,[6, 36, 46] causing the cell to increasingly rely on glycolysis. Increased glycolytic flux results in glucose depletion, which we saw functionally with depression of glycolysis, tricarboxylic acid (TCA) cycle, and pentose phosphate pathway intermediates. Additionally, depletion of amino acid anaplerosis precursors in ACP KD cells indicates an upregulation in gluconeogenesis, meaning that the cell is attempting to compensate for glucose depletion. More directly, we found that media glucose levels were reduced in ACP KD cultures.

Interestingly, with increased mtFASII function through mitochondrial *trans*-2-enoyl-CoA reductase overexpression (MECR OX), markers of glucose utilization were not simply unchanged but were elevated, indicating a decreased reliance on glucose compared to control. Additionally, intermediates of the γ-glutamyl cycle, which can serve as indicators of oxidative stress levels, were reduced compared to control in MECR OX.[192, 195, 196] It appears, then, that increased mtFASII function may actually bolster ETC function. This could occur in several ways. It is possible that mtFASII produces fatty acids that enhance mitochondrial inner membrane impermeability, thus improving the efficiency of the ETC by reducing any H^+ leakage across the inner membrane. ETC complex function is also known to improve in certain lipid environments:

cardiolipin organizes ETC complexes into “supercomplexes”, making their interactions more efficient due to their proximity.[216-218]

Knockdown of any component of the mtFASII pathway is known to result in respiratory deficiency.[3, 6, 10, 19, 22, 48] To examine whether all changes we saw in ACP KD cells, mitochondria, and secretomes were simply due to respiratory deficiency, we also examined CI KD cells, mitochondria, and secretomes. Some changes observed in ACP KD were also seen in CI KD, such as evidence of respiratory deficiency and increased oxidative stress markers. Many changes, however, were specific to ACP KD. These included changes in the levels of bioactive lipids and dipeptides.

Alteration of mtFASII function resulted in changes in bioactive lipid levels, including lysophospholipids and sphingolipids. Lysophospholipids were depleted in ACP KD cells, and were at increased levels in MECR OX cells. In CI KD cells and in isolated mitochondria, there was no clear pattern of regulation. Decreased lysophospholipid levels in ACP KD cells could indicate that the mtFASII pathway contributes to the *de novo* synthesis of lysophospholipids, especially considering that lysophospholipid levels correlate directly with mtFASII function in whole cells. The mtFASII pathway could directly provide acyl chains needed for lysophospholipid synthesis. Alternatively, mtFASII-produced fatty acids could indirectly affect lysophospholipid levels, perhaps by acylation of the enzymes involved in *de novo* lysophospholipid synthesis, such as mitochondrial glycerol-3-phosphate acyltransferase (GPAM). Acylation of GPAM, however, has not yet been demonstrated.

Alternatively, decreased lysophospholipid levels could indicate increased degradation by lysophospholipases. Isolated mitochondria have lysophospholipase activity when the mitochondrial membrane potential is compromised.[219] In the case of ACP KD, mitochondrial respiration is dysfunctional, and the mitochondrial membrane potential is presumably disrupted. In this case, mitochondrial phospholipase activity would be elevated, reducing lysophospholipid levels. In MECR OX cells, lysophospholipid levels are elevated. Since mitochondrial

lysophospholipase activity is negligible in healthy mitochondria, little lysophospholipid degradation would occur in MECR OX mitochondria. However, it appears as though MECR OX mitochondria are healthier than control cells, having reduced oxidative stress markers and a possible decreased reliance on glycolysis. Thus, it is possible that MECR OX mitochondria have even less than normal baseline lysophospholipase activity, leading to increased lysophospholipid levels compared to control.

The mtFASII pathway appears to participate in regulation of sphingolipids, though the mechanism has not been identified. In whole cells, sphingosine and sphinganine levels correlated directly with mtFASII function. At the mitochondrial level, sphingosine and sphinganine were not altered by changes in mtFASII function, but this result could be due to the exclusion of the mitochondria-associated ER membrane (MAM) from mitochondria isolated in the manner used in our studies. In the mitochondrial secretome, ACP KD mitochondria secreted less sphingosine than control or CI KD mitochondria, though the difference did not reach significance. Reduced sphingosine secretion in ACP KD is consistent with the whole-cell data, in which ACP KD cells showed reduced sphingosine levels. Sphingosine-1-phosphate (S1P) levels were increased in ACP KD cells, though mitochondrial secretion of S1P was unchanged. The sphingosine:S1P ratio, however, is increased in ACP KD mitochondria compared to control mitochondria, though the difference is nonsignificant. This change in the sphingosine:S1P ratio does not appear at the whole-cell level. It appears, then, that the mtFASII pathway is involved in sphingolipid regulation, possibly in a mitochondria-specific manner. Importantly, mitochondrial sphingosine and S1P levels are important determinants of whether or not a cell undergoes apoptosis.

In addition to levels of smaller sphingolipids, we investigated the effects of mtFASII alterations on ceramide levels. ACP KD elevated markers of oxidative stress in the γ-glutamyl pathway, and oxidative stress is a trigger for ceramide synthesis.[122] Despite the increase in ROS levels, ceramide levels were unchanged in ACP KD whole cells and mitochondria. It is

likely that the apparent failure to upregulate ceramide levels despite increased ROS levels is due to ACP KD-related reductions in baseline ceramide levels. Because levels of sphingosine and sphinganine are reduced in ACP KD, it is likely that ceramide levels are also down compared to control. Thus, ROS-related increases in ceramide levels might still occur in ACP KD, but because baseline ceramide levels are reduced, it appears as if no change in ceramide levels has occurred.

The mechanism by which alterations in the mtFASII pathway affect sphingolipid levels is not known. Because sphingolipid levels correlate directly with mtFASII function, it is likely that the products of mtFASII contribute in some way to sphingolipid synthesis. In the most direct scenario, mtFASII would produce palmitate, which is combined with serine by SPT to initiate sphingolipid synthesis. Alternatively, the products of the mtFASII pathway could indirectly affect sphingolipid synthesis. Because CI KDs did not display the same sphingolipid changes seen in ACP KD, it is not likely that mtFASII product-mediated effects on sphingolipid synthesis are related to respiratory changes. It is possible that the activities of sphingolipid synthesis enzymes are affected by acylation that stems from the mtFASII pathway; in this case, the function of sphingolipid synthesis enzymes would be dependent on acylation of proteins using fatty acids from the mtFASII pathway. No sphingolipid synthesis enzyme has been identified as an acylated enzyme, however.

In addition to changes in sphingolipid synthesis, changes in sphingolipid degradation could account for the altered sphingolipid levels seen in ACP KD and MECR OX. Reduced sphingolipid levels in ACP KD could indicate that sphingolipid degradation is increased, while higher sphingolipid levels in MECR OX could indicate reduced sphingolipid degradation. Typically, both sphingosine and sphinganine are phosphorylated by sphingosine kinase and then degraded by sphingosine-1-phosphate lyase.[121, 220] Increased activity of either sphingosine kinase or sphingosine-1-phosphate lyase could result in reduced sphingosine and sphinganine levels, as is seen in ACP KD. Reduced activities of these enzymes could result in elevated

sphingosine and sphinganine levels, as is seen in MECR OX. In fact, unpublished RNAseq data from our lab indicates that sphingosine kinase 2 (SPHK2) expression is upregulated in ACP KD cells, so it is possible that SPHK2 activity is also increased in ACP KD cells (data not shown).

Regardless of the mechanism, changes in mtFASII function alter lysophospholipid and sphingolipid homeostasis, perhaps in a mitochondria-specific manner. Interestingly, mtFASII-related changes in lipid levels are specific to known signaling lipids, as phospholipid levels overall do not appear changed. For these reasons, we believe that the mtFASII pathway is involved in lipid-based mitochondrial signaling.

We found that in both isolated mitochondria and in the mitochondrial secretome, alterations in mtFASII function resulted in changes in dipeptide levels. Control, ACP KD, and CI KD mitochondria all secreted dipeptides, consistent with previous data indicating that proteolysis in plant mitochondria is constitutive.[214] However, the fact that ACP KD mitochondria contained higher dipeptide levels and trended toward increased secretion of dipeptides indicates that the mtFASII pathway may be involved in regulation of the mitochondrial unfolded protein response (mtUPR).

There are several possible ways in which knockdown of the mtFASII pathway could lead to mtUPR activation. First, mtFASII knockdown could lead to activation of the mtUPR through the failure of proper complex I assembly (Chapter II). A loss of proper complex I assembly in ACP KD would result in increased levels of unassembled proteins in the mitochondria and, therefore, more protein folding stress. Secondly, ACP KD could stimulate mtUPR activation through elevated expression of mtDNA-encoded proteins. In ACP KD cells and mitochondria, NAD^+ levels are elevated, which can lead to increased mitochondrial-encoded gene expression through SIRT3.[106, 109, 221] Thus, it is possible that elevated mitochondrial NAD^+ levels leads to increased expression of mtDNA-encoded genes, resulting in mitonuclear imbalance and activation of the mtUPR.

A third possible mechanism for mtFASII to regulate the mtUPR is through sphingolipids. We have shown that ACP KD depletes cellular sphingosine levels. Additionally, ACP KD increases the mitochondrial sphingosine:S1P ratio, though technically nonsignificant in our study. Thus, sphingosine levels are reduced in ACP KD, and mitochondrial S1P levels are low compared to those of sphingosine. In each case, less mitochondrial S1P is being produced. Typically, mitochondrial S1P binds prohibitin 2 (PHB2), promoting complex IV function and inhibiting activity of the m-AAA protease.[168, 170] The m-AAA protease includes ClpP, the protease responsible for protein degradation in the mtUPR.[106, 108, 109, 111, 115] With a lack of S1P available to bind PHB2, PHB2 may not be able to inhibit the m-AAA protease, resulting in disinhibition of protein degradation, leading to activation of the mtUPR.

Limitations

Although we are confident in our approach, every set of experiments has limitations. One limitation of our work is due to the fact that changes to mtFASII function have multiple effects on the cell, mitochondria, and secretome. To ensure that the ACP KD phenotype was not simply due to respiratory dysfunction, we performed similar experiments in CI KD cells. However, we were not able to confirm whether other mtFASII-related changes were due to the products of mtFASII themselves, or of secondary functions of mtFASII components. For experiments using isolated mitochondria or the mitochondrial secretome, we could not confirm whether any of the observed changes were due to the mitochondrial isolation procedure itself. Though we could have compared multiple mitochondrial isolation techniques, any mitochondrial isolation procedure has potential to stress mitochondria and cannot prevent situations inherent to mitochondrial isolation, such as mitonuclear protein imbalance. Additionally, when characterizing the mitochondrial secretome, the difficulty in identifying lipid species by LC-MS prevented us from being able to specifically identify which lipid species were secreted by the mitochondria (Chapter IV).

Future Directions

Since the mtFASII pathway's roles and effects in the cell are not well characterized, there are many experiments that could be done in the future. One unknown factor in mtFASII research is the ultimate use of mtFASII products, such as the types of molecules mtFASII products are used to assemble as well as their subcellular localization. The products of the mtFASII pathway could be tracked using malonate linked to a stable isotope combined with lipid-specific mass spectrometry. Because acyl-CoA synthetase family member 3 (ACSF3), which converts malonate to malonyl-CoA, is present in the mitochondria but not the cytosol, malonate specifically feeds into the mtFASII pathway. Thus, a stable isotope-linked malonate would label any mtFASII product with the stable isotope. In mass spectrometry, this stable isotope would cause any labeled molecule to show a mass shift on the mass spectrum. In identifying molecules with mass shifts, mtFASII products are identified. When combined with cell fractionation, the subcellular localization of mtFASII products could also be determined. These experiments could confirm previous data regarding which fatty acids are produced by the mtFASII pathway but also identify what becomes of mtFASII products in terms of incorporation into larger lipid molecules and subcellular localization. Additionally, stable isotope tracing could work to identify mtFASII-related molecules that appear in the mitochondrial secretome.

To expand upon our findings related to sphingolipids, lipidomics could be performed. In this set of experiments, HeLa cells would undergo shRNA-mediated ACP KD and vector-mediated MECR OX. Control cells to complement ACP KD would be scrambled shRNA-treated cells; control cells to complement MECR OX would be empty vector-treated cells. To ensure that ACP's effects are not simply due to respiratory deficiency, another group of cells would receive 96 hours of CI KD. After 96 hours of ACP or CI KD or 24 hours of MECR OX, HeLa cells would be harvested whole, or mitochondria would be isolated. Lipids would be extracted from each whole-cell or mitochondrial sample using a modified Folch extraction.[179] Samples would

then undergo LC-MS/MS to identify the presence and amounts of a panel of lipids, particularly sphingolipids. These experiments would provide an overview of the classes of lipids altered by changes in mtFASII function and would provide a more in-depth look into the nature of mtFASII's effects on sphingolipid synthesis and metabolism. Changes in phospholipids would provide insight into whether or not the mtFASII pathway plays a potential role in the composition and thus physical properties of cellular membranes, which we were not able to determine in the metabolomics experiments we have conducted so far. We would be able to identify whether sphingosine levels are reduced in ACP KD cells because of reduced sphingosine synthesis or because of sphingosine's conversion into other molecular species. Additionally, we would have a better understanding of the mtFASII pathway's role in sphingolipid-mediated signaling, as lipidomics would provide more specific data on the exact sphingolipid species affected by alterations in mtFASII function.

Another set of experiments could be performed to determine whether the changes in dipeptides seen in ACP KD mitochondria and secretomes are related to activation of the mtUPR or to nonspecific protein degradation. As in the previous set of experiments, HeLa cells would undergo 96 hours of ACP KD or treatment with scrambled shRNA, or 24 hours of MECR OX or treatment with empty vector. One experiment that would be helpful toward understanding the mtFASII pathway's involvement in mtUPR regulation has already been done: our lab has an unpublished set of RNAseq data for ACP KD and MECR OX cells in which several mtUPR-related genes are upregulated in ACP KD. Since mRNA expression is not necessarily representative of protein expression and activity, protein-level assays would need to be performed as well. Western blots for JNK and c-Jun would allow visualization of their expression levels; band shifts would indicate that they have been activated by phosphorylation. Additionally, isolation of the nucleus followed by western blotting would identify if JNK and c-Jun have translocated to the nucleus, which is required for them to activate transcription of CHOP and

C/EBPβ. Also, since CHOP and C/EBPβ bind to activate transcription of mtUPR-related genes, co-immunoprecipitation assays could be done to confirm their binding subsequent to ACP KD.

Conclusions

The experiments described in the preceding chapters provide an interesting insight into a pathway about which little is known. The mtFASII pathway may, at first blush, appear to be a vestigial, nearly impotent pathway that is easily superseded by the abilities of the cytosolic fatty acid synthesis pathway (FASI). Our data, however, indicate that the mtFASII pathway is more involved and more vital than simply producing fatty acids in the mitochondria. We have shown that the mtFASII pathway is capable of regulating levels of bioactive lipids, which indicates that the mtFASII pathway is potentially involved in lipid signaling. Additionally, the mtFASII pathway regulates mitochondrial and secretome levels of dipeptides, pointing toward a role for the mtFASII pathway in mtUPR regulation. In both cases, these experiments provide new information regarding how the mitochondria communicate to other parts of the cell. Additionally, involvement of the mtFASII pathway in regulation of anything beyond the mitochondria is a novel finding. Our findings must be replicated and extended to fully understand the role of the mtFASII pathway in the mitochondria and the cell. However, these experiments are an exciting first step toward a better understanding of mitochondrial function and communication.

REFERENCES

1. Smith, S., Witkowski, A. & Joshi, A.K. Structural and functional organization of the animal fatty acid synthase. *Progress in lipid research* **42**, 289-317 (2003).

2. Witkowski, A., Joshi, A.K. & Smith, S. Coupling of the de novo fatty acid biosynthesis and lipoylation pathways in mammalian mitochondria. *The Journal of biological chemistry* **282**, 14178-14185 (2007).

3. Hiltunen, J.K., Chen, Z., Haapalainen, A.M., Wierenga, R.K. & Kastaniotis, A.J. Mitochondrial fatty acid synthesis--an adopted set of enzymes making a pathway of major importance for the cellular metabolism. *Progress in lipid research* **49**, 27-45 (2010).

4. Stuible, H.P., Meier, S., Wagner, C., Hannappel, E. & Schweizer, E. A novel phosphopantetheine:protein transferase activating yeast mitochondrial acyl carrier protein. *The Journal of biological chemistry* **273**, 22334-22339 (1998).

5. Lambalot, R.H. & Walsh, C.T. Cloning, overproduction, and characterization of the Escherichia coli holo-acyl carrier protein synthase. *The Journal of biological chemistry* **270**, 24658-24661 (1995).

6. Tehlivets, O., Scheuringer, K. & Kohlwein, S.D. Fatty acid synthesis and elongation in yeast. *Biochimica et biophysica acta* **1771**, 255-270 (2007).

7. Joshi, A.K., Zhang, L., Rangan, V.S. & Smith, S. Cloning, expression, and characterization of a human 4'-phosphopantetheinyl transferase with broad substrate specificity. *The Journal of biological chemistry* **278**, 33142-33149 (2003).

8. Bunkoczi, G. *et al.* Mechanism and substrate recognition of human holo ACP synthase. *Chem Biol* **14**, 1243-1253 (2007).

9. Schonauer, M.S., Kastaniotis, A.J., Hiltunen, J.K. & Dieckmann, C.L. Intersection of RNA processing and the type II fatty acid synthesis pathway in yeast mitochondria. *Molecular and cellular biology* **28**, 6646-6657 (2008).

10. Hiltunen, J.K., Okubo, F., Kursu, V.A., Autio, K.J. & Kastaniotis, A.J. Mitochondrial fatty acid synthesis and maintenance of respiratory competent mitochondria in yeast. *Biochem Soc Trans* **33**, 1162-1165 (2005).

11. Sloan, J.L. *et al.* Exome sequencing identifies ACSF3 as a cause of combined malonic and methylmalonic aciduria. *Nature genetics* **43**, 883-886 (2011).

12. Witkowski, A., Thweatt, J. & Smith, S. Mammalian ACSF3 protein is a malonyl-CoA synthetase that supplies the chain extender units for mitochondrial fatty acid synthesis. *The Journal of biological chemistry* **286**, 33729-33736 (2011).

13. Gurvitz, A. Physiological function of mycobacterial mtFabD, an essential malonyl-CoA:AcpM transacylase of type 2 fatty acid synthase FASII, in yeast mct1Delta cells. *Comp Funct Genomics*, 836172 (2009).

14. Harington, A., Herbert, C.J., Tung, B., Getz, G.S. & Slonimski, P.P. Identification of a new nuclear gene (CEM1) encoding a protein homologous to a beta-keto-acyl synthase which is essential for mitochondrial respiration in Saccharomyces cerevisiae. *Molecular microbiology* **9**, 545-555 (1993).

15. Zhang, L., Joshi, A.K., Hofmann, J., Schweizer, E. & Smith, S. Cloning, expression, and characterization of the human mitochondrial beta-ketoacyl synthase. Complementation of the yeast CEM1 knock-out strain. *The Journal of biological chemistry* **280**, 12422-12429 (2005).

16. Christensen, C.E., Kragelund, B.B., von Wettstein-Knowles, P. & Henriksen, A. Structure of the human beta-ketoacyl [ACP] synthase from the mitochondrial type II fatty acid synthase. *Protein Sci* **16**, 261-272 (2007).

17. Venkatesan, R. *et al.* Insights into mitochondrial fatty acid synthesis from the structure of heterotetrameric 3-ketoacyl-ACP reductase/3R-hydroxyacyl-CoA dehydrogenase. *Nat Commun* **5**, 4805 (2014).

18. Wroblewski, T. *et al.* Comparative large-scale analysis of interactions between several crop species and the effector repertoires from multiple pathovars of Pseudomonas and Ralstonia. *Plant Physiol* **150**, 1733-1749 (2009).

19. Hiltunen, J.K. *et al.* Mitochondrial fatty acid synthesis and respiration. *Biochimica et biophysica acta* **1797**, 1195-1202 (2010).

20. Zhang, Y., Ning, F., Li, X. & Teng, M. Structural insights into cofactor recognition of yeast mitochondria 3-oxoacyl-ACP reductase OAR1. *IUBMB life* **65**, 154-162 (2013).

21. Autio, K.J. *et al.* An ancient genetic link between vertebrate mitochondrial fatty acid synthesis and RNA processing. *FASEB journal : official publication of the Federation of American Societies for Experimental Biology* **22**, 569-578 (2008).

22. Kastaniotis, A.J., Autio, K.J., Sormunen, R.T. & Hiltunen, J.K. Htd2p/Yhr067p is a yeast 3-hydroxyacyl-ACP dehydratase essential for mitochondrial function and morphology. *Molecular microbiology* **53**, 1407-1421 (2004).

23. Miinalainen, I.J. *et al.* Characterization of 2-enoyl thioester reductase from mammals. An ortholog of YBR026p/MRF1'p of the yeast mitochondrial fatty acid synthesis type II. *The Journal of biological chemistry* **278**, 20154-20161 (2003).

24. Masuda, N. *et al.* Nuclear receptor binding factor-1 (NRBF-1), a protein interacting with a wide spectrum of nuclear hormone receptors. *Gene* **221**, 225-233 (1998).

25. Parl, A. *et al.* The mitochondrial fatty acid synthesis (mtFASII) pathway is capable of mediating nuclear-mitochondrial cross talk through the PPAR system of transcriptional activation. *Biochemical and biophysical research communications* **441**, 418-424 (2013).

26. Chen, Z.J. *et al.* Structural enzymological studies of 2-enoyl thioester reductase of the human mitochondrial FAS II pathway: new insights into its substrate recognition properties. *Journal of molecular biology* **379**, 830-844 (2008).

27. Runswick, M.J., Fearnley, I.M., Skehel, J.M. & Walker, J.E. Presence of an acyl carrier protein in NADH:ubiquinone oxidoreductase from bovine heart mitochondria. *FEBS letters* **286**, 121-124 (1991).

28. Sackmann, U., Zensen, R., Rohlen, D., Jahnke, U. & Weiss, H. The acyl-carrier protein in Neurospora crassa mitochondria is a subunit of NADH:ubiquinone reductase (complex I). *European journal of biochemistry / FEBS* **200**, 463-469 (1991).

29. Cronan, J.E., Fearnley, I.M. & Walker, J.E. Mammalian mitochondria contain a soluble acyl carrier protein. *FEBS letters* **579**, 4892-4896 (2005).

30. Triepels, R. *et al.* The human nuclear-encoded acyl carrier subunit (NDUFAB1) of the mitochondrial complex I in human pathology. *J Inherit Metab Dis* **22**, 163-173 (1999).

31. Roujeinikova, A. *et al.* Structural studies of fatty acyl-(acyl carrier protein) thioesters reveal a hydrophobic binding cavity that can expand to fit longer substrates. *Journal of molecular biology* **365**, 135-145 (2007).

32. Carroll, J., Fearnley, I.M., Shannon, R.J., Hirst, J. & Walker, J.E. Analysis of the subunit composition of complex I from bovine heart mitochondria. *Mol Cell Proteomics* **2**, 117-126 (2003).

33. Meyer, E.H., Heazlewood, J.L. & Millar, A.H. Mitochondrial acyl carrier proteins in Arabidopsis thaliana are predominantly soluble matrix proteins and none can be confirmed as subunits of respiratory Complex I. *Plant Mol Biol* **64**, 319-327 (2007).

34. Brody, S., Oh, C., Hoja, U. & Schweizer, E. Mitochondrial acyl carrier protein is involved in lipoic acid synthesis in Saccharomyces cerevisiae. *FEBS letters* **408**, 217-220 (1997).

35. Schulte, U. Biogenesis of respiratory complex I. *J Bioenerg Biomembr* **33**, 205-212 (2001).

36. Schneider, R., Massow, M., Lisowsky, T. & Weiss, H. Different respiratory-defective phenotypes of Neurospora crassa and Saccharomyces cerevisiae after inactivation of the gene encoding the mitochondrial acyl carrier protein. *Current genetics* **29**, 10-17 (1995).

37. Wakil, S.J.M., W.; Warshaw, J.B. Synthesis of fatty acids by mitochondria. *The Journal of biological chemistry* **235**, PC31-PC32 (1960).

38. Gueguen, V., Macherel, D., Jaquinod, M., Douce, R. & Bourguignon, J. Fatty acid and lipoic acid biosynthesis in higher plant mitochondria. *The Journal of biological chemistry* **275**, 5016-5025 (2000).

39. Perham, R.N. Swinging arms and swinging domains in multifunctional enzymes: catalytic machines for multistep reactions. *Annu Rev Biochem* **69**, 961-1004 (2000).

40. Mayr, J.A., Feichtinger, R.G., Tort, F., Ribes, A. & Sperl, W. Lipoic acid biosynthesis defects. *J Inherit Metab Dis* **37**, 553-563 (2014).

41. Kikuchi, G., Motokawa, Y., Yoshida, T. & Hiraga, K. Glycine cleavage system: reaction mechanism, physiological significance, and hyperglycinemia. *Proc Jpn Acad Ser B Phys Biol Sci* **84**, 246-263 (2008).

42. Morikawa, T., Yasuno, R. & Wada, H. Do mammalian cells synthesize lipoic acid? Identification of a mouse cDNA encoding a lipoic acid synthase located in mitochondria. *FEBS letters* **498**, 16-21 (2001).

43. Schonauer, M.S., Kastaniotis, A.J., Kursu, V.A., Hiltunen, J.K. & Dieckmann, C.L. Lipoic acid synthesis and attachment in yeast mitochondria. *The Journal of biological chemistry* **284**, 23234-23242 (2009).

44. Wada, H., Shintani, D. & Ohlrogge, J. Why do mitochondria synthesize fatty acids? Evidence for involvement in lipoic acid production. *Proceedings of the National Academy of Sciences of the United States of America* **94**, 1591-1596 (1997).

45. Jordan, S.W. & Cronan, J.E., Jr. A new metabolic link. The acyl carrier protein of lipid synthesis donates lipoic acid to the pyruvate dehydrogenase complex in Escherichia coli and mitochondria. *The Journal of biological chemistry* **272**, 17903-17906 (1997).

46. Feng, D., Witkowski, A. & Smith, S. Down-regulation of mitochondrial acyl carrier protein in mammalian cells compromises protein lipoylation and respiratory complex I and results in cell death. *The Journal of biological chemistry* **284**, 11436-11445 (2009).

47. Smith, S. *et al.* Compromised mitochondrial fatty acid synthesis in transgenic mice results in defective protein lipoylation and energy disequilibrium. *PloS one* **7**, e47196 (2012).

48. Kursu, V.A. *et al.* Defects in mitochondrial fatty acid synthesis result in failure of multiple aspects of mitochondrial biogenesis in Saccharomyces cerevisiae. *Molecular microbiology* **90**, 824-840 (2013).

49. Gurvitz, A. A C. elegans model for mitochondrial fatty acid synthase II: the longevity-associated gene W09H1.5/mecr-1 encodes a 2-trans-enoyl-thioester reductase. *PloS one* **4**, e7791 (2009).

50. Torkko, J.M. *et al.* Candida tropicalis Etr1p and Saccharomyces cerevisiae Ybr026p (Mrf1'p), 2-enoyl thioester reductases essential for mitochondrial respiratory competence. *Molecular and cellular biology* **21**, 6243-6253 (2001).

51. Chen, Z. *et al.* Myocardial overexpression of Mecr, a gene of mitochondrial FAS II leads to cardiac dysfunction in mouse. *PloS one* **4**, e5589 (2009).

52. Ojala, D., Montoya, J. & Attardi, G. tRNA punctuation model of RNA processing in human mitochondria. *Nature* **290**, 470-474 (1981).

53. Rossmanith, W. Of P and Z: mitochondrial tRNA processing enzymes. *Biochimica et biophysica acta* **1819**, 1017-1026 (2012).

54. Rossmanith, W., Tullo, A., Potuschak, T., Karwan, R. & Sbisa, E. Human mitochondrial tRNA processing. *The Journal of biological chemistry* **270**, 12885-12891 (1995).

55. Holzmann, J. *et al.* RNase P without RNA: identification and functional reconstitution of the human mitochondrial tRNA processing enzyme. *Cell* **135**, 462-474 (2008).

56. Rossmanith, W. & Karwan, R.M. Characterization of human mitochondrial RNase P: novel aspects in tRNA processing. *Biochemical and biophysical research communications* **247**, 234-241 (1998).

57. Daoud, R., Forget, L. & Lang, B.F. Yeast mitochondrial RNase P, RNase Z and the RNA degradosome are part of a stable supercomplex. *Nucleic Acids Res* **40**, 1728-1736 (2012).

58. Alfares, A. *et al.* Combined malonic and methylmalonic aciduria: exome sequencing reveals mutations in the ACSF3 gene in patients with a non-classic phenotype. *Journal of medical genetics* **48**, 602-605 (2011).

59. Lustbader, J.W. *et al.* ABAD directly links Abeta to mitochondrial toxicity in Alzheimer's disease. *Science* **304**, 448-452 (2004).

60. Dirix, G. *et al.* Peptide signal molecules and bacteriocins in Gram-negative bacteria: a genome-wide in silico screening for peptides containing a double-glycine leader sequence and their cognate transporters. *Peptides* **25**, 1425-1440 (2004).

61. Michiels, J., Dirix, G., Vanderleyden, J. & Xi, C. Processing and export of peptide pheromones and bacteriocins in Gram-negative bacteria. *Trends Microbiol* **9**, 164-168 (2001).

62. Yuan, Y., Sachdeva, M., Leeds, J.A. & Meredith, T.C. Fatty acid biosynthesis in Pseudomonas aeruginosa is initiated by the FabY class of beta-ketoacyl acyl carrier protein synthases. *J Bacteriol* **194**, 5171-5184 (2012).

63. Kleerebezem, M., Quadri, L.E., Kuipers, O.P. & de Vos, W.M. Quorum sensing by peptide pheromones and two-component signal-transduction systems in Gram-positive bacteria. *Molecular microbiology* **24**, 895-904 (1997).

64. Fuqua, C., Parsek, M.R. & Greenberg, E.P. Regulation of gene expression by cell-to-cell communication: acyl-homoserine lactone quorum sensing. *Annu Rev Genet* **35**, 439-468 (2001).

65. Miller, M.B. & Bassler, B.L. Quorum sensing in bacteria. *Annu Rev Microbiol* **55**, 165-199 (2001).

66. Hoang, T.T., Sullivan, S.A., Cusick, J.K. & Schweizer, H.P. Beta-ketoacyl acyl carrier protein reductase (FabG) activity of the fatty acid biosynthetic pathway is a determining factor of 3-oxo-homoserine lactone acyl chain lengths. *Microbiology* **148**, 3849-3856 (2002).

67. Yates, E.A. *et al.* N-acylhomoserine lactones undergo lactonolysis in a pH-, temperature-, and acyl chain length-dependent manner during growth of Yersinia pseudotuberculosis and Pseudomonas aeruginosa. *Infect Immun* **70**, 5635-5646 (2002).

68. Shaw, P.D. *et al.* Detecting and characterizing N-acyl-homoserine lactone signal molecules by thin-layer chromatography. *Proceedings of the National Academy of Sciences of the United States of America* **94**, 6036-6041 (1997).

69. Hall, R.A. *et al.* The quorum-sensing molecules farnesol/homoserine lactone and dodecanol operate via distinct modes of action in Candida albicans. *Eukaryot Cell* **10**, 1034-1042 (2011).

70. Schaefer, A.L., Val, D.L., Hanzelka, B.L., Cronan, J.E., Jr. & Greenberg, E.P. Generation of cell-to-cell signals in quorum sensing: acyl homoserine lactone synthase activity of a purified Vibrio fischeri LuxI protein. *Proceedings of the National Academy of Sciences of the United States of America* **93**, 9505-9509 (1996).

71. Viana, E.S., Campos, M.E., Ponce, A.R., Mantovani, H.C. & Vanetti, M.C. Biofilm formation and acyl homoserine lactone production in Hafnia alvei isolated from raw milk. *Biol Res* **42**, 427-436 (2009).

72. Urbanowski, M.L., Lostroh, C.P. & Greenberg, E.P. Reversible acyl-homoserine lactone binding to purified Vibrio fischeri LuxR protein. *J Bacteriol* **186**, 631-637 (2004).

73. Meighen, E.A. Molecular biology of bacterial bioluminescence. *Microbiol Rev* **55**, 123-142 (1991).

74. Hanzelka, B.L. & Greenberg, E.P. Quorum sensing in Vibrio fischeri: evidence that S-adenosylmethionine is the amino acid substrate for autoinducer synthesis. *J Bacteriol* **178**, 5291-5294 (1996).

75. Engebrecht, J., Nealson, K. & Silverman, M. Bacterial bioluminescence: isolation and genetic analysis of functions from Vibrio fischeri. *Cell* **32**, 773-781 (1983).

76. Choi, S.H. & Greenberg, E.P. The C-terminal region of the Vibrio fischeri LuxR protein contains an inducer-independent lux gene activating domain. *Proceedings of the National Academy of Sciences of the United States of America* **88**, 11115-11119 (1991).

77. Havarstein, L.S., Diep, D.B. & Nes, I.F. A family of bacteriocin ABC transporters carry out proteolytic processing of their substrates concomitant with export. *Molecular microbiology* **16**, 229-240 (1995).

78. Weinrauch, Y., Penchev, R., Dubnau, E., Smith, I. & Dubnau, D. A Bacillus subtilis regulatory gene product for genetic competence and sporulation resembles sensor protein members of the bacterial two-component signal-transduction systems. *Genes Dev* **4**, 860-872 (1990).

79. Lazazzera, B.A. & Grossman, A.D. The ins and outs of peptide signaling. *Trends Microbiol* **6**, 288-294 (1998).

80. Ansaldi, M., Marolt, D., Stebe, T., Mandic-Mulec, I. & Dubnau, D. Specific activation of the Bacillus quorum-sensing systems by isoprenylated pheromone variants. *Molecular microbiology* **44**, 1561-1573 (2002).

81. Magnuson, R., Solomon, J. & Grossman, A.D. Biochemical and genetic characterization of a competence pheromone from B. subtilis. *Cell* **77**, 207-216 (1994).

82. Solomon, J.M., Lazazzera, B.A. & Grossman, A.D. Purification and characterization of an extracellular peptide factor that affects two different developmental pathways in Bacillus subtilis. *Genes Dev* **10**, 2014-2024 (1996).

83. Weinrauch, Y., Guillen, N. & Dubnau, D.A. Sequence and transcription mapping of Bacillus subtilis competence genes comB and comA, one of which is related to a family of bacterial regulatory determinants. *J Bacteriol* **171**, 5362-5375 (1989).

84. Tossa, P. *et al.* Early markers of airways inflammation and occupational asthma: rationale, study design and follow-up rates among bakery, pastry and hairdressing apprentices. *BMC Public Health* **9**, 113 (2009).

85. Roggiani, M. & Dubnau, D. ComA, a phosphorylated response regulator protein of Bacillus subtilis, binds to the promoter region of srfA. *J Bacteriol* **175**, 3182-3187 (1993).

86. Turgay, K., Hamoen, L.W., Venema, G. & Dubnau, D. Biochemical characterization of a molecular switch involving the heat shock protein ClpC, which controls the activity of ComK, the competence transcription factor of Bacillus subtilis. *Genes Dev* **11**, 119-128 (1997).

87. Turgay, K., Hahn, J., Burghoorn, J. & Dubnau, D. Competence in Bacillus subtilis is controlled by regulated proteolysis of a transcription factor. *EMBO J* **17**, 6730-6738 (1998).

88. van Sinderen, D., ten Berge, A., Hayema, B.J., Hamoen, L. & Venema, G. Molecular cloning and sequence of comK, a gene required for genetic competence in Bacillus subtilis. *Molecular microbiology* **11**, 695-703 (1994).

89. van Sinderen, D. & Venema, G. comK acts as an autoregulatory control switch in the signal transduction route to competence in Bacillus subtilis. *J Bacteriol* **176**, 5762-5770 (1994).

90. Hahn, J., Kong, L. & Dubnau, D. The regulation of competence transcription factor synthesis constitutes a critical control point in the regulation of competence in Bacillus subtilis. *J Bacteriol* **176**, 5753-5761 (1994).

91. Solomon, J.M., Magnuson, R., Srivastava, A. & Grossman, A.D. Convergent sensing pathways mediate response to two extracellular competence factors in Bacillus subtilis. *Genes Dev* **9**, 547-558 (1995).

92. Lazazzera, B.A., Kurtser, I.G., McQuade, R.S. & Grossman, A.D. An autoregulatory circuit affecting peptide signaling in Bacillus subtilis. *J Bacteriol* **181**, 5193-5200 (1999).

93. Lazazzera, B.A., Solomon, J.M. & Grossman, A.D. An exported peptide functions intracellularly to contribute to cell density signaling in B. subtilis. *Cell* **89**, 917-925 (1997).

94. Pottathil, M. & Lazazzera, B.A. The extracellular Phr peptide-Rap phosphatase signaling circuit of Bacillus subtilis. *Front Biosci* **8**, d32-45 (2003).

95. Burbulys, D., Trach, K.A. & Hoch, J.A. Initiation of sporulation in B. subtilis is controlled by a multicomponent phosphorelay. *Cell* **64**, 545-552 (1991).

96. Kolodkin-Gal, I., Hazan, R., Gaathon, A., Carmeli, S. & Engelberg-Kulka, H. A linear pentapeptide is a quorum-sensing factor required for mazEF-mediated cell death in Escherichia coli. *Science* **318**, 652-655 (2007).

97. Kumar, S. & Engelberg-Kulka, H. Quorum sensing peptides mediating interspecies bacterial cell death as a novel class of antimicrobial agents. *Curr Opin Microbiol* **21**, 22-27 (2014).

98. Kolodkin-Gal, I. & Engelberg-Kulka, H. The extracellular death factor: physiological and genetic factors influencing its production and response in Escherichia coli. *J Bacteriol* **190**, 3169-3175 (2008).

99. Engelberg-Kulka, H., Amitai, S., Kolodkin-Gal, I. & Hazan, R. Bacterial programmed cell death and multicellular behavior in bacteria. *PLoS Genet* **2**, e135 (2006).

100. Hazan, R., Sat, B. & Engelberg-Kulka, H. Escherichia coli mazEF-mediated cell death is triggered by various stressful conditions. *J Bacteriol* **186**, 3663-3669 (2004).

101. Aizenman, E., Engelberg-Kulka, H. & Glaser, G. An Escherichia coli chromosomal "addiction module" regulated by guanosine [corrected] 3',5'-bispyrophosphate: a model for programmed bacterial cell death. *Proceedings of the National Academy of Sciences of the United States of America* **93**, 6059-6063 (1996).

102. Zhang, Y., Zhang, J., Hara, H., Kato, I. & Inouye, M. Insights into the mRNA cleavage mechanism by MazF, an mRNA interferase. *The Journal of biological chemistry* **280**, 3143-3150 (2005).

103. Zhang, Y. *et al.* MazF cleaves cellular mRNAs specifically at ACA to block protein synthesis in Escherichia coli. *Mol Cell* **12**, 913-923 (2003).

104. Kamada, K., Hanaoka, F. & Burley, S.K. Crystal structure of the MazE/MazF complex: molecular bases of antidote-toxin recognition. *Mol Cell* **11**, 875-884 (2003).

105. Belitsky, M. *et al.* The Escherichia coli extracellular death factor EDF induces the endoribonucleolytic activities of the toxins MazF and ChpBK. *Mol Cell* **41**, 625-635 (2011).

106. Mottis, A., Jovaisaite, V. & Auwerx, J. The mitochondrial unfolded protein response in mammalian physiology. *Mamm Genome* **25**, 424-433 (2014).

107. Zhao, Q. *et al.* A mitochondrial specific stress response in mammalian cells. *EMBO J* **21**, 4411-4419 (2002).

108. Bernales, S., Soto, M.M. & McCullagh, E. Unfolded protein stress in the endoplasmic reticulum and mitochondria: a role in neurodegeneration. *Front Aging Neurosci* **4**, 5 (2012).

109. Jovaisaite, V. & Auwerx, J. The mitochondrial unfolded protein response-synchronizing genomes. *Curr Opin Cell Biol* **33**, 74-81 (2015).

110. Nargund, A.M., Pellegrino, M.W., Fiorese, C.J., Baker, B.M. & Haynes, C.M. Mitochondrial import efficiency of ATFS-1 regulates mitochondrial UPR activation. *Science* **337**, 587-590 (2012).

111. Choi, K.H. & Licht, S. Control of peptide product sizes by the energy-dependent protease ClpAP. *Biochemistry* **44**, 13921-13931 (2005).

112. Haynes, C.M., Yang, Y., Blais, S.P., Neubert, T.A. & Ron, D. The matrix peptide exporter HAF-1 signals a mitochondrial UPR by activating the transcription factor ZC376.7 in C. elegans. *Mol Cell* **37**, 529-540 (2010).

113. Yoneda, T. *et al.* Compartment-specific perturbation of protein handling activates genes encoding mitochondrial chaperones. *J Cell Sci* **117**, 4055-4066 (2004).

114. Young, L., Leonhard, K., Tatsuta, T., Trowsdale, J. & Langer, T. Role of the ABC transporter Mdl1 in peptide export from mitochondria. *Science* **291**, 2135-2138 (2001).

115. Pellegrino, M.W., Nargund, A.M. & Haynes, C.M. Signaling the mitochondrial unfolded protein response. *Biochimica et biophysica acta* **1833**, 410-416 (2013).

116. Martinus, R.D. *et al.* Selective induction of mitochondrial chaperones in response to loss of the mitochondrial genome. *European journal of biochemistry / FEBS* **240**, 98-103 (1996).

117. Aldridge, J.E., Horibe, T. & Hoogenraad, N.J. Discovery of genes activated by the mitochondrial unfolded protein response (mtUPR) and cognate promoter elements. *PloS one* **2**, e874 (2007).

118. Dean, M., Hamon, Y. & Chimini, G. The human ATP-binding cassette (ABC) transporter superfamily. *Journal of lipid research* **42**, 1007-1017 (2001).

119. Horibe, T. & Hoogenraad, N.J. The chop gene contains an element for the positive regulation of the mitochondrial unfolded protein response. *PloS one* **2**, e835 (2007).

120. Aguilera-Romero, A., Gehin, C. & Riezman, H. Sphingolipid homeostasis in the web of metabolic routes. *Biochimica et biophysica acta* **1841**, 647-656 (2014).

121. Gault, C.R., Obeid, L.M. & Hannun, Y.A. An overview of sphingolipid metabolism: from synthesis to breakdown. *Advances in experimental medicine and biology* **688**, 1-23 (2010).

122. Kogot-Levin, A. & Saada, A. Ceramide and the mitochondrial respiratory chain. *Biochimie* **100**, 88-94 (2014).

123. Bertea, M. *et al.* Deoxysphingoid bases as plasma markers in diabetes mellitus. *Lipids Health Dis* **9**, 84 (2010).

124. Kanehisa, M. & Goto, S. KEGG: kyoto encyclopedia of genes and genomes. *Nucleic Acids Res* **28**, 27-30 (2000).

125. Edsall, L.C., Pirianov, G.G. & Spiegel, S. Involvement of sphingosine 1-phosphate in nerve growth factor-mediated neuronal survival and differentiation. *J Neurosci* **17**, 6952-6960 (1997).

126. Mandala, S.M. *et al.* Molecular cloning and characterization of a lipid phosphohydrolase that degrades sphingosine-1- phosphate and induces cell death. *Proceedings of the National Academy of Sciences of the United States of America* **97**, 7859-7864 (2000).

127. Edsall, L.C., Cuvillier, O., Twitty, S., Spiegel, S. & Milstien, S. Sphingosine kinase expression regulates apoptosis and caspase activation in PC12 cells. *Journal of neurochemistry* **76**, 1573-1584 (2001).

128. Kohama, T. *et al.* Molecular cloning and functional characterization of murine sphingosine kinase. *The Journal of biological chemistry* **273**, 23722-23728 (1998).

129. Ulrich, S., Huwiler, A., Loitsch, S., Schmidt, H. & Stein, J.M. De novo ceramide biosynthesis is associated with resveratrol-induced inhibition of ornithine decarboxylase activity. *Biochemical pharmacology* **74**, 281-289 (2007).

130. Cuvillier, O. *et al.* Suppression of ceramide-mediated programmed cell death by sphingosine-1-phosphate. *Nature* **381**, 800-803 (1996).

131. Castillo, S.S. & Teegarden, D. Sphingosine-1-phosphate inhibition of apoptosis requires mitogen-activated protein kinase phosphatase-1 in mouse fibroblast C3H10T 1/2 cells. *The Journal of nutrition* **133**, 3343-3349 (2003).

132. Obeid, L.M., Linardic, C.M., Karolak, L.A. & Hannun, Y.A. Programmed cell death induced by ceramide. *Science* **259**, 1769-1771 (1993).

133. Xu, J. *et al.* Involvement of de novo ceramide biosynthesis in tumor necrosis factor-alpha/cycloheximide-induced cerebral endothelial cell death. *The Journal of biological chemistry* **273**, 16521-16526 (1998).

134. Spiegel, S. & Milstien, S. Sphingosine 1-phosphate, a key cell signaling molecule. *The Journal of biological chemistry* **277**, 25851-25854 (2002).

135. Perry, D.K. *et al.* Serine palmitoyltransferase regulates de novo ceramide generation during etoposide-induced apoptosis. *The Journal of biological chemistry* **275**, 9078-9084 (2000).

136. Strelow, A. *et al.* Overexpression of acid ceramidase protects from tumor necrosis factor-induced cell death. *J Exp Med* **192**, 601-612 (2000).

137. Gudz, T.I., Tserng, K.Y. & Hoppel, C.L. Direct inhibition of mitochondrial respiratory chain complex III by cell-permeable ceramide. *The Journal of biological chemistry* **272**, 24154-24158 (1997).

138. Zigdon, H. *et al.* Ablation of ceramide synthase 2 causes chronic oxidative stress due to disruption of the mitochondrial respiratory chain. *The Journal of biological chemistry* **288**, 4947-4956 (2013).

139. Hassoun, S.M. *et al.* Sphingosine impairs mitochondrial function by opening permeability transition pore. *Mitochondrion* **6**, 149-154 (2006).

140. Ghafourifar, P. *et al.* Ceramide induces cytochrome c release from isolated mitochondria. Importance of mitochondrial redox state. *The Journal of biological chemistry* **274**, 6080-6084 (1999).

141. Siskind, L.J., Kolesnick, R.N. & Colombini, M. Ceramide forms channels in mitochondrial outer membranes at physiologically relevant concentrations. *Mitochondrion* **6**, 118-125 (2006).

142. Novgorodov, S.A. *et al.* Essential roles of neutral ceramidase and sphingosine in mitochondrial dysfunction due to traumatic brain injury. *The Journal of biological chemistry* **289**, 13142-13154 (2014).

143. Olivera, A. *et al.* Sphingosine kinase expression increases intracellular sphingosine-1-phosphate and promotes cell growth and survival. *J Cell Biol* **147**, 545-558 (1999).

144. Morita, Y. *et al.* Oocyte apoptosis is suppressed by disruption of the acid sphingomyelinase gene or by sphingosine-1-phosphate therapy. *Nat Med* **6**, 1109-1114 (2000).

145. Cuvillier, O. & Levade, T. Sphingosine 1-phosphate antagonizes apoptosis of human leukemia cells by inhibiting release of cytochrome c and Smac/DIABLO from mitochondria. *Blood* **98**, 2828-2836 (2001).

146. Kim, D.S., Hwang, E.S., Lee, J.E., Kim, S.Y. & Park, K.C. Sphingosine-1-phosphate promotes mouse melanocyte survival via ERK and Akt activation. *Cell Signal* **15**, 919-926 (2003).

147. Olivera, A. & Spiegel, S. Sphingosine-1-phosphate as second messenger in cell proliferation induced by PDGF and FCS mitogens. *Nature* **365**, 557-560 (1993).

148. Liu, H. *et al.* Molecular cloning and functional characterization of a novel mammalian sphingosine kinase type 2 isoform. *The Journal of biological chemistry* **275**, 19513-19520 (2000).

149. Xia, P. *et al.* Tumor necrosis factor-alpha induces adhesion molecule expression through the sphingosine kinase pathway. *Proceedings of the National Academy of Sciences of the United States of America* **95**, 14196-14201 (1998).

150. Gomez, L. *et al.* A novel role for mitochondrial sphingosine-1-phosphate produced by sphingosine kinase-2 in PTP-mediated cell survival during cardioprotection. *Basic Res Cardiol* **106**, 1341-1353 (2011).

151. Yabu, T. *et al.* Stress-induced ceramide generation and apoptosis via the phosphorylation and activation of nSMase1 by JNK signaling. *Cell death and differentiation* **22**, 258-273 (2015).

152. Heinrich, M. *et al.* Cathepsin D links TNF-induced acid sphingomyelinase to Bid-mediated caspase-9 and -3 activation. *Cell death and differentiation* **11**, 550-563 (2004).

153. Chalfant, C.E., Szulc, Z., Roddy, P., Bielawska, A. & Hannun, Y.A. The structural requirements for ceramide activation of serine-threonine protein phosphatases. *Journal of lipid research* **45**, 496-506 (2004).

154. Muller, G. *et al.* PKC zeta is a molecular switch in signal transduction of TNF-alpha, bifunctionally regulated by ceramide and arachidonic acid. *EMBO J* **14**, 1961-1969 (1995).

155. Dobrowsky, R.T., Kamibayashi, C., Mumby, M.C. & Hannun, Y.A. Ceramide activates heterotrimeric protein phosphatase 2A. *The Journal of biological chemistry* **268**, 15523-15530 (1993).

156. Bourbon, N.A., Sandirasegarane, L. & Kester, M. Ceramide-induced inhibition of Akt is mediated through protein kinase Czeta: implications for growth arrest. *The Journal of biological chemistry* **277**, 3286-3292 (2002).

157. Bourbon, N.A., Yun, J. & Kester, M. Ceramide directly activates protein kinase C zeta to regulate a stress-activated protein kinase signaling complex. *The Journal of biological chemistry* **275**, 35617-35623 (2000).

158. Coroneos, E., Wang, Y., Panuska, J.R., Templeton, D.J. & Kester, M. Sphingolipid metabolites differentially regulate extracellular signal-regulated kinase and stress-activated protein kinase cascades. *The Biochemical journal* **316 (Pt 1)**, 13-17 (1996).

159. Rosen, H., Gonzalez-Cabrera, P.J., Sanna, M.G. & Brown, S. Sphingosine 1-phosphate receptor signaling. *Annu Rev Biochem* **78**, 743-768 (2009).

160. Malek, R.L. *et al.* Nrg-1 belongs to the endothelial differentiation gene family of G protein-coupled sphingosine-1-phosphate receptors. *The Journal of biological chemistry* **276**, 5692-5699 (2001).

161. Van Brocklyn, J.R. *et al.* Dual actions of sphingosine-1-phosphate: extracellular through the Gi-coupled receptor Edg-1 and intracellular to regulate proliferation and survival. *J Cell Biol* **142**, 229-240 (1998).

162. Lee, M.J. *et al.* Vascular endothelial cell adherens junction assembly and morphogenesis induced by sphingosine-1-phosphate. *Cell* **99**, 301-312 (1999).

163. Mattie, M., Brooker, G. & Spiegel, S. Sphingosine-1-phosphate, a putative second messenger, mobilizes calcium from internal stores via an inositol trisphosphate-independent pathway. *The Journal of biological chemistry* **269**, 3181-3188 (1994).

164. Meyer zu Heringdorf, D. *et al.* Stimulation of intracellular sphingosine-1-phosphate production by G-protein-coupled sphingosine-1-phosphate receptors. *Eur J Pharmacol* **414**, 145-154 (2001).

165. Desai, N.N., Zhang, H., Olivera, A., Mattie, M.E. & Spiegel, S. Sphingosine-1-phosphate, a metabolite of sphingosine, increases phosphatidic acid levels by phospholipase D activation. *The Journal of biological chemistry* **267**, 23122-23128 (1992).

166. Kiss, Z. & Mukherjee, J.J. Phosphocholine and sphingosine-1-phosphate synergistically stimulate DNA synthesis by a MAP kinase-dependent mechanism. *FEBS letters* **412**, 197-200 (1997).

167. Tamama, K. *et al.* Extracellular mechanism through the Edg family of receptors might be responsible for sphingosine-1-phosphate-induced regulation of DNA synthesis and migration of rat aortic smooth-muscle cells. *The Biochemical journal* **353**, 139-146 (2001).

168. Steglich, G., Neupert, W. & Langer, T. Prohibitins regulate membrane protein degradation by the m-AAA protease in mitochondria. *Molecular and cellular biology* **19**, 3435-3442 (1999).

169. Richter-Dennerlein, R. *et al.* DNAJC19, a mitochondrial cochaperone associated with cardiomyopathy, forms a complex with prohibitins to regulate cardiolipin remodeling. *Cell metabolism* **20**, 158-171 (2014).

170. Strub, G.M. *et al.* Sphingosine-1-phosphate produced by sphingosine kinase 2 in mitochondria interacts with prohibitin 2 to regulate complex IV assembly and respiration. *FASEB journal : official publication of the Federation of American Societies for Experimental Biology* **25**, 600-612 (2011).

171. Clay, H.B. *et al.* Altering the Mitochondrial Fatty Acid Synthesis (mtFASII) Pathway Modulates Cellular Metabolic States and Bioactive Lipid Profiles as Revealed by Metabolomic Profiling. *PloS one* **11**, e0151171 (2016).

172. Misra, A., Surolia, N. & Surolia, A. Catalysis and mechanism of malonyl transferase activity in type II fatty acid biosynthesis acyl carrier proteins. *Molecular bioSystems* **5**, 651-659 (2009).

173. Mikolajczyk, S. & Brody, S. De novo fatty acid synthesis mediated by acyl-carrier protein in Neurospora crassa mitochondria. *European journal of biochemistry / FEBS* **187**, 431-437 (1990).

174. Wakil, S.J. Enzymatic synthesis of fatty acids. *Comparative biochemistry and physiology* **4**, 123-158 (1962).

175. Zensen, R., Husmann, H., Schneider, R., Peine, T. & Weiss, H. De novo synthesis and desaturation of fatty acids at the mitochondrial acyl-carrier protein, a subunit of NADH:ubiquinone oxidoreductase in Neurospora crassa. *FEBS letters* **310**, 179-181 (1992).

176. Ronnebaum, S.M. *et al.* Chronic suppression of acetyl-CoA carboxylase 1 in beta-cells impairs insulin secretion via inhibition of glucose rather than lipid metabolism. *The Journal of biological chemistry* **283**, 14248-14256 (2008).

177. Hiltunen, J.K. *et al.* Mitochondrial fatty acid synthesis type II: more than just fatty acids. *The Journal of biological chemistry* **284**, 9011-9015 (2009).

178. Zhang, L., Joshi, A.K. & Smith, S. Cloning, expression, characterization, and interaction of two components of a human mitochondrial fatty acid synthase. Malonyltransferase and acyl carrier protein. *The Journal of biological chemistry* **278**, 40067-40074 (2003).

179. Folch, J., Lees, M. & Sloane Stanley, G.H. A simple method for the isolation and purification of total lipides from animal tissues. *The Journal of biological chemistry* **226**, 497-509 (1957).

180. Morrison, W.R. & Smith, L.M. Preparation of Fatty Acid Methyl Esters and Dimethylacetals from Lipids with Boron Fluoride--Methanol. *Journal of lipid research* **5**, 600-608 (1964).

181. Sreekumar, A. *et al.* Metabolomic profiles delineate potential role for sarcosine in prostate cancer progression. *Nature* **457**, 910-914 (2009).

182. Boudonck, K.J. *et al.* Discovery of metabolomics biomarkers for early detection of nephrotoxicity. *Toxicologic pathology* **37**, 280-292 (2009).

183. Lawton, K.A. *et al.* Analysis of the adult human plasma metabolome. *Pharmacogenomics* **9**, 383-397 (2008).

184. Evans, A.M., DeHaven, C.D., Barrett, T., Mitchell, M. & Milgram, E. Integrated, nontargeted ultrahigh performance liquid chromatography/electrospray ionization

tandem mass spectrometry platform for the identification and relative quantification of the small-molecule complement of biological systems. *Analytical chemistry* **81**, 6656-6667 (2009).

185. Dehaven, C.D., Evans, A.M., Dai, H. & Lawton, K.A. Organization of GC/MS and LC/MS metabolomics data into chemical libraries. *Journal of cheminformatics* **2**, 9 (2010).

186. Storey, J.D. & Tibshirani, R. Statistical significance for genomewide studies. *Proceedings of the National Academy of Sciences of the United States of America* **100**, 9440-9445 (2003).

187. Kadish, A.H. & Hall, D.A. A new method for the continuous monitoring of blood glucose by measurement of dissolved oxygen. *Clin Chem* **11**, 869-875 (1965).

188. Bielawski, J. *et al.* Comprehensive quantitative analysis of bioactive sphingolipids by high-performance liquid chromatography-tandem mass spectrometry. *Methods Mol Biol* **579**, 443-467 (2009).

189. DeBerardinis, R.J., Lum, J.J., Hatzivassiliou, G. & Thompson, C.B. The biology of cancer: metabolic reprogramming fuels cell growth and proliferation. *Cell metabolism* **7**, 11-20 (2008).

190. Stanton, R.C. Glucose-6-phosphate dehydrogenase, NADPH, and cell survival. *IUBMB life* **64**, 362-369 (2012).

191. Richardson, D.K. & Czech, M.P. Primary role of decreased fatty acid synthesis in insulin resistance of large rat adipocytes. *The American journal of physiology* **234**, E182-189 (1978).

192. Wang, X.F. & Cynader, M.S. Astrocytes provide cysteine to neurons by releasing glutathione. *Journal of neurochemistry* **74**, 1434-1442 (2000).

193. Srivastava, S.K. & Beutler, E. The transport of oxidized glutathione from human erythrocytes. *The Journal of biological chemistry* **244**, 9-16 (1969).

194. Griffith, O.W. Biologic and pharmacologic regulation of mammalian glutathione synthesis. *Free radical biology & medicine* **27**, 922-935 (1999).

195. Berkeley, L.I., Cohen, J.F., Crankshaw, D.L., Shirota, F.N. & Nagasawa, H.T. Hepatoprotection by L-cysteine-glutathione mixed disulfide, a sulfhydryl-modified prodrug of glutathione. *Journal of biochemical and molecular toxicology* **17**, 95-97 (2003).

196. Gao, L., Kim, K.J., Yankaskas, J.R. & Forman, H.J. Abnormal glutathione transport in cystic fibrosis airway epithelia. *The American journal of physiology* **277**, L113-118 (1999).

197. Tkachenko, A.G. & Nesterova, L.Y. Polyamines as modulators of gene expression under oxidative stress in Escherichia coli. *Biochemistry. Biokhimiia* **68**, 850-856 (2003).

198. Tkachenko, A.G., Akhova, A.V., Shumkov, M.S. & Nesterova, L.Y. Polyamines reduce oxidative stress in Escherichia coli cells exposed to bactericidal antibiotics. *Research in microbiology* **163**, 83-91 (2012).

199. Smirnova, O.A. *et al.* Chemically induced oxidative stress increases polyamine levels by activating the transcription of ornithine decarboxylase and spermidine/spermine-N1-acetyltransferase in human hepatoma HUH7 cells. *Biochimie* **94**, 1876-1883 (2012).

200. Morgan, D.M. Polyamines. An overview. *Molecular biotechnology* **11**, 229-250 (1999).

201. Park, M.H. & Igarashi, K. Polyamines and their metabolites as diagnostic markers of human diseases. *Biomolecules & therapeutics* **21**, 1-9 (2013).

202. Coleman, R.A. & Lee, D.P. Enzymes of triacylglycerol synthesis and their regulation. *Progress in lipid research* **43**, 134-176 (2004).

203. Coleman, R.A., Lewin, T.M. & Muoio, D.M. Physiological and nutritional regulation of enzymes of triacylglycerol synthesis. *Annual review of nutrition* **20**, 77-103 (2000).

204. Lewin, T.M., Schwerbrock, N.M., Lee, D.P. & Coleman, R.A. Identification of a new glycerol-3-phosphate acyltransferase isoenzyme, mtGPAT2, in mitochondria. *The Journal of biological chemistry* **279**, 13488-13495 (2004).

205. Stiban, J., Fistere, D. & Colombini, M. Dihydroceramide hinders ceramide channel formation: Implications on apoptosis. *Apoptosis : an international journal on programmed cell death* **11**, 773-780 (2006).

206. Goetzl, E.J. *et al.* Mechanisms of lysolipid phosphate effects on cellular survival and proliferation. *Annals of the New York Academy of Sciences* **905**, 177-187 (2000).

207. Ohta, T. *et al.* Untargeted metabolomic profiling as an evaluative tool of fenofibrate-induced toxicology in Fischer 344 male rats. *Toxicologic pathology* **37**, 521-535 (2009).

208. Evans, A.M.B., B.R.; Miller, L.A.D.; Mitchell, M.W.; Robinson, R.J.; Dai, H.; Stewart, S.J.; DeHaven, C.D.; Liu, Q. High resolution mass spectrometry improves data quantity and quality as compared to unit mass resolution mass spectrometry in high-throughput profiling metabolomics. *Metabolomics* **4** (2014).

209. Houtkooper, R.H., Canto, C., Wanders, R.J. & Auwerx, J. The secret life of NAD+: an old metabolite controlling new metabolic signaling pathways. *Endocr Rev* **31**, 194-223 (2010).

210. Jayaram, H.N., Kusumanchi, P. & Yalowitz, J.A. NMNAT expression and its relation to NAD metabolism. *Curr Med Chem* **18**, 1962-1972 (2011).

211. Ying, W. NAD+/NADH and NADP+/NADPH in cellular functions and cell death: regulation and biological consequences. *Antioxid Redox Signal* **10**, 179-206 (2008).

212. Sweetlove, L.J. *et al.* The impact of oxidative stress on Arabidopsis mitochondria. *Plant J* **32**, 891-904 (2002).

213. Ehrmann, D.C. *et al.* Glutathionylated gammaG and gammaA subunits of hemoglobin F: a novel post-translational modification found in extremely premature infants by LC-MS and nanoLC-MS/MS. *J Mass Spectrom* **49**, 178-183 (2014).

214. Halperin, T., Zheng, B., Itzhaki, H., Clarke, A.K. & Adam, Z. Plant mitochondria contain proteolytic and regulatory subunits of the ATP-dependent Clp protease. *Plant Mol Biol* **45**, 461-468 (2001).

215. Palmieri, L. *et al.* Identification of the yeast mitochondrial transporter for oxaloacetate and sulfate. *The Journal of biological chemistry* **274**, 22184-22190 (1999).

216. Schug, Z.T., Frezza, C., Galbraith, L.C. & Gottlieb, E. The music of lipids: how lipid composition orchestrates cellular behaviour. *Acta oncologica* **51**, 301-310 (2012).

217. Pfeiffer, K. *et al.* Cardiolipin stabilizes respiratory chain supercomplexes. *The Journal of biological chemistry* **278**, 52873-52880 (2003).

218. McKenzie, M., Lazarou, M., Thorburn, D.R. & Ryan, M.T. Mitochondrial respiratory chain supercomplexes are destabilized in Barth Syndrome patients. *Journal of molecular biology* **361**, 462-469 (2006).

219. Broekemeier, K.K., S. Activation of mitochondrial lysophospholipase by mitochondrial depolarization: role in organelle turnover. *FASEB journal : official publication of the Federation of American Societies for Experimental Biology* **28**, Supplement 758.754 (2014).

220. Berdyshev, E.V. *et al.* De novo biosynthesis of dihydrosphingosine-1-phosphate by sphingosine kinase 1 in mammalian cells. *Cell Signal* **18**, 1779-1792 (2006).

221. Yang, Y. *et al.* NAD+-dependent deacetylase SIRT3 regulates mitochondrial protein synthesis by deacetylation of the ribosomal protein MRPL10. *The Journal of biological chemistry* **285**, 7417-7429 (2010).